

UNIVERSITÄTSKLINIKUM HAMBURG-EPPENDORF

Klinik und Poliklinik für Neurologie
Prof. Dr. med. Tim Magnus, Prof. Dr. med. Götz Thomalla

The exploration of microglial immune tolerance induction on post-stroke inflammation

Dissertation

zur Erlangung des Grades eines Doktors der Medizin/Zahnmedizin
an der Medizinischen Fakultät der Universität Hamburg.

vorgelegt von:
Haodi Cai,
aus Jiangsu, China

Hamburg 2024

(wird von der Medizinischen Fakultät ausgefüllt)

**Angenommen von der
Medizinischen Fakultät der Universität Hamburg am: 14.01.2025**

**Veröffentlicht mit Genehmigung der
Medizinischen Fakultät der Universität Hamburg.**

Prüfungsausschuss, der/die Vorsitzende: Prof. Dr. Thomas Oertner

Prüfungsausschuss, zweite/r Gutachter/in: PD Dr. Mathias Gelderblom

Content

Content	3
1. Aims of the study	7
2. Introduction	8
2.1 Acute ischemic stroke is still a noteworthy topic	8
2.2 Mechanisms of acute ischemic stroke	9
2.3 Experimental stroke modelling by tMCAO – an ideal but not perfect model ...	10
2.4 Immune activation during stroke pathology.....	10
2.4.1 Microglia play a vital role in stroke.....	11
2.4.2 Infiltrated peripheral immune cells have various functions during stroke ..	12
Myeloid cells	13
Lymphocytes and lymphoid cells	15
2.5 Mechanisms of innate immunity	16
2.5.1 Innate immunity introduction	16
2.5.2 Innate immune memory	17
2.6 Peripheral administration of LPS can induce innate immune response in rodents in the brain.....	19
2.7 Microglia-induced trained immunity shapes CNS diseases	21
3. Material and methods	23
3.1 Design of the study.....	23
3.1.1 Guideline and animal protocol.....	23
3.1.2 Mouse information.....	23
3.1.3 Time schedule of short-term study.....	23
3.1.4 Time schedule of long-term study.....	24
3.2 Immune tolerance induction.....	25
3.3 tMCAO stroke modelling	25
3.4 MRI quantification of mouse stroke lesion	26
3.5 Behavioral test.....	27
3.5.1 Open field test.....	27

3.5.2 Y-maze test.....	28
3.6 FACS measurement of immune cell infiltration.....	29
3.6.1 Tissue isolation and cell pellet suspension preparation	29
3.6.1.1 Spleen and cervical lymph nodes isolation and cell suspension preparation.....	29
3.6.1.2 Meninges isolation and cell suspension preparation	29
3.6.1.3 Brain isolation and preparation of cell suspension.....	30
3.6.1.4 Cell suspension distribution	31
3.6.2 Infiltration staining and quantification.....	31
3.6.3 T cell activation and intracellular staining.....	33
3.7 Microglia FACS sorting	35
3.7.1 Tissue isolation and cell pellet suspension preparation	35
3.7.2 Cell staining	35
3.7.3 FACS measurement and sorting.....	36
3.8 RNA preparation and bulk-RNA sequencing	36
3.8.1 RNA extraction	36
3.8.2 RNA quality control by Agilent RNA 6000 Pico Kit.....	36
3.8.3 Bulk-RNA sequencing	37
3.9 Statistical analysis	38
4. Results	39
4.1 Induction of immune tolerance by peripheral injections of LPS.....	39
4.1.1 Bodyweight changes indicate the induction of immune tolerance	39
4.1.2 Acute exposure to LPS does not alter the psychoneurological function of mice	40
4.2 Immune tolerance in microglia does not affect the stroke-induced immune landscape in the CNS post-stroke.....	44
4.2.1 The acute inflammatory reaction remains unaffected after induction of microglial immune tolerance	44
4.2.2 Meningeal immunity remains unchanged after induction of microglial	

immune tolerance.....	47
4.2.3 T cells secrete similar proinflammatory cytokines after induction of immune tolerance.....	51
4.3 Exploration of immune tolerance induction on long-term outcome post-stroke	52
4.3.1 Stroke lesion size decreases after inductions of immune tolerance in microglia	52
4.3.2 Immune tolerance modified behavior outcome post-stroke.....	54
4.3.2.1 Immune tolerance improved the locomotor functions in open field test 14 days post-ischemia	54
4.3.2.2 Microglial immune tolerance does not improve short-term memory....	56
4.3.3 Immune landscape 14 days post-stroke showed no changes in immune tolerance-induced mice	57
4.3.3.1 Cell counts and UMAP distribution showed similarities between PBS and LPS group in the CNS	57
4.3.3.2 Cell counts and subtypes are comparable between PBS and LPS groups in meninges.....	58
4.3.3.3 T cell functions are similar on the respect of pro-inflammatory cytokine releasing.....	59
4.4 Exploration of microglia gene expression difference between cortex and subcortical regions.....	61
4.4.1 Quality control and sample distribution.....	61
4.4.2 Differentially expressed genes between the PBS and LPS group are only found in subcortical microglia	62
4.4.3 Downstream analyses of Bulk-RNA sequencing data indicated pathways involved in immune tolerance during stroke recovery	63
5. Discussion.....	65
5.1 Continuous peripheral LPS injections are able to induce immune tolerance in mice	65
5.2 Immune tolerance is able to alleviate stroke lesion size during the early but not	

the late-stage post-stroke	67
5.3 Immune tolerance did not alter the immune landscapes after stroke onset.....	68
5.4 Immune tolerance alters anxiety-like behavior and locomotor function at different stages but does not influence short-term spatial memory function	71
5.5 Differentially expressed genes and pathways involved in microglia-mediated immune tolerance	72
5.6 Limitations of the study.....	76
6. Summary	77
7. Bibliography	80
8. Acknowledgements	91
9. Resume	93
10. Eidesstattliche Erklärung	94

1. Aims of the study

Acute ischemic stroke poses a significant global health challenge, characterized by a high incidence, a high morbidity and high mortality rates (Guzik and Bushnell, 2017, Saini et al., 2021). Despite the advanced diagnostic and treatment methods, a substantial number of people are still suffering from the disease itself as well as its sequela. Hence understanding the inflammatory mechanisms that contribute to stroke severity and exploit that knowledge to alleviate the outcome is very important.

Microglia are a group of brain-residential immune cells that play pivotal roles in stroke onset, progression and recovery (Prinz et al., 2019, Prinz et al., 2021). They exist in a great variety of subtypes that strongly depend on environmental disease-specific signals (Paolicelli et al., 2022, Pannell et al., 2016). Microglia participate in innate immunity, but also assist acquired immunity during stroke (Kanazawa et al., 2017).

Similar to acquired immunity, the innate immune system can gain a memory function after certain stimuli without the development of antigen-specific memory. Immune training and tolerance are two induced states of immunological memory that can be acquired by microglia through induced modifications in the epigenetic profile (Lin et al., 2023). In particular, it is proven that immune tolerance of microglia obtains an anti-inflammatory function and improves the outcome of some CNS diseases (Wendeln et al., 2018) whereas immune training aggravates neurological pathology. However, in stroke the impact of microglial immune tolerance on the acute inflammatory response is not fully understood.

We hypothesized that the induction of immune tolerance prior to stroke onset is able to alleviate the severity of stroke, and supports the regenerative capacity of the CNS post-stroke. In order to test this hypothesis, the aims of the study are as followed: (i) to investigate potential global immune landscape changes during acute und subacute phase post-stroke after induction of microglial immune tolerance; (ii) to explore the regenerative capacity of microglial innate immune tolerance during subacute phase of stroke; and (iii) to explore the change of microglia gene expression levels following immune tolerance during stroke.

2. Introduction

2.1 Acute ischemic stroke is still a noteworthy topic

Acute ischemic stroke is a global health issue due to its high incidence, high morbidity and high mortality (Guzik and Bushnell, 2017, Saini et al., 2021). According to the data from America Stroke Association, about 795,000 people suffer from new or recurrent stroke every year and 87% of them are ischemic stroke. On average, every 197 seconds, someone died from a stroke (Tsao et al., 2023). It is predicted that stroke mortality will increase by 50% from 2020 to 2050 (Feigin et al., 2023). The heavy burden caused by stroke requires fundamental scientific progress in stroke prevention, treatment, and rehabilitation.

Clinically, the mechanisms leading to stroke are classified into several categories: large artery atherosclerosis (LAA), cardioembolism, small vessel occlusion, stroke of other determined etiology, and stroke of undetermined etiology. Among all, LAA and cardioembolism are the major causes of stroke (Jr. et al., 1993). These stroke etiologies are prominent for the insufficiency of large artery blood supply as well as the swift onset, making them extremely dependent on fast recanalization treatment (Zotter et al., 2021). However, according to the strict limitation of current treatment window, only a small proportion of stroke patients is able to undergo on-time treatment. In addition to the poor functional outcome rate, still a large amount of people is suffering from stroke and its subsequent sequela such as physiological and psychological impairments in daily life (Marsh and Keyrouz, 2010, Feil et al., 2020).

The symptoms of stroke are various, including movement impairment, speech changes, visual changes, and mental disorders (Helboe et al., 2023, Handley et al., 2009). Such symptoms can last for a long period and can aggravate. For example, stroke with hippocampus involvement might lead to a memory impairment or cognitive disorder (Szabo, 2014). Most of the stroke symptoms will have a long-lasting influence on patients and further impede their independent living ability. Hence the burdens on care-givers are unignorable (Hu et al., 2018, Kazemi et al., 2021).

2.2 Mechanisms of acute ischemic stroke

Pathological reactions are triggered in central nervous system (CNS) directly after the onset of CNS ischemia. Thereby, the acute ischemic injury and the subsequent reperfusion-associated inflammation are the major parts contributing to tissue damaging processes (Hossmann, 2012).

Initial artery occlusion leads to an insufficiency of oxygen and energy supply, directly causing neuronal dysfunction. The shortage of oxygen and energy results in ionic pump disruptions, including a disturbance of intracellular sodium ion (Na^+), potassium ion (K^+) and calcium ion (Ca^{2+}) concentration. The membrane depolarizes and leads to an increased release of excitatory neurotransmitter glutamate (Radak et al., 2017) resulting in excitotoxicity. Higher level of glutamate reversely causes overloaded Ca^{2+} influx (Chen et al., 2014, Xu et al., 2023). This ionic impairment eventually activates necrotic and apoptosis pathway of neurons (Azad et al., 2016).

The excessive Ca^{2+} accumulation further impairs mitochondria function by excessive calcium uptake in mitochondria. Such ion imbalance results in the opening of mitochondrial permeability transitional pore, which allows mitochondria swelling and outer membrane lysis, leading to the leakage of cytochrome C. Release of cytochrome C in mitochondria initiates caspase-dependent cellular death pathways (Jemmerson et al., 2005). Free radicals, generated mainly in anaerobic environment in mitochondria, also contribute to CNS damage. Accumulated or accelerated produced reactive oxygen species (ROS) induce modifications on protein, lipid, and DNA, ultimately leading to cell dysfunction or apoptosis (Qian et al., 2024, Karsy et al., 2017).

Following reperfusion, ROS release further contributes to ongoing tissue damage as nicotinamide dinucleotide phosphate oxidase, an enzyme complex in mitochondria, donates electrons to oxygen and produces more ROS after reperfusion (Kumar Saini and Singh, 2024). The blood-brain-barrier (BBB), which loses the barrier function during ischemic insults, can also be harmed by reperfusion through increased vasogenic edema and angiogenesis. The injury of BBB can lead to worse complications, such as hemorrhagic transformation (Lin et al., 2016).

2.3 Experimental stroke modelling by tMCAO – an ideal but not perfect model

Rodents, especially mice and rats are mostly applied for stroke modelling. It is because of the similarity of the central nervous system (CNS) structure and anatomy among them and human beings. The cellular mechanisms of stroke based on research in rodent disease models is comparatively well-established (Howells et al., 2010). To mimic the ischemic-reperfusion process of stroke, transient middle cerebral artery occlusion model (tMCAO) model is widely applied in experimental research.

To perform tMCAO, a filament is inserted into internal carotid artery (ICA) until the MCA. The filament is kept in the MCA for certain time period and removed afterwards to mimic the process of ischemic-reperfusion (Longa et al., 1989). The fast reperfusion after tMCAO treatment can simulate the successful recanalization in clinic, through intravenous thrombolysis and mechanical thrombectomy. TMCAO is one of the standard procedures to study stroke because of its privilege to study reperfusion mechanisms and associated inflammatory cell infiltration (Pan et al., 2007, Nour et al., 2013).

The tMCAO model allows the reperfusion of brain blood flow in the middle cerebral artery. Such fully recanalization differs from human stroke because it only obtains a small proportion in clinic (Mcbride and Zhang, 2017). This drawback has already been mentioned in previous stroke studies, and the researchers suggest permanent MCAO (pMCAO), a stroke model without allowing the reperfusion at last, as an alternative ((Stair), 1999, Hossmann, 2012). However, pMCAO is also doubted with its disturbance of intracranial environment due to its surgical invasive nature, leaving it an imperfect model as well (Crupi et al., 2018).

The diversity of stroke mechanisms indicate that no single model can represent all variables known to affect human stroke. Choosing a suitable disease model based on the research question is the best method to reach the study goal (Howells et al., 2010).

2.4 Immune activation during stroke pathology

Stressed and dying neurons during acute ischemia/reperfusion release danger-

associated molecular pattern (DAMPs), such as purines (i.e., adenosine triphosphate, ATP) or heat shock-proteins (HSP), which activate and attract a variety of immune cells including resident glial cells (astrocytes, microglia, oligodendrocytes, etc.), peripheral immune cells such as lymphocytes, granulocytes or monocytes (Campbell et al., 2019). The cells play either alleviation or deterioration roles during stroke process. In the following introduction, several important immune cells involved in stroke process will be described.

2.4.1 Microglia play a vital role in stroke

Microglia are the primary brain-resident immune cells and contribute to the brain development, homeostasis maintenance, immune reaction, and disease onset and recovery (Prinz et al., 2019). They obtain a ramified morphology with highly branched processes during homeostatic stage. However, when microglia sense changes in the physiologic microenvironment, they become activated and transform into an amoeboid or spheric shape and migrate to the site of the lesion (Lier et al., 2021, Spiteri et al., 2022). Microglia also interact with other cells of the CNS, including neurons. They participate in engulfment of synapses and constantly signal via the CX3CR1-CX3CL1 axis with neurons (Lenz and Nelson, 2018). These immune surveillance processes guarantee a healthy environment for neuron development and functioning (Borst et al., 2021). The impairment of microglia function is related with CNS diseases of neuroinflammatory, neurodegenerative or demyelinating origin (Chen and Holtzman, 2022, Hughes et al., 2023).

As resident immune cells of the brain, microglia respond to not only the acute phase but during the recovery phase of stroke. They are the first cells reacting to stroke onset by sensing damage associated motif patterns (DAMPs) and migrating to the site of the lesion where they release pro-inflammatory mediators such as cytokines or ROS (Wicks et al., 2022). Besides the release of pro-inflammatory cytokines, microglia are also involved in cell debris engulfment and antigen presenting functions (Kanazawa et al., 2017), which contribute to the resolution of the inflammatory environment. A variety of studies classified activated microglia into pro-inflammatory M1 microglia and anti-

inflammatory M2 microglia (Zheng et al., 2019). Such simple categorizing can in fact simplify the problem, but ignores the underlying complexity of functions (Paolicelli et al., 2022, Var et al., 2021). Increasing studies based on sequencing technique reveal a strong heterogeneity of microglia populations. For instance, a study focused on microglia activation during traumatic brain injury in both wild type mice and *Ccr2*^{-/-} mice. Single cell RNA-sequencing results reveal that in *Ccr2* deficiency condition, microglia activation is influenced by infiltrating monocytes and macrophages. Microglia tend to promote a type I interferon response with reduced *Irf7* gene expression (Somebang et al., 2021). More studies are warranted for more detailed microglia subpopulation research in CNS diseases.

2.4.2 Infiltrating peripheral immune cells and their functions during stroke

Peripheral immune cells are recruited after the activation of the residential immune cells and release of inflammatory mediators such as cytokines and chemokines. They migrate to the brain and contribute tissue damage aggravation. The study from Gelderblom et al. analyzed the temporal dynamics of residential cell activation as well as circulatory immune cell infiltration, and reflects the highly controlled immune-cell activation during stroke in the CNS (**Figure 1**) (Gelderblom et al., 2009). After microglia activation, macrophages, neutrophils, and myeloid dendritic cells (DCs) rapidly react to the ischemia. They activate and migrate toward the CNS, and their amounts reach the peak within 3 days post-stroke. Lymphocytes, nature killer (NK) T cells and non-myeloid DCs aggregate slower in ischemic tissue, and exhibit moderate quantitative change during the whole acute processes. NK cells, however, show less sensitive to the stroke insult and remain generally unchanged in amount after stroke.

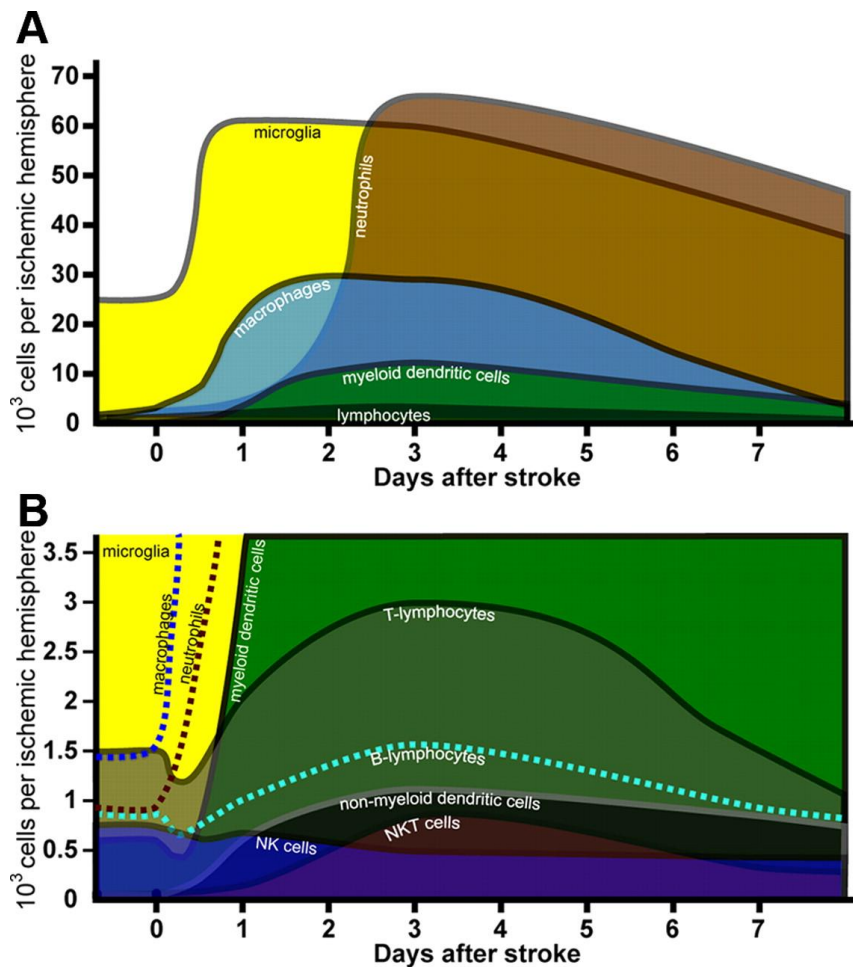


Figure 1. Schematics of temporal dynamics of post-stroke inflammation (Gelderblom et al., 2009). After microglia activation, macrophages, neutrophils, and myeloid DCs rapidly react to the ischemia. They activate and migrate toward the CNS, and their amounts reach the peak within 3 days post-stroke. Lymphocytes, NKT cells and non-myeloid DCs aggregate slower in ischemic tissue, and exhibit moderate quantitative change during the whole acute processes. NK cells, however, show less sensitive to the stroke insult and remain generally unchanged in amount after stroke. A: data obtained from sham conditions, 12 hours, 1, 3, 7 days postreperfusion; B: magnification of lower part of A.

Myeloid cells

The majority of myeloid cells comprise granulocytes, DC, macrophages and monocytes. Among them, neutrophils as well as monocyte are highly related with stroke.

Neutrophils proliferate and infiltrate into the brain parenchyma as soon as they receive chemokine-derived signals such as CXCL-1 (Gelderblom et al., 2012). Neutrophils can be detected adhering to the luminal surface of microvessels as early as 15 hours after stroke onset. The peak infiltrate into brain parenchyma happens 24-48 hours after stroke onset. Neutrophil aggregation can occlude capillary microvessels, leading to a ‘no-

reflow' phenomenon (Easton, 2013). Too much neutrophils in circulation also disturbs the consistency of BBB and impedes post-stroke repairment (Denorme et al., 2021). Controlling the number or modulating the functions of neutrophils is associated with better outcomes after AIS. Kang et al. showed that inhibiting the formation of neutrophil extracellular traps (NETs) can sufficiently increase neovascularization and vascular repair, as well as improve functional recovery (Kang et al., 2020). Yan et al. found that prophylactic anti-Ly6G antibody treatment in mice, which specifically blocks neutrophils, is able to reduce neutrophil accumulation as well as ameliorate stroke outcome in subacute phase (Yan et al., 2023). Gelderblom et al. also discovered the protective function of IL-17 neutralization. IL-17A produced by $\gamma\delta$ T cells recruits circulation neutrophils. The inhibition of such infiltration is probable via IL-17A neutralization by anti-IL-17A, which effectively reduced stroke lesion size and improved stroke outcome. (Gelderblom et al., 2012).

Monocytes are mononuclear leukocytes in the peripheral circulation. They sense pathological stimuli with chemokine and pathogen recognition receptors (PRRs) and react by performing phagocytosis, releasing cytokines or producing ROS or reactive nitrogen species (RNS) (Garcia-Culebras et al., 2018). Monocytes can further polarize into macrophages of different subpopulations and contribute to both damage and regeneration in areas close to the stroke lesion. Beuker et al. found a population of stroke-associated myeloid cells, mainly consisting of microglia, macrophages and monocytes, by single cell RNA sequencing (scRNAseq). These cells are characterized by enhanced lipid metabolism and phagocytosis. Blocking the markers of these cells alleviates injury and improves outcome (Beuker et al., 2022). Some clinical studies also found that excessive monocyte in circulation can predict poor stroke outcome. Parameters such as monocyte-to-leukocyte ratio and monocyte-to-high-density-lipoprotein ratio are related to poor outcome (Gong et al., 2021, Liu et al., 2020). However, similar to microglia, the polarization of monocytes also involves an anti-inflammatory subtype, which is named as M2 phenotype. They protect the CNS by secreting remodeling factors and anti-inflammatory cytokines in order to promote

protective functions, axonal outgrowth, and angiogenesis (Kanazawa et al., 2017). Surprisingly, in a mouse study, a Ly6C^{hi} monocyte subtype was observed to be neuroprotective. The administration of Ccr2 antagonist led to stroke deterioration and M2 macrophages decreasing, indicating an anti-inflammatory function of certain monocyte subtypes (Chu et al., 2015).

As a kind of important antigen-presenting cell (APC), DCs are necessary in the communication between innate and acquired immunity. However, DCs are less mentioned in stroke immunity due to their limited quantity in healthy brain parenchyma (Jian et al., 2019). Due to the antigen-presenting function of CNS residential cells, DCs were regarded as not existent in CNS for a long period. However, a study found that peripheral DCs only occupied less than 5% DCs in healthy brain but raised up to around 40% in stroked hemisphere. It proved the existence of residential DCs and a strong infiltration of circulatory DCs during stroke (Felger et al., 2010). Further studies about the functions of different DC subpopulations are still needed.

Lymphocytes and lymphoid cells

Lymphocytes arrive later in stroke stage and reach the peak of infiltration at around 3-7 days after stroke onset (Gelderblom et al., 2009). Especially, T cells and B cells further accumulate for 2-7 weeks after stroke (Zbesko et al., 2021). $\alpha\beta$ T cells mainly act as pro-inflammatory cells. CD8⁺ T cells cause direct cell damage by apoptosis induction as well as perforin releasing. CD4⁺ T helper (Th) 1 cells amplify the inflammatory reaction by increasing vascular permeability, promoting activation of neutrophils, microglia, and brain endothelial cells. Depletion of T cells is able to alleviate stroke severity (Arumugam et al., 2005). Moreover, $\gamma\delta$ T cells with their IL-17 producing function also cause damage on the penumbra region by initiating the infiltration of neutrophils into the brain parenchyma (Gelderblom et al., 2012).

However, not all T cell subtypes are pro-inflammatory. Some T cells also obtain the ability of controlling inflammation and damage. CD4⁺ Th2 cells, are capable of suppressing Th1 cells by anti-inflammatory cytokines including interleukin-10 (IL-10), transform growth factor-1 (TGF-1) (Arumugam et al., 2005). Recently, increasing

studies focus on regulatory lymphocytes (Tregs and Bregs), especially CD4⁺CD25⁺Foxp3⁺Tregs. Treg can be detected 14 to 30 days post-stroke. The depletion of Treg in experimental stroke area leads to stroke deterioration, but the therapeutic enhancement of them improves stroke outcome. The mechanism is under investigation. Possible mechanisms include the production of anti-inflammatory cytokines (such as IL-10, TGF- β), the suppression of reactive T cell proliferation, reduction of microglia/monocyte activation or induction of microglia/monocyte polarizing toward anti-inflammatory phenotypes (Liesz et al., 2015).

B cells are regarded less involved in stroke previously, even though they exist from early stage of stroke onset to several weeks after stroke. B cells are related to long-term cognitive impairment (Malone et al., 2023). A study applied anti-CD20 antibody in order to deplete circulation B cells. The results showed that the treated mice did not show cognitive impairment 7-week post-stroke but the controlled mice did. It proved the role of delayed cognitive influence of B cells (Doyle et al., 2015).

Nature killer (NK) cells are a kind of innate lymphoid cells that are involved during stroke. It is reported that NK cells are related with post-stroke inflammation, immunodepression and infection (Rolfes et al., 2022). A bioinformatic-based study found that NK cells were positively correlated with stroke, and pro-inflammatory genes such as *IL1B*, *IL1R1* were observed upregulated in NK cells during stroke (Feng et al., 2022). However, limited to the quantity during stroke, NK cells are rarely studied as a potent treatment or prophylactic target. More studies are warranted for further clarifying the function of NK cells during stroke.

2.5 Mechanisms of innate immunity

2.5.1 Innate immunity introduction

Innate immunity shares the same molecular pathways in the majority of multicellular organisms. By sensing pathogen-associated molecule patterns (PAMPs) and DAMPs such as LPS and bacteria CpG DNA, innate immunity forms the first-line defense to infections and pathological insults (Janeway and Medzhitov, 2002) and protects against

a large spectrum of pathogens. Innate immunity can be mediated by tissue-specific macrophages (including microglia), monocytes, Langerhans cells, dendritic cells, tissue-associated lymphocytes including NK cells and $\gamma\delta$ T cells (Hackett, 2003).

The innate immune system detects PAMPs via pattern-associated molecular patterns (PRRs), including Toll-like receptors (TLRs), nucleotide-binding oligomerization domain (NOD)-like receptors, retinoic acid-inducible gene I (RIG-I)-like receptors, and C-type lectin receptors (Stambas et al., 2020). After recognition, innate immune cells become activated and initiate the removal of invading pathogens, or express co-stimulatory molecules to subsequently activate the acquired immune system (Janeway and Medzhitov, 2002).

In non-infectious inflammations, innate immunity also plays important roles. In stroke, DAMPs from dying or dead neurons bind to TLRs and scavenger receptors on microglia. The subsequent induction of the neutrophil recruitment further enhances the process of tissue damage. Lymphocytes are activated by either antigen presenting innate immune cells or by direct signals leaked from the CNS (Mayer-Barber and Barber, 2015).

2.5.2 Innate immune memory

As acquired immunity, innate immunity can also obtain ‘memory’ functions. This means that innate immune cells exhibit adaptive characteristics and respond with an adjusted response towards a reinfection including a non-specific defense on similar infections. This process lacks adaptive immune system and fully completes by innate-like immune system (Netea et al., 2020), which is termed as ‘innate immune memory’. Innate immune memory probably lasts for more than 3 months in monocytes (**Figure 2**). However, a recent study showed that hematopoietic cells from COVID-19 infected individual can keep the epigenetic memory up to 1 year, indicating a long-lasting functional effect after first activation (Cheong et al., 2023).

In difference from the gene rearrangement of lymphocytes, innate immune memory is characterized by its long-term functional reprogramming of innate immune cells, based on epigenetic modifications and metabolic reprogramming (**Figure 2**).

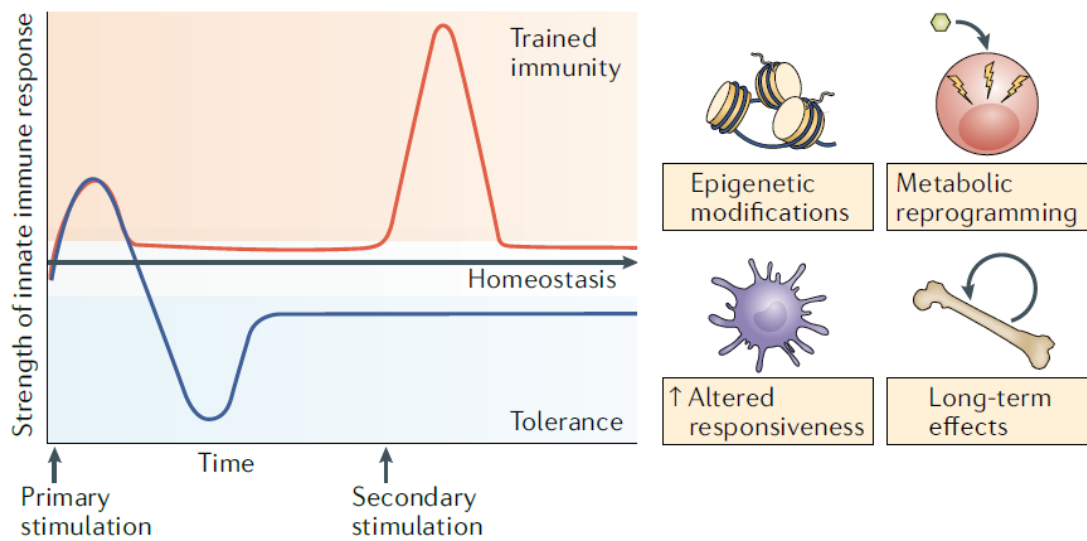


Figure 2. Trained immunity and tolerance: two opposite functional programs of innate immunity (Netea et al., 2020). Infections or sterile tissue triggers induce inflammation and the activation of immune effector mechanisms. In trained immunity, innate immunity remains low-level activated after primary stimulation. The secondary stimulation triggers stronger and faster reaction. Immune tolerance refers to the hypoactivity of innate immunity after primary stimulation. The reaction keeps under homeostatic level and becomes inertia to secondary stimulation. During the altered responsiveness, epigenetic modification, along with metabolic reprogramming characterize the innate immune memory. The effects are usually long-lasting, for 3 months to 1 years.

Epigenetic modifications are mainly mediated through chemical modifications of the DNA and histone subunits by acetylation and methylation processes (Cruz-Carrillo and Camacho-Morales, 2021). Detailed modification depends on the primary stimuli to induce innate immune memory. In general, the activation of innate immune cells can leave an ‘epigenetic scar’ at the level of stimulated genes, changing their long-term responsiveness towards a secondary new stimulus (**Figure 2**).

The cellular metabolism is closely linked with epigenetic modifications. Increasing energy demands of innate immune cells occurs after the sensing of the inflammatory insult. The changes directly alter the energy metabolic forms as well as the metabolite by-products, which are known regulators (such as methyl-transferases) of the epigenetic landscapes (Ochando et al., 2023). Thus, metabolic adjustments can modulate the accessibility of chromatin, leading to the modification gene expression and in turn cellular function.

A process of innate immune memory formation is called ‘immune training’. It refers to the process that the innate immune system reacts with an enhanced immune response when a secondary stimulus is presented (**Figure 2**). This idea has been applied in vaccine designs. For instance, Bacillus Calmette–Guérin (BCG) vaccine is a widely applied vaccine for neonatal tuberculosis protection. It serves as a PAMP, activates the innate immune system via TLR and causes further signals of immune reactions. It is proven that the BCG vaccine is subsequently able to defend unspecific respiratory infection, malaria, yellow fever, and bladder cancer by the induction of immune training effects (Divangahi et al., 2021). BCG can also manipulate transcriptional and functional profiles of hematopoietic stem and progenitor cells (HSPCs) and enhance myelopoiesis. Such influence on immune progenitor cells can keep the epigenetic characters and hence elongate function during cell proliferation (Geckin et al., 2022, Han et al., 2020). Besides immune training, the induction of an immune tolerance condition could also be induced by a primary immune stimulus, which in turn dampens the immune reaction of the host upon a secondary inflammatory insult (**Figure 2**). Immune tolerance may be able to prevent certain diseases caused by excessive immune system activation. Organ transplantation patients are always required to induce immune tolerance in order to get rid of rejections (Stolp et al., 2019). Moreover, immune tolerance also has the potential of treating diseases. Zhang et al. discovered that the immune training of liver Kupffer cells leads to a higher resistance toward hepatic ischemic-reperfusion injury on mouse model. With preoperative exercise therapy, mice experienced less inflammation during disease (Zhang et al., 2021b).

2.6 Peripheral administration of LPS can induce innate immune response in rodents in the brain

LPS is a cytotoxic molecule mainly produced by Gram negative bacteria. It is one of the main components of the bacterial outer membrane. LPS is composed of lipid A, core polysaccharide, and O-antigen repeats. The toxicity is majorly on lipid A, and mechanisms vary from different microorganisms (Wang and Quinn, 2010). Recognized

by TLR4, it can activate the innate immune system and subsequently initiate an immune response (Longa et al., 1989). Studies in mice identified the prophylactic function of LPS pretreatment on endotoxin rechallenging, indicating the occurrence of an induced immune tolerance mechanism (West and Heagy, 2002).

Apart from the immune cells in the circulation, peripheral LPS administration can also activate microglia as the primary innate immune effector cells of the CNS and induce innate immune memory (Ahmed et al., 2000). In rostral ventrolateral medulla (RVLM) inflammation model, LPS was infused intraperitoneally for 14 days and induced a significant increase of central IL-1 β , IL-6 and TNF- α level as well as microglia activation with higher ROS production. These signs indicate a successful induction CNS innate immune response with merely peripheral LPS administration (Wu et al., 2012). Additionally, Schaafsma et al. found that in microglia and macrophages, LPS preconditioning is accompanied by a reduction in active histone modifications in the promoters of the IL-1 β and TNF- α genes, as well as an increase of repressive histone modification on IL-1 β promoter indicating epigenetic reprogramming (Schaafsma et al., 2015).

Moreover, another study proved the immune memory induction by histological analysis. Mice were infected with *Salmonella typhimurium*, which cause diseases by LPS. These mice and other non-infectious mice were then intracerebrally injected with LPS 4 weeks after the primary infection. Compared to non-infectious mice, these mice exhibit higher level of microglia activation marker on staining, indicating a trained immunity in CNS (Püntener et al., 2012).

Interestingly, LPS can induce different forms of innate immune memory according to the exposure methods. In the research from Sousa et al., microglia originated from peripheral LPS-injected mice expressed lower level of homeostatic and anti-inflammatory genes and higher level of pro-inflammatory genes than sham mice (Sousa et al., 2018). However, peripheral LPS administration can also induce immune tolerance. Norden et al. found that 4 repeated injections of 0.66mg/kg LPS led to induction of immune tolerance in microglia. In detail, the pro-inflammatory cytokine

IL-6 was no longer elevated 24 hours after the 4th LPS injection. Moreover, microglia after repeated LPS injections exhibited lower inflammatory cytokine mRNA level and higher YM-1 level, indicating the microglia shift towards an anti-inflammatory subtype (Norden et al., 2016).

2.7 Microglia-induced trained immunity shapes CNS diseases

Acute LPS exposure leads to long-lasting functional reprogramming of microglia in CNS. This means that microglia induced with trained immunity may respond differently to neurological disease. Understanding the underlying mechanism is beneficial to identify new targets and explore new treatment possibilities.

Wendeln et al. analyzed the relationship between microglia immune training and Alzheimer's disease (AD). They found that immune training by LPS injection led to increased cerebral β -amyloidosis, which exacerbate AD. However, LPS injection-induced immune tolerance alleviated the condition of β -amyloidosis in the brain parenchyma (Wendeln et al., 2018). These findings identified microglia trained immunity is important in CNS neuropathology. Thus, inducing immune tolerance on microglia could be a possible way to AD alleviation and recovery.

Moreover, microglia trained immunity is also related with brain ischemia. Ischemic preconditioning (IPC) refers to the protective effect of brief ischemia induction. Such mild treatment can lead to an alleviation to a prolonged ischemic event. A mouse study found the protective effect of IPC on white matter during ischemia. It included the activation of TLR4 and type 1 interferon receptor (IFNAR1), proving the activation of innate immunity. By microglia-targeted IFNAR1 knockdown, the experiment showed the specific involvement of microglia (Hamner et al., 2015). The process caused epigenetic modifications, proving the existence of trained immunity (McDonough and Weinstein, 2020).

The abovementioned studies show that inducing immune memory has a long-lasting protective effect in neurological disease. Especially, a preconditioning treatment to induce microglia immune tolerance may be a therapeutic approach to alleviate disease

pathology.

This study aims at exploring the potential protective effect of microglia immune tolerance via peripheral LPS injection on stroke pathology.

3. Material and methods

3.1 Design of the study

3.1.1 Guideline and animal protocol

Animal experiments were all conducted under the regulation of the national and animal facility of the University Medical Center Hamburg-Eppendorf. All experiments were approved by the local animal care committee (Behörde für Lebensmittelsicherheit und Veterinärwesen, project number: TVA 28/22).

3.1.2 Mouse information

10-12 weeks old male C57/BL6 wildtype mice (internal mouse line number: #6060 and #7070) were applied in this study. The mice were bought from Charles River Laboratories (Germany), and maintained at the animal facility of University Medical Center Hamburg-Eppendorf. Mice were identified by earmarks.

3.1.3 Time schedule of short-term study

The short-term study included a baseline experiment, a day-1 experiment and day-3 experiment. Mice in each experiment were assigned into PBS group and LPS group randomly. The time schedule is shown in **Figure 3**.

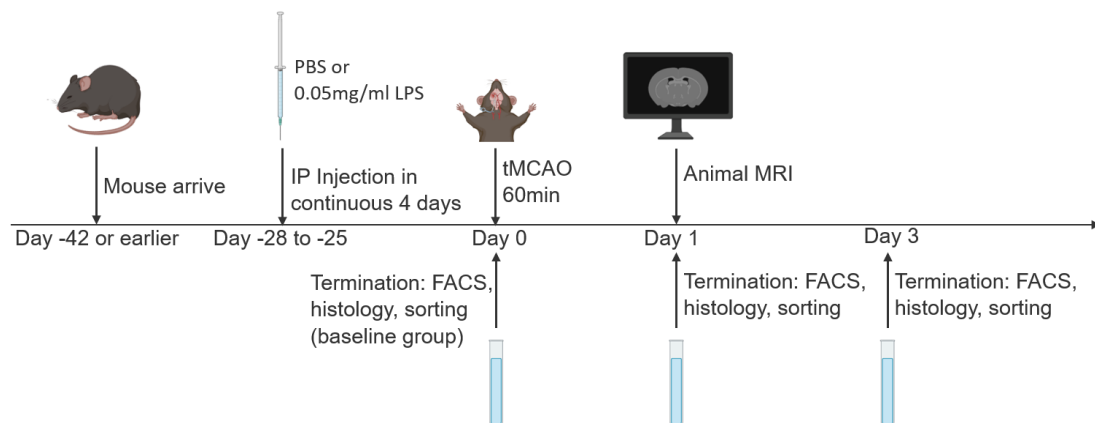


Figure 3. Time schedule of short-term study. Abbreviations: PBS, phosphate-buffered saline; LPS: lipopolysaccharide; IP: intraperitoneal; tMCAO, temporary middle cerebral artery occlusion; FACS: fluorescence-activated cell sorting; MRI, magnetic resonance imaging.

Mice were housed in the animal facility for at least 2 weeks until first injection (day -42 or earlier). The injections were performed in continuous 4 days (day -28 to day -25). Bodyweight of every mouse was recorded on each injection day and every 7th day after

the week of injection. The mice in baseline group were sacrificed on day 0. Other mice received additional tMCAO surgery. Animal magnetic resonance imaging (MRI) was performed on all mice to identify the ischemic lesion and lesion size calculation was performed 24 hours after tMCAO (day 1). Mice were sacrificed on 1 day (day-1 experiment) or 3 days (day-3 experiment) after stroke. The isolated tissues from the sacrificed mice were applied for FACS measurement, histology staining or microglia sorting.

3.1.4 Time schedule of long-term study

To further validate the long-term changes of mice after stroke, a long-term experiment was applied. The schedule is shown in **Figure 4**.

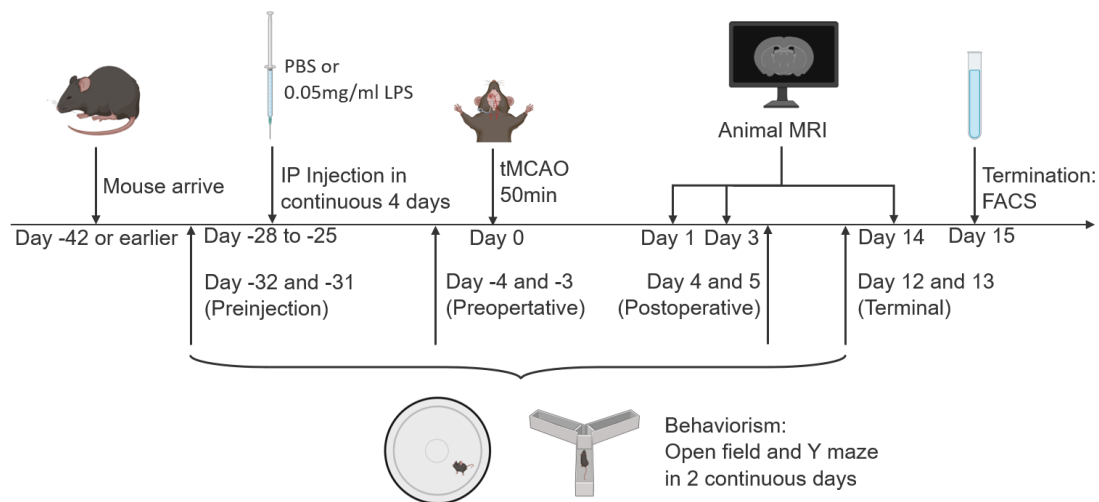


Figure 4. Time schedule of long-term study. Abbreviations: PBS, phosphate-buffered saline; LPS: lipopolysaccharide; IP: intraperitoneal; tMCAO, temporary middle cerebral artery occlusion; FACS: fluorescence-activated cell sorting; MRI, magnetic resonance imaging.

The long-term study shared the same schedule with the short-term study on mouse housing, injection and stroke modelling. The MRI was performed on 1 day, 3 days and 14 days after stroke modelling to reflect the stroke or recovery condition of baseline, acute stage and chronic stage. To further explore the behavior changes, open field (OF) tests and Y-maze (YM) tests were performed at the 4 indicated time points: preinjection stage (day -32 and -31), preoperative stage (day -4 and -3), postoperative stage (day 4 and day 5), and terminal stage (day 12 and day 13). The mice were sacrificed on the 15th or 16th day after stroke for FACS measurement.

3.2 Immune tolerance induction

The way of immune tolerance induction was according to previous studies (Wendeln et al., 2018, Neher and Cunningham, 2019). After at least 2 weeks of acclimatization, mice were injected intraperitoneally with PBS (Gibco, #14190-144) or LPS solution according to the previous grouping.

Lipopolysaccharides from *Salmonella enterica* serotype typhimurium powder (Sigma, L6511-10MG) was first dissolved in PBS solution as stock solution (1 mg/mL). The stock solution was sterile by filtered (rotilabo-Spritzenfilter PVDF steril, pore size 0.45 μm , outer diameter 33 mm, Roth, P667.1) and stored at 4°C. Before every injection, LPS was further diluted into 50 $\mu\text{g}/\text{ml}$ by PBS solution. The injected LPS dose was 500 μg per kg bodyweight.

The bodyweights were recorded on each injection day and every 7th day in the following weeks before stroke modelling. A successful induction was described as a drastic drop in bodyweight after the first LPS injection and a gradual rise thereafter.

3.3 tMCAO stroke modelling

tMCAO stroke modelling was performed by experienced technicians blinded to group information. The protocol was modified from previous studies (Gelderblom et al., 2012, Gelderblom et al., 2023). Mice were anesthetized with isoflurane (1% to 2% v/v oxygen). Buprenorphine (0.1ml) was injected intraperitoneally for analgesia. A 1-centimeter vertical cut was made on the ventral skin of the neck. The muscles and connective tissues were then blunt separated and the common carotid artery (CCA) was exposed. After isolating the carotid sheath, the external carotid artery (ECA) was ligated and a tiny cut was made on the proximal end of ECA. A filament was then inserted from the cutting to CCA. The ECA was then isolated. The filament was adjusted into internal carotid artery (ICA) and further inserted till the resistance getting stronger (reached in middle cerebral artery, MCA). The blood flow of MCA was blocked by the filament, and the mouse was placed on a heating pad for a certain period. Durations of blood

vessel occlusion vary in different experiments and are specified in different result sections. The filament was removed afterwards for reperfusion. Mice were placed on a heating pad (37°C) for post-operative recovery. Wet food and water containing 0.12 mg/ml sucrose and 1 mg/ml tramadol were regularly added into the cages. The caregivers visited and cared the mice for at least twice a day at first 3 days, and at least once a day afterwards. Sterofundin and buprenorphine were administered when malnutrition or pain were observed. The bodyweights were recorded at every caring time.

3.4 MRI quantification of mouse stroke lesion

MRI was applied for stroke lesion quantification and set on the indicated time point as shown in the study design. Mice were anesthetized with isoflurane (3% v/v oxygen for anesthesia induction and 0.8% to 1% v/v oxygen for scanning) and located on the machine. Their head was fixed with a cap. The MRI test included localization, T2 sequencing scanning, and DWI sequencing scanning. After scanning, the mice were put back to the previous cage and resuscitated on the heating pad (37°C) till waking up.

The results of T2 sequences were analyzed by Image J (1.53t, USA). 19 continuous slides in T2 sequence were chosen. Size of ipsilateral hemisphere, contralateral hemisphere, and lesion area were measured according to the mouse brain anatomy (Xiong et al., 2017). For the MRI measured on day 1 and day 3, infarct volume is calculated with edema correction. The formula was as followed:

$$\text{Infarct volume} = \text{calculated infarct volume} * \frac{\text{total area of contralateral hemisphere}}{\text{total area of ipsilateral hemisphere}}$$

For the MRI measured on day 14, atrophy volume was determined by a healthy tissue preserved rate, which is calculated as followed:

$$\text{healthy tissue preserved rate} = \frac{\text{total area of ipsilateral hemisphere}}{\text{total area of contralateral hemisphere}} * 100\%$$

The tissue selection method can be reflected on **Figure 5**.

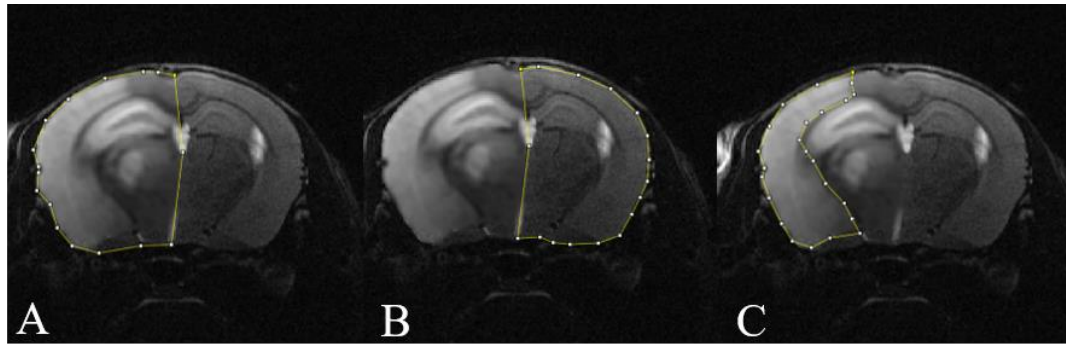


Figure 5. Method of tissue selection on animal MRI. A: selection method of ipsilateral hemisphere. The middle line was set and the whole hemisphere was included in a closed shape; B: selection method of contralateral hemisphere. The middle line was kept the same with the ipsilateral hemisphere. The contralateral hemisphere was included in a closed shape with the reference of the middle line; C: selection method of stroked tissue. The region higher signal was figured out. The posterior cerebral artery supply region, including brainstem and hippocampus, were avoided. Abbreviation: MRI, magnetic resonance imaging.

3.5 Behavioral test

All behavioral tests were performed between 10:00 am and 4:00 pm under dim light conditions. Prior testing, mice were put in the dark room with red light for 30 minutes in order to acclimatize the environment. All tests are recorded by a video camera (ELP 2.0 Megapixel USB camera, China). The chambers were all cleaned with soap water, tape water and 75% ethanol consequently before the next test to get avoid of odor interference. The analyses were finished by AnyMaze Video Tracking System 7.30a beta (Stoeling Co., USA).

3.5.1 Open field test

Open field test was performed for locomotor activity identification. Mice were put in the dark room with red light for 30 minutes in order to acclimatize the environment. The apparatus consisted of a white cylinder arena with 60 centimeters diameter and 30 centimeters height. The arena was divided into 3 regions (**Figure 6**): center region (10-centimeter-diameter circle area), peripheral region (a ring region with 60 centimeters outer diameter and 50 centimeters inner diameter), and middle region (the area among middle and peripheral region). The regions were mapped on a paper and always recorded before every day's experiment. The location of the arena was fixed and mice were put from a certain corner of the arena and allowed to explore for 10 minutes. The

distance travelled, and speed in center zone, peripheral zone, and whole travelling period were recorded.

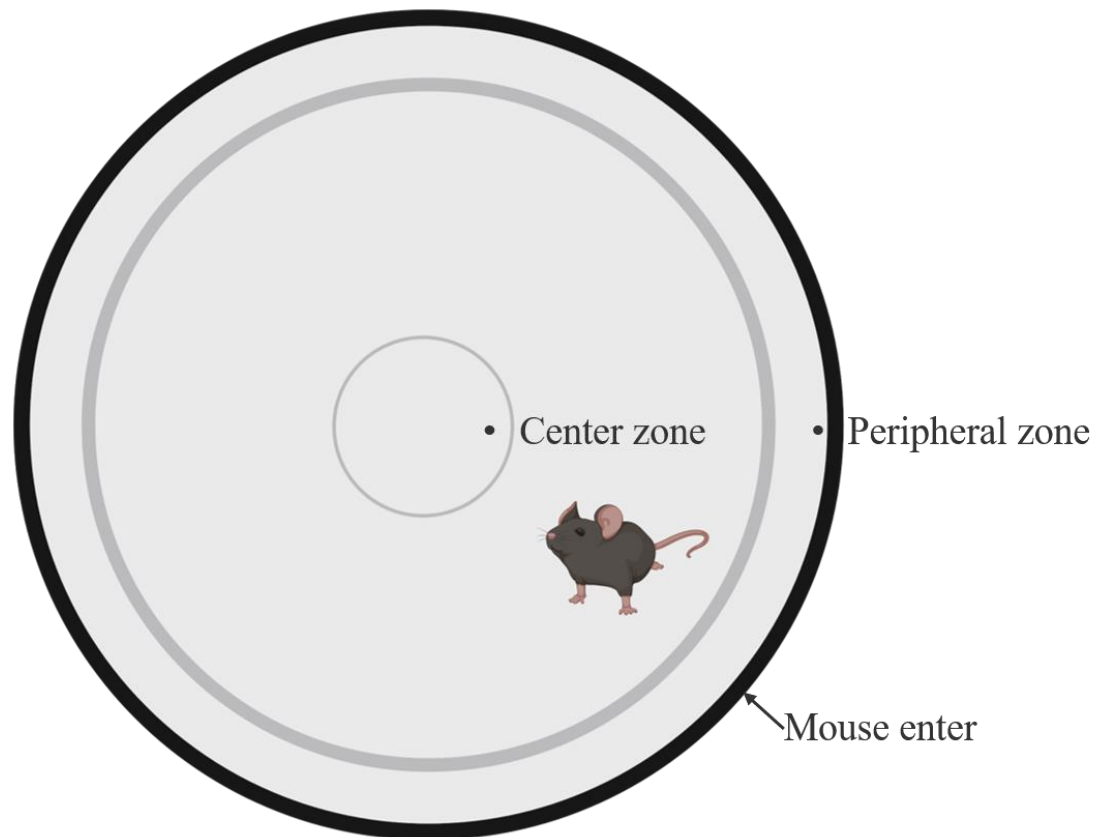


Figure 6. The map of the Open field arena.

3.5.2 Y-maze test

Y-maze test was performed to investigate short-term learning. The apparatus consisted of a 3-armed Y-maze chamber (arm length: 35 centimeters) and a plastic isolation card. The chamber was decorated with paper with different patterns for location identification. All decoration was isolated from mice with plastic boards. The arms were named as: open arm, closed arm and entry arm (**Figure 7**). All mice underwent 2-round exploration. In the first round, the isolation board was set at the entrance of closed arm. Mice were first placed at the end of the entry arm, and freely explored for 7 minutes. The mice were put back to their previous cages until 30 minutes after the first entry. Then the isolation board was removed, and the mice were placed at the same place again. The exploration time of the second round is 7 minutes as well. The counts of

entry into the open arm and the closed arm were recorded.

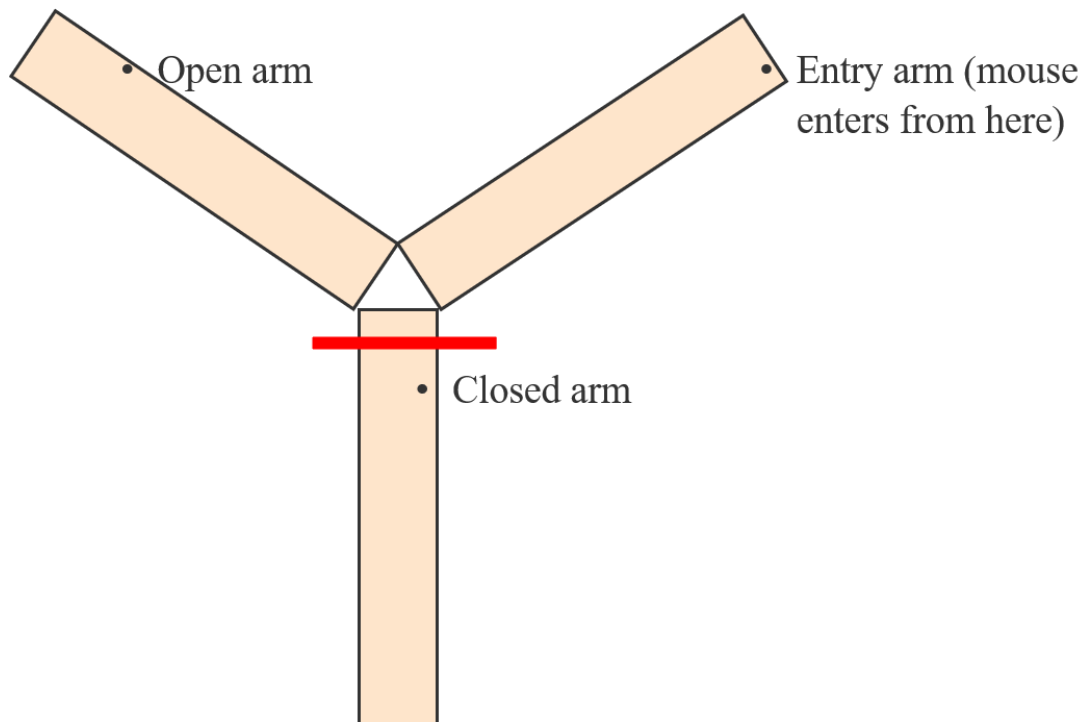


Figure 7. The map of the Y-maze chamber.

3.6 FACS measurement of immune cell infiltration

3.6.1 Tissue isolation and cell pellet suspension preparation

Mice were euthanized via carbon dioxide and perfused with cold PBS from the left ventricle (speed level 8, 2 minutes, pumped by Pumpdrive 5201, Heidolph Instrument GmbH & Co.). The spleen, cervical lymph nodes, meninges and ipsilateral brain hemisphere were isolated according to previous publications (Scheyltjens et al., 2022, Gelderblom et al., 2009) with some minute modifications.

3.6.1.1 Spleen and cervical lymph nodes isolation and cell suspension preparation

The spleen was isolated directly from the abdominal cavity. The cervical lymph nodes were collected after a ventral cervical incision. Both spleen and lymph nodes were stored in cold PBS and smashed directly via a plunger from a 3 ml syringe through a 40 μm cell strainer. The cell suspensions were washed with 50 ml PBS and the final pellet was kept for further staining.

3.6.1.2 Meninges isolation and cell suspension preparation

The head was isolated from the thorax. Skin, muscles, eye balls and optic nerves on the

skull were removed. Os zygomaticus was cut from both sides, and frontal part of nose was cut as well. The superior part of skull was collected. The dura was peeled from the skull under a binocular microscope (Carl Zeiss Microscopy Stand C LED, 435420-0000-000) and transferred to a 5 ml Eppendorf tube with 500 μ l 4°C Dulbecco's Modified Eagle Medium (DMEM, Gibco, 41965-039) inside. The dura was further cut into small pieces by scissors and 500 μ l meninges digestion solution was added (DMEM + 2.0mg/ml Collagenase + 0.2 mg/ml DNase) (DNase: Roche, 11284932001; Collagenase: Sigma, C2139). The tissue was digested in a 37°C-water bath (Grant, GLS400) for 15 minutes with agitation. After digestion, 1 ml DMEM+10% Fetal Bovine Serum (FBS) (PAN Biotech, P40-37500) was added to terminate the enzyme reaction. The mixed solution was then smashed by a plunger from a 3 ml syringe through a 40 μ m cell strainer. The tube was rinsed by 35 ml DMEM+10% FBS solution. After centrifugation (700g, 10 minutes, 4°C), the pellets were preserved for further staining.

3.6.1.3 Brain isolation and preparation of cell suspension

Brain was harvested, and ipsilateral hemisphere was collected. The hemisphere was first dissected by a scalpel and transferred into 5ml of digestion solution (containing 1 mg/ml collagenase and 0.1 mg/ml DNase I in DMEM). The tissue was digested in the 37°C-water bath for 30 minutes with agitation. The digested tissue solution was then smashed through a 40 μ m cell strainer by a plunger from a 3 ml syringe and washed by 50 ml PBS (700 x g, 10 minutes, 4°C). The supernatant was removed after washing. 5 ml erythrocyte lysis buffer (Biolegend, 422401) was added and incubated for 5 minutes on ice in order to lyse and remove red blood cells. The cells were washed again with 50 ml PBS (700 x g, 10 minutes, 4°C). Stock Percoll solution was prepared beforehand (90% v/v in 10x PBS) (Percoll, Cytiva, 10341908; 10x PBS: Sigma Aldrich, D1408-500ML). The pellets were resuspended in 2.8 ml Percoll B solution (30% v/v in DMEM). 2.8 ml Percoll A solution (78% v/v in 1xPBS) was underlaid via a 3 ml Pasteur pipette. After centrifugation (1350 x g, 30 minutes, 4°C accelerations off, brake off), 2 ml cloudy middle layer fluid was extracted and washed in 10 ml FACS buffer (5g/l BSA

and 0.1% 0.5M EDTA in PBS) (700 x g, 10 minutes, 4°C) (BSA: Thermofisher, A34785; EDTA: Sigma-Aldrich, 03690). The pellets were further washed in 10 ml FACS buffer (400 x g, 10 minutes, 4°C). The final pellets were collected for further staining.

3.6.1.4 Cell suspension distribution

The cell pellet suspensions were dissolved in a small volume of FACS buffer and distributed into two different 96-well plates for infiltration staining and T cell activation staining, separately. The distribution methods were as followed: CNS, 25% of the suspension for infiltration staining (20 % for measurement and 5% for isotype control) and 75% of the suspension for T cell activation staining (65% for measurement and 10% for isotype control); meninges, 35% of the suspension for infiltration staining (30 % for measurement and 5% for isotype control) and 65% of the suspension for T cell activation staining (60% for measurement and 10% for isotype control); lymph nodes, 100% of the suspension for T cell activation staining (80% for measurement and 20% for isotype control); spleen, 300 µl out of 3 ml total suspension for T cell activation panel test run. The isotype controls of every tissue on each plate were pooled into a well and served as a control for the certain experiment.

3.6.2 Infiltration staining and quantification

After transferring cell suspensions into well plates, cells were washed with 200 µl ice-cold PBS (350 x g, 5 minutes, 4°C) and incubated with 50 µl infiltration panel surface antibody cocktail. The incubation lasted for 30 minutes in 4°C environments. The ingredients were as followed: FITC anti-mouse MHC II, dilution: 1:100, clone: M5/114.15.2 (eBioscience, 11-5321-82); PerCP-Cyanine 5.5 anti-mouse TCR γ/δ , dilution: 1:100, clone: GL-3 (Biolegend, 118118); PE anti-mouse Ly6G, dilution: 1:200, clone: 1A8 (Biolegend, 127680); PE-Cyanine 7 anti-mouse CD11b, dilution: 1:100, clone: M1/70 (Biolegend, 101216); APC anti-mouse CD206 (MMR), dilution: 1:100, clone: C068C2 (Biolegend, 141707); APC-Fluor780 anti-mouse CD45, dilution: 1:100, clone: 30-F11 (eBioscience, 47-0451-82); BRILLIANT VIOLET421 anti-mouse CD3, dilution: 1:100, clone: 17A2 (Biolegend, 100228); BRILLIANT VIOLET570 anti-mouse CD45R/B220, dilution: 1:100, clone: RA36-B2 (Biolegend, 123133);

BRILLIANT VIOLET605 anti-mouse F4/80, dilution: 1:100, clone: GL-3 (Biolegend, 47-0451-82); BRILLIANT VIOLET650 anti-mouse CD8, dilution: 1:100, clone: 53-6.7 (Biolegend, 100741); BRILLIANT VIOLET711 anti-mouse NK1.1, dilution: 1:100, clone: PK136 (Biolegend, 108745); BRILLIANT VIOLET785 anti-mouse CD4, dilution: 1:100, clone: RM4-5 (Biolegend, 100551); BUV395 anti-mouse CD11c, dilution: 1:100, clone: HL 3 (BD, 564080). Specially, the isotype control cells were set for CD206 controlling. Anti-CD206 (MMR) antibody was replaced by APC Isootype antibody (dilution: 1:100, clone: RTK2758, Biolegend, 400512) in previous antibody cocktail ingredient. The cells were washed by 150 μ l FACS buffer (350g, 5 minutes, 4°C) and then resuspended in 250 μ l FACS buffer. The cell suspension was finally transferred to a Trucount™ Absolute Counting Tube (BD, 663028). The gating strategy was shown in **Figure 8**.

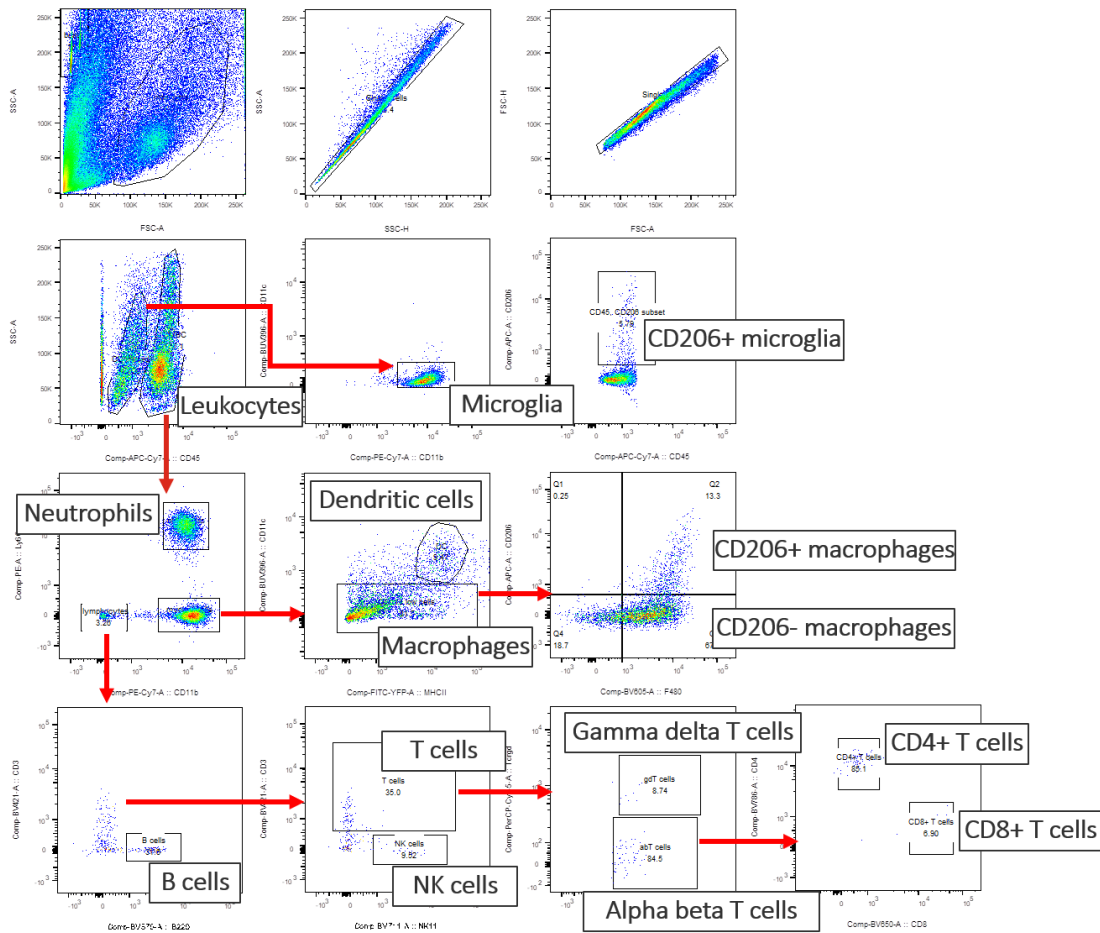


Figure 8. Gating strategy of FACS infiltration staining panel. Abbreviation: NK cells, nature killer cells.

The total bead count of each tube was recorded for cell quantification. Due to the previous splitting of cells, the total cell counts were calculated based on the previous percentage. The method of calculation was as followed:

$$total\ cell\ count = cell\ read * \frac{1}{cell\ percentage} * \frac{total\ bead\ count}{bead\ count\ read}$$

All samples were measured with BD FACS Symphony A3.

3.6.3 T cell activation and intracellular staining

Transferred cell suspensions were centrifuged (350 x g, 5 minutes, 4°C) and then stimulated by RPMI 1640 medium (Gibco, 21875-034) with phorbol 12-myristate 13-acetate (100 ng/ml, Sigma-Aldrich, P1585) and ionomycin (1 µg/ml, Sigma-Aldrich, 56092-81-0) in the presence of brefeldin A (1:1000, eBioscience, 00-4506-51) for 4 h at 37 °C, 5% CO₂ to analyze T cell cytokine production. After washing twice, the cells were stained with activation panel surface antibodies for 30 minutes in 4°C environments. The ingredients applied were as followed: PerCp-Cyanine 5.5 anti-mouse/human CD45R/B220, dilution: 1:100, clone: RA3-6B2 (Biolegend, 103236); PE-Cyanine 7 anti-mouse NK1.1, dilution: 1:100, clone: PK136 (Biolegend, 108714); Alexa Fluor 700 anti-mouse CD4, dilution: 1:100, clone: RM4-5 (Biolegend, 100536); BRILLIANT VIOLET421 anti-mouse CD3, dilution: 1:100, clone: 17A2 (Biolegend, 100228); Brilliant Violet 510 anti-mouse CD45, dilution: 1:100, clone: 30-F11 (Biolegend, 103138); Brilliant Violet 605 anti-mouse TCR γ/δ, dilution: 1:100, clone: GL-3 (Biolegend, 118129); BV650 anti-mouse CD8a, dilution: 1:100, clone: 53-6.7 (Biolegend, 100742).

After surface staining, the cells were fixed by True nuclear Transkription Factor Buffer Set (Biolegend, 424401) for 20 minutes in room temperature and washed by permeabilization buffer (eBioscience, 00-8333-56, 1:10 dilution by dH₂O) (350g, 5 minutes, 4°C). Subsequent intracellular cytokine staining was done in permeabilization buffer for 20 minutes at room temperature. The components of cell staining were as followed: Alexa Fluor 488 anti-mouse interferon-γ, dilution: 1:100, clone: XMG 1.2 (Biolegend, 505813); APC anti-mouse TNF-α, dilution: 1:100, clone: MP6XT22 (Biolegend, 506308). The final gating strategy is shown in **Figure 9**.

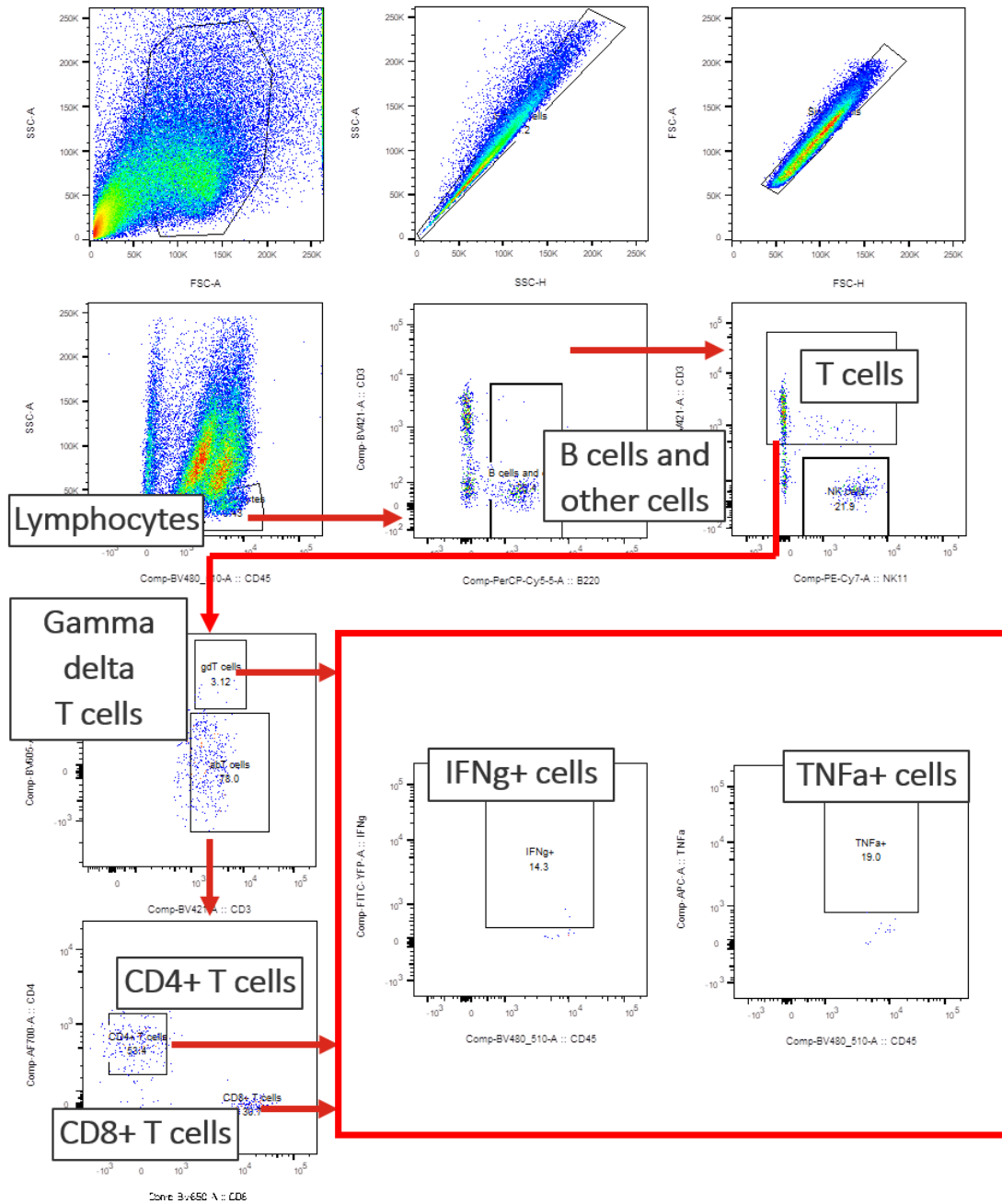


Figure 9. Gating strategy of T cell activation panel. Abbreviation: IFN γ , interferon- γ ; TNF α , tumor necrotic factor- α .

The components of isotype control staining were as followed: Alexa Fluoro 488 anti-mouse isotype control, dilution: 1:100, clone: RTK2071 (Biolegend, 400417); PE anti-mouse isotype control, dilution: 1:30, clone: eBR2a (eBioscience, 12-4321-82); APC anti-mouse isotype control, dilution: 1:100, clone: eBRG1 (eBioscience, 17-4301-82). The cells were washed in 150 μ l permeabilization buffer and resuspended in 250 μ l FACS buffer. The cell suspension was transferred into a FACS tube and measured on

BD FACS Symphony A3.

3.7 Microglia FACS sorting

The protocol of microglia FACS sorting was modified on previous publications (Schadlich et al., 2022, Ortega et al., 2013).

3.7.1 Tissue isolation and cell pellet suspension preparation

Brain was harvested following transcardial perfusion with ice cold PBS. The cerebellum and olfactory bulbs were removed. Ipsilateral hemisphere was dissected and preserved. The hemisphere was isolated under the microscope into cortex and subcortical region. Isolated tissues were smashed in KIMBLE dounce tissue homogenizer (Merck, D9063) with 2 ml PBS solution. The tissues were grinded by loose dounce A and followed by tight dounce B to form homogenized suspensions. The tissue suspension was then transferred to a 5 ml Eppendorf tube. PBS was removed by centrifugation (300 x g, 5 minutes, 4°C). Tissue pellets were further digested for 20 minutes in Papain (Warthington, LK003176) dissolved in Hibernate E (Gibco, A12476-01) and continued with 10 minutes in at 37 °C after addition of 1 mg/ml collagenase and 0.1 mg/ml DNase I in DMEM. Protease inhibitor (1:25, Roche, 11697498001) was applied to terminate the digestion. After one time PBS washing (700 x g, 10 minutes, 4°C), cells were then isolated from the middle cloudy layer after the two-phase Percoll centrifugation (30% v/v and 78% v/v in DMEM and PBS respectively) and washed in FACS buffer (700 x g, 10 minutes, 4°C). The supernatant was removed, and the pellet was preserved for surface staining.

3.7.2 Cell staining

Cell pellets were stained with surface antibody: PE-Texas red anti-mouse CD11b, dilution: 1:100, clone: M1/70 (BD, 562287); APC-eFluor 780 anti-mouse CD45, dilution: 1:100, clone: 30-F11 (eBioscience, 47-0451-82); PE anti-mouse ESAM, dilution: 1:50, clone: 1G8/ESAM (Biolegend, 136203); PE anti-mouse endomucin, dilution: 1:20, clone: eBioV.7C7 (Invitrogen, 12-5851-82); PE-Cyanine 7 anti-mouse CD140a, dilution: 1:30, clone: APA5 (Biolegend, 135912); APC anti-mouse O4,

dilution: 1:50, clone: O4 (Miltenyi, 130-119-155); FITC anti-mouse ASCA-2, dilution: 1:30, clone: REA969 (MACS, 130-116-24), for 30 minutes at 4°C. The cell suspension was diluted to 15 ml and got through the 100 µm strainer via pipetting. The cells were last centrifuged (700g, 10 minutes, 4°C). The pellets were resuspended into 150 µl PBS containing 0.3% v/v EDTA for sorting.

3.7.3 FACS measurement and sorting

Cells were sorted on FACS Aria Fusion. Microglia were defined as CD45^{med}/CD11b^{high}/CD11c^{low} cells. The cells were sorted into Hibernate E medium in tubes coated with FCS. Cell counting was recorded by FACS Aria Fusion. Cells were collected for qPCR or bulk-RNA sequencing.

3.8 RNA preparation and bulk-RNA sequencing

3.8.1 RNA extraction

Sorted microglia suspension were initially centrifuged (21130 x g, 3 minutes, 4°C) to remove the supernatant. The cell pellet was then treated with RNeasy Micro Kit (Qiagen, 74034) and Qia Shredder (Qiagen, 79654). The pellet was lysed in RLT buffer with 2-mercaptoethanol and centrifuged on Qia Shredder (21130 x g, 2 minutes, 4°C). The flow-through was further centrifuged on a gDNA eliminator (8000 x g, 30 seconds, room temperature). Collected flow through was added on the MinElute spin column. The sample was subsequently washed by 70% ethanol, RW1 buffer, RPE buffer and 80% ethanol on RNeasy MinElute column. The RNA sample was ultimately eluted in 17 µl RNase free water. 1.5 µl sample were taken out for further quality control.

3.8.2 RNA quality control by Agilent RNA 6000 Pico Kit

RNA sample quality control was performed with Agilent RNA 6000 Pico Kit (Agilent Technologies, 5067-1513). Ladder was prepared in advance with 70°C heat denaturation and stored at -80°C environment. Gel was prepared no earlier than 1 month of the experiment. Gel was further aliquoted into 65 µl vials and stored at 4°C environments. On the day of measurement, all reagents were allowed to equilibrate to room temperature for 30 minutes. 1 µl dye was added to the aliquoted gel after vortex

and spinning down. The gel-dye mix was then centrifuged (13000 x g, 10 minutes, room temperature) and used within 1 day.

RNA chip was firstly loaded on the priming station. 9 μ l gel-dye mix were applied on the marked place and pressed the plunge for 30 seconds as described in the protocol. Then, 9 μ l gel-dye mix, 9 μ l conditioning solution, 5 μ l RNA marker were added to certain wells subsequently. 1 μ l samples and ladder were at last added to the wells according to the previous marks. After vortex (2400 rpm, 60 seconds, room temperature), the chip was loaded and measured on 2100 Bioanalyzer instrument. RNA concentration, RNA integrity number (RIN) values, electropherograms figures and parameters were recorded for further analyses.

3.8.3 Bulk-RNA sequencing

Bulk-RNA sequencing was performed by Novogene Co. (China). Microglia RNA samples with RIN value over 6 and concentration over 300pg/ μ l were regarded as qualified samples. The samples both qualified from cortex and subcortical tissues from the same mouse were collected for further sequencing. 5 pair of samples from PBS group and 5 pair of samples from LPS group were eventually chosen for sequencing. Samples were delivered in dry ice box and sequenced by Novogene Co. The treatment steps included sample quality control, library construction, library quality control, sequencing, data quality control, and QC report generation. The raw data were saved as pair-ended sequenced files. All samples obtained 0.01% error rate and nearly 50% GC pair percentage.

The sample quality information, differentially expressed genes (DEGs) analyses and downstream analyses were performed by UKE Bioinformatics core facility. A gene is considered significantly differentially expressed if the corresponding False Discovery Rate (FDR) is smaller than or equal to 0.1 and the absolute log₂-foldchange (log₂FC) is larger than or equal to 1 (FDR \leq 0.1 AND |log₂FC| \geq 1). Annotation source was Ensembl (version: GRCm39.110); quality control was performed by fastp (version: 0.23.0); Mapping and RNA quantification is performed by STAR (2.7.10a).

Downstream analyses included enrichment analysis by Gene Set Enrichment Analysis

(GSEA) (Subramanian et al., 2005) and transcription regulatory activity by discriminant regulon expression analysis (DoRothEA) (Garcia-Alonso et al., 2019). GSEA used a list of all genes ranked by the shrunked log₂ fold change from the DE analysis and tested if an entry of the abovementioned databases was significantly enriched at the top or bottom of this list. The enrichment was measured by the normalized enrichment score (NES). DoRothEA provided a gene set database containing signed transcription factor (TF) - target interactions (regulons). Each regulon was assigned a confidence class (A-E) based on literature sources and experimental data. For this analysis, the classes A-C were included. The regulon activity was estimated based on the TF target expression data.

3.9 Statistical analysis

Statistical analysis was performed on GraphPad Prism for Windows 64 9.5.0 (730) (GraphPad Software). Kolmogorov–Smirnov test was used for the test of normality on a continuous variable. Unpaired t-test was used for comparing normality variables with same square differences. Welch t-test was applied if the square differences were not the same. Mann–Whitney U-test was used for comparing non-normality variables. Specifically, due to the repeated measurement, bodyweights and behaviorism data were compared via two-way ANOVA. Šídák multiple comparison analysis was applied for individual analysis after two-way ANOVA. $p < 0.05$ was regarded as a significant difference. In figures, the sign of *, **, ***, and **** represented $p < 0.05$, $p < 0.01$, $p < 0.005$, $p < 0.001$ respectively.

4. Results

This study aims (i) to investigate potential global immune landscape changes during acute and subacute phase post-stroke after induction of microglial immune tolerance, (ii) to explore the regenerative capacity of microglial innate immune tolerance during subacute phase of stroke and (iii) to explore gene expression changes in spatially distinct microglia subpopulations following immune tolerance during stroke.

4.1 Induction of immune tolerance by peripheral injections of LPS

According to Wendeln et al. the induction of long-lasting immune tolerance in murine microglia can be accomplished by intraperitoneal injections of 500 μ g LPS/kg bodyweight at four consecutive days. Acute LPS injections were shown to cause an acute sickness behavior reflected in a bodyweight drop with a subsequent recovery of the bodyweight to baseline values.

4.1.1 Bodyweight changes indicate the induction of immune tolerance

To validate the induction of immune tolerance by peripheral LPS injections, mice were weighed on every injection day and once a week for 4 weeks. Only mice injected at the first 3 months of the project (January, 2023 to March, 2023) were enrolled for this analysis. Totally 88 mice bodyweights were included (PBS group, n=43; LPS group, n=45). The bodyweight timelines are shown in **Figure 10**.

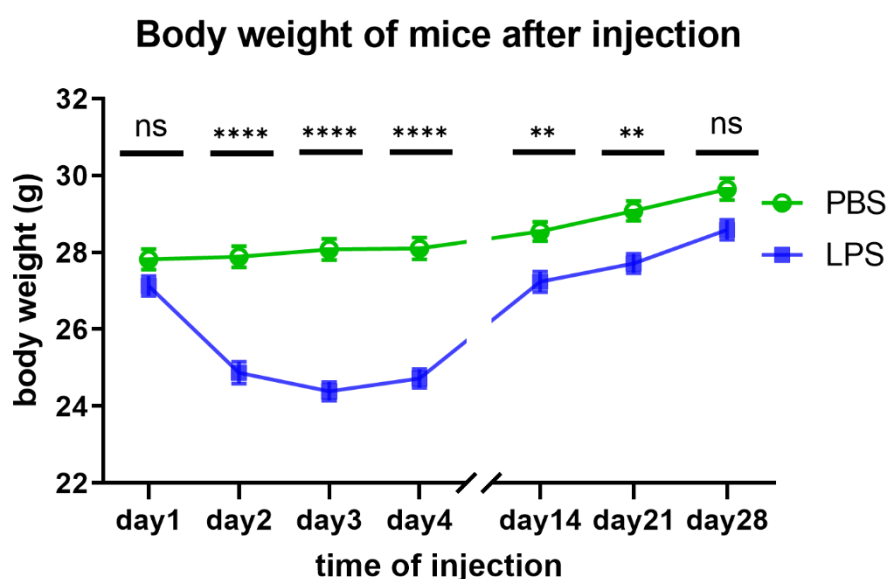


Figure 10. Timeline of mice bodyweight after peripheral injection of LPS/PBS. Bodyweights were recorded on the 1st, 2nd, 3rd, 4th, 14th, 21st, 28th day after the first injection. Mice were peritoneally injected with either PBS (control) or LPS according to their bodyweight. All data are shown as mean \pm s.e.m. Mouse count: PBS, n=43; LPS, n=45. (ns: $p>0.05$; *: $p<0.05$; ** $p<0.01$; ***: $p<0.005$; ****: $p<0.001$. Statistics: two-way ANOVA.) Abbreviation: PBS: phosphate-buffer saline; LPS: lipopolysaccharide; s.e.m: standard error mean; ns: not significant; ANOVA: analysis of variance.

The bodyweight exhibited no difference on the first injection day (1st day: PBS, 27.82 \pm 1.76g, LPS, 27.13 \pm 1.77g; $p=0.40$), indicating a homogenous cohort and thus excludes influences on the immune response due to exogenous factors. From the second day of injection, the LPS group showed a drastic drop of weight (percentage of bodyweight change from baseline: PBS: 0.3%; LPS: -8.3%) which was significantly lower than in PBS group (2nd day: PBS, 27.89 \pm 1.81g, LPS, 24.87 \pm 1.94g; $p<0.001$). The difference continued to increase until the third day (3rd day: PBS, 28.08 \pm 1.81g, LPS, 24.39 \pm 1.65g; $p<0.001$) (percentage of bodyweight change from baseline: PBS: 0.9%; LPS: -10.1%). On the fourth day the bodyweight in the LPS group did not show a further drop but remained constant indicating the development of tolerance as described by Wendeln et al (4th day: PBS, 28.11 \pm 1.89g, LPS, 24.72 \pm 1.65g; $p<0.001$) (percentage of bodyweight change from baseline: PBS: 1.0%; LPS: -8.9%). After stopping LPS injections, the LPS-induced difference in bodyweight in comparison to PBS injected mice became diminished within the following weeks (14th day: PBS, 28.54 \pm 1.68g, LPS, 27.23 \pm 1.79g; $p=0.005$; 21st day: PBS, 29.08 \pm 1.68g, LPS, 27.71 \pm 1.67g; $p=0.002$) (percentage of bodyweight change from baseline: day 14: PBS: 2.6%; LPS: 0.4%; day 21: PBS: 4.5%; LPS: 2.1%) and finally the bodyweights became comparable at week 4 post-injections (28th day: PBS, 29.65 \pm 1.86g, LPS 28.59 \pm 1.77g; $p=0.053$) (percentage of bodyweight change from baseline: PBS: 6.6%; LPS: 5.4%) indicating a return to a physiological condition of the mouse.

4.1.2 Acute exposure to LPS does not alter the psychoneurological function of mice

To observe the acute effects of LPS injections on anxiety, locomotor behavior and short-term memory, totally 18 mice (PBS: n=9; LPS: n=9) underwent Open field and Y-maze testing both at baseline (pre-injection) and on the first and second day after LPS injection (post-injection).

Figure 11A shows the results for anxiety-like behavior whereas **Figure 11B** displays locomotor ability. Both tested behavioral characteristics do not show differences between treatment groups after LPS injection. The heatmap confirms an unspecific bias of mice staying in the peripheral zone in both groups (**Figure 11C**).

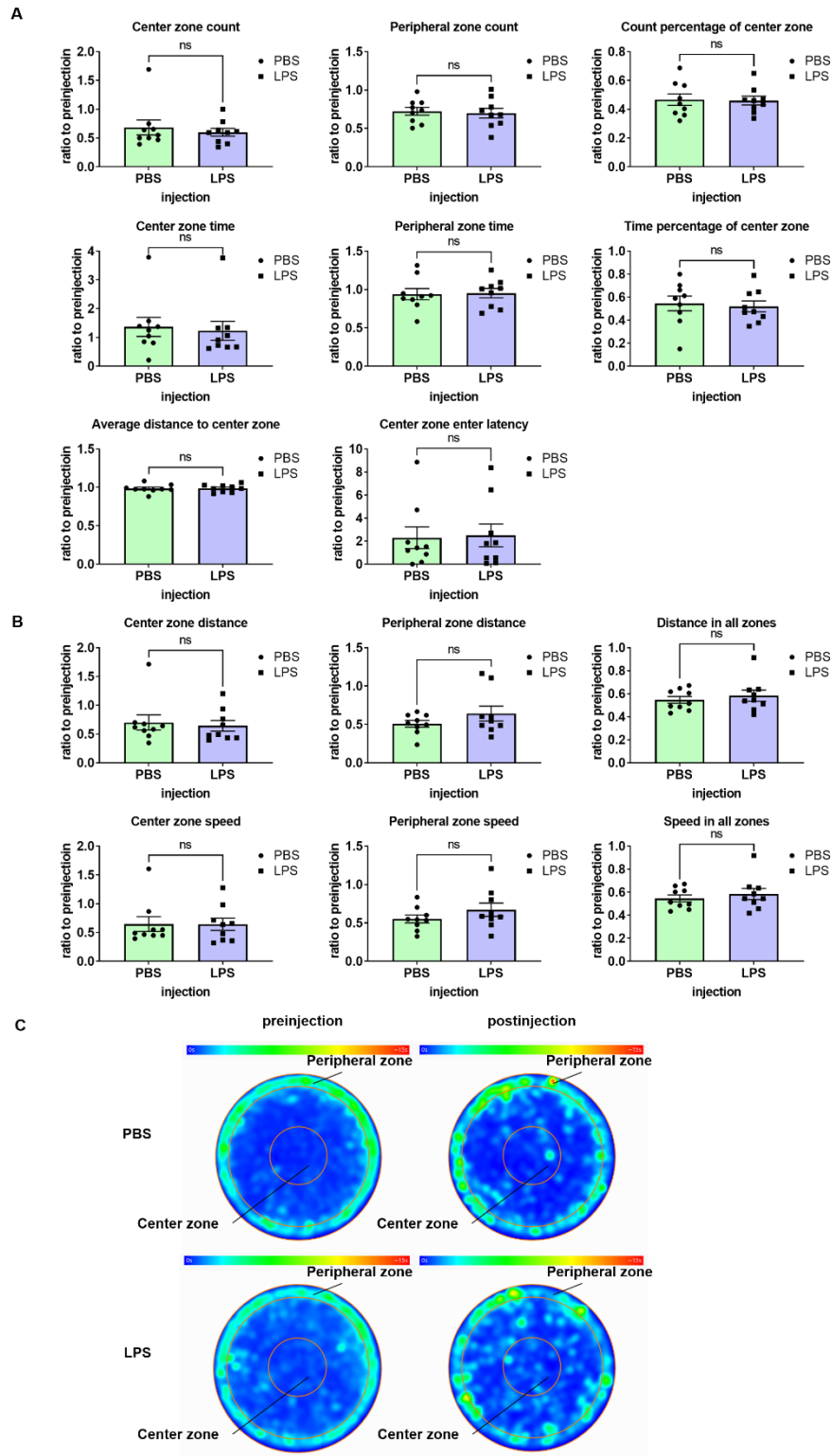


Figure 11. Results of Open field test 1 day after final injection (A) Analysis of Open field parameter regarding anxiety-like behavior normalized to preinjection. (B) Analysis of Open field parameter regarding locomotor function normalized to preinjection. (C) Heatmap of mice staying time in different location in the open field arena. All data are shown as mean \pm s.e.m. Mouse count: PBS, $n=5$; LPS, $n=5$. (ns: $p>0.05$. Statistics: two-way ANOVA.) Abbreviation: PBS: phosphate-buffered saline; LPS: lipopolysaccharide; s.e.m: standard error mean; ns: not significant; ANOVA: analysis of variance.

Y-maze tests to test short-term memory were performed on baseline condition (preinjection) and the 2nd day after the final injection (postinjection). Total counts in the open and closed arm were normalized to preinjection data, count distribution is shown as proportion entering the open or closed arm from the total count of entering both arms. As shown in **Figure 12A**, mice in the LPS and PBS group exhibited a similar trend of arm entering. **Figure 12B** shows that both groups (LPS and PBS injected mice) visit the closed arm more often than the open arm independently of prior LPS/PBS injections. Moreover, both groups shared the same ratio of entering both closed and open arms **Figure 12C**. In the heatmap, mice from LPS/PBS groups exhibit similar moving and staying traces in the Y-maze arms (**Figure 12D**).

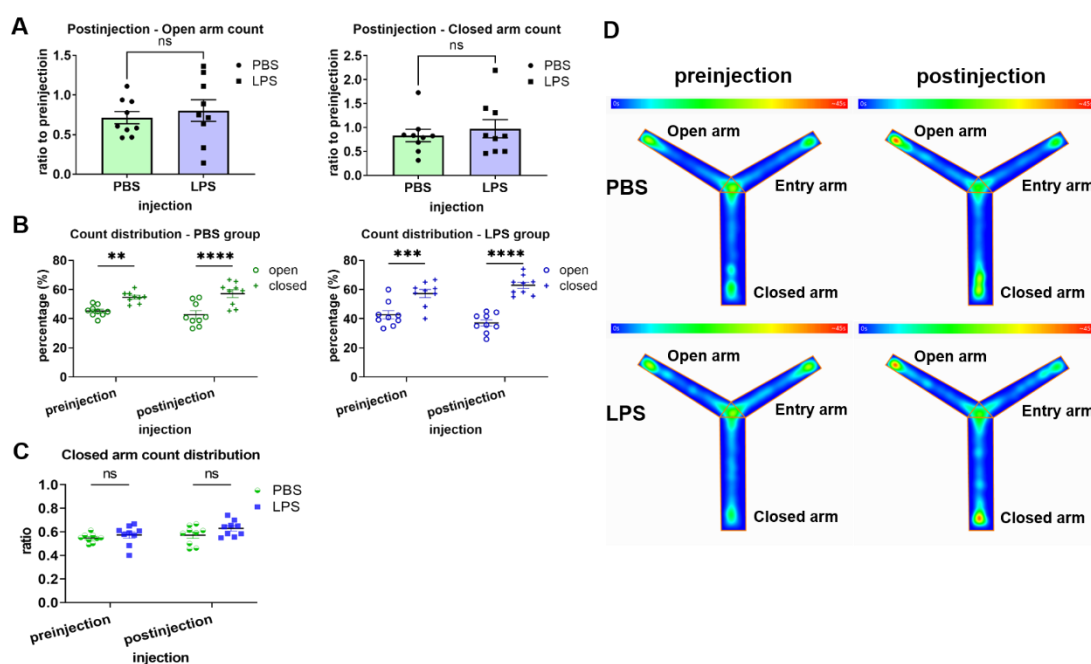


Figure 12. Results of Y-maze test 2 days after final injection (A) Comparison of open arm entering count and closed arm entering count in the Y-maze arena at postinjection stage. Results are standardized to preinjection data. (B) Comparison of the distribution of different arms entering count from total counts at pre- and postinjection stage. (C) Group comparison (LPS vs PBS) of the proportions to enter the closed arm. (D) Heatmap of mice staying time in the different arms in the Y-maze arena. Mouse count: PBS, n=5; LPS, n=5. (ns: $p > 0.05$; *: $p < 0.05$; **: $p < 0.01$; ***: $p < 0.005$; ****: $p < 0.001$. Statistics: two-way ANOVA.) All data are shown as mean \pm s.e.m. Abbreviation: PBS: phosphate-buffered saline; LPS: lipopolysaccharide; s.e.m: standard error mean; ns: not significant; ANOVA: analysis of variance.

4.2 Immune tolerance in microglia does not affect the stroke-induced immune landscape in the CNS post-stroke

Microglia are the primary immune effector cells in the brain. Thus, they are among the first cells that get activated through DAMPs released by dying and stressed neurons. As a consequence, microglia release inflammatory mediators such as IL-1 β or TNF- α that contribute to the inflammatory sequelae as well as immune cell infiltration. To validate the effect of microglial immune tolerance on the immune landscape of infiltrating immune cells under ischemic conditions, tMCAO surgery was performed in mice 4 weeks post LPS/PBS injections a timepoint when initial LPS injections do not impair the mouse' physiology. The occlusion time for tMCAO surgery of this group was set as 60 minutes. An MRI recorded at day 1 post-stroke was used to identify lesion size. Mice were sacrificed either on day 1 or 3 post-stroke for FACS experiments. In total, 19 mice (PBS, n=10; LPS, n=9) were enrolled for 1-day post-stroke analysis and 18 mice (PBS, n=10; LPS, n=8) were included for 3-day post-stroke analysis. Moreover, other 24 mice (PBS, n=12; LPS, n=12) were also involved as a naïve control group.

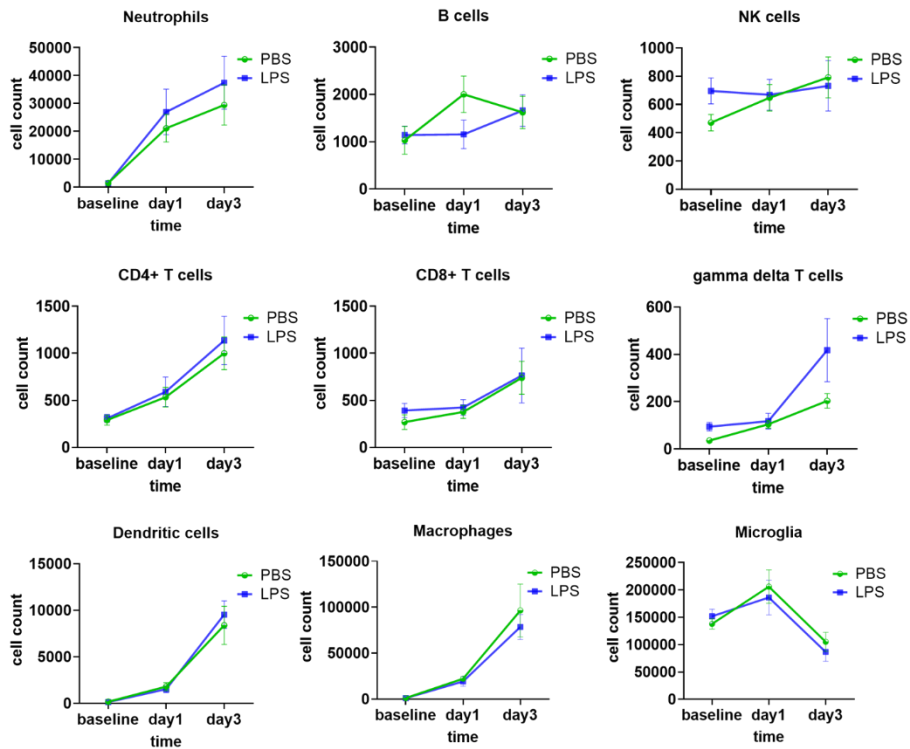
4.2.1 The acute inflammatory reaction remains unaffected after induction of microglial immune tolerance

To investigate the impact of microglial immune tolerance on the subsequent immune cell infiltration and activation of leucocytes, cell counts of neutrophils, B cells, nature killer cells (NK cells), CD4⁺ T cells, CD8⁺ T cells, $\gamma\delta$ T cells, dendritic cells, macrophages and also microglia as resident immune cells from the ipsilateral hemisphere were recorded at day 1 and 3 post-ischemia by FACS analyses. The dynamics of immune cell infiltration from baseline to day 1 and day 3 are shown in **Figure 13A**. Overall, the timeline reflects the well-studied trend of increased parenchymal cell counts with stroke onset (Gelderblom et al., 2009) with only the microglia cells count dropped on the 3rd day. When comparing immune cell infiltration between the LPS and PBS group, the same trends of increased immune cells were detectable. However, though not significant, the B cell count tended to be decreased in

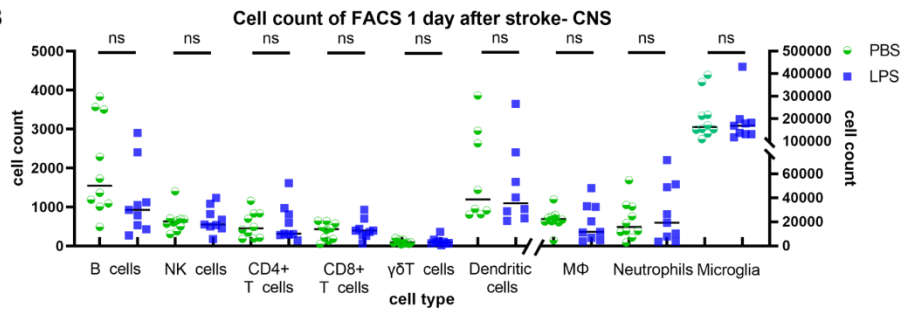
the LPS group at day 1. But at day 3 the B cell count exhibited similar counts between treatment groups.

For a detailed analyses of the individual cell counts per time points, cellular counts are displayed in **Figure 13B** and **C**. An indistinguishable pattern of immune cell infiltration between LPS und PBS pretreatment can be observed among all cell groups at both time points.

A



B



C

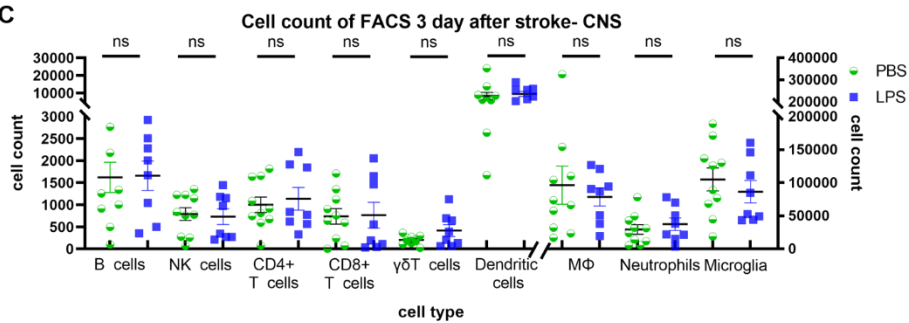


Figure 13. FACS analysis of CNS tissue from PBS- and LPS- injected mice in naïve, 1-day post-stroke and 3-day post-stroke conditions. (A) Timelines of cell count changes at indicated time points post-stroke. (B, C) Detailed distribution of cell counts 1-day (B) and 3-day (C) post-stroke in the ipsilateral hemisphere. All data are shown as mean \pm s.e.m. (ns: $p > 0.05$. Statistics: unpaired t-test.) Abbreviation: PBS: phosphate-buffered saline; LPS: lipopolysaccharide; s.e.m: standard error mean; ns: not significant.

Additionally, the distribution of cells was depicted as Uniform Manifold Approximation and Projection (UMAP) (**Figure 14**). Of note on the 3rd day, the macrophage subpopulation from LPS treated mice (green) (**Figure 14B**) exhibited a variation in comparison to the PBS group (blue). In all other comparisons, The LPS and PBS group show a high overlap of the analyzed cell populations.

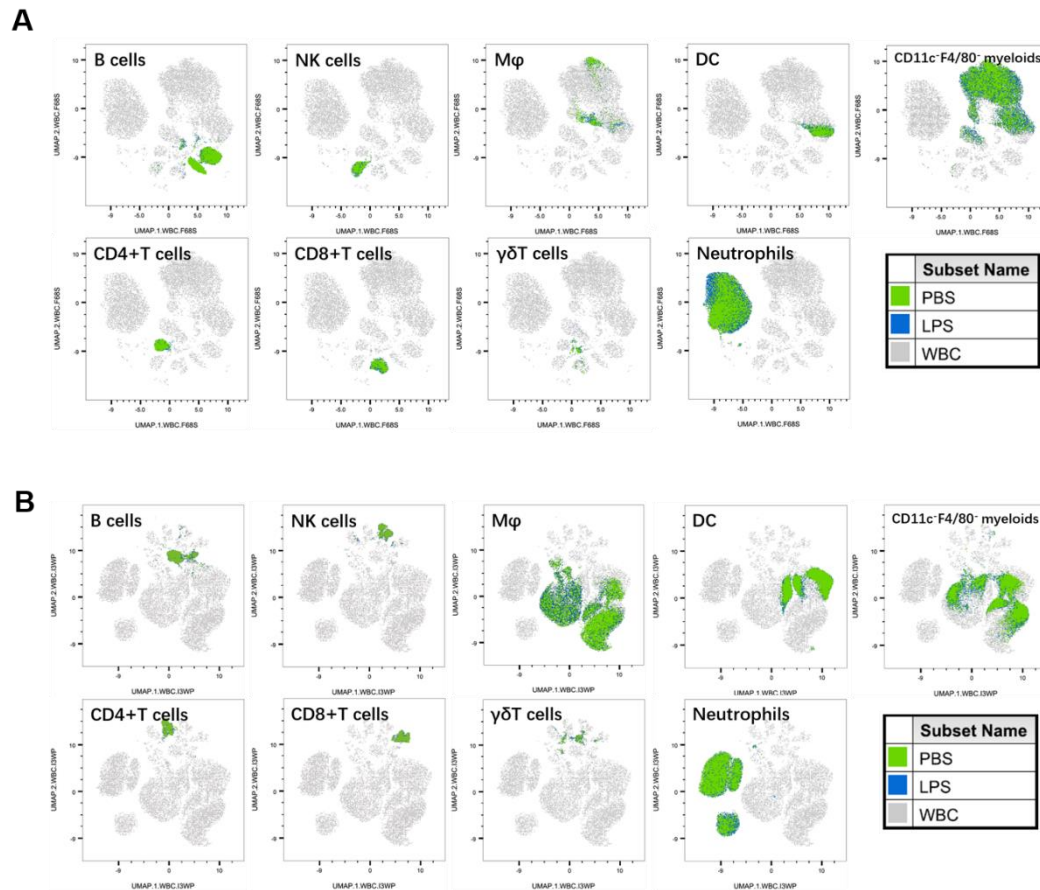


Figure 14. UMAP of cell distribution in different injection groups 1-day (A) and 3-day (B) after stroke in the CNS. Abbreviation: WBC: white blood cells; Mφ: macrophages; PBS: phosphate-buffered saline; LPS: lipopolysaccharide; UMAP: Uniform Manifold Approximation and Projection.

4.2.2 Meningeal immunity remains unchanged after induction of microglial immune tolerance

Meningeal immunity has recently been identified to be affected by neurological diseases such as ischemic stroke (Su et al., 2023). However, if immune tolerance can affect meningeal immunity also in the context of ischemic stroke has not been addressed so far. To study the immune landscape of dural tissue after induction of immune

tolerance but also after secondary stroke induction cell counts of neutrophils, B cells, nature killer cells (NK cells), CD4⁺ T cells, CD8⁺ T cells, $\gamma\delta$ T cells, dendritic cells and macrophages were analyzed (**Figure 15**).

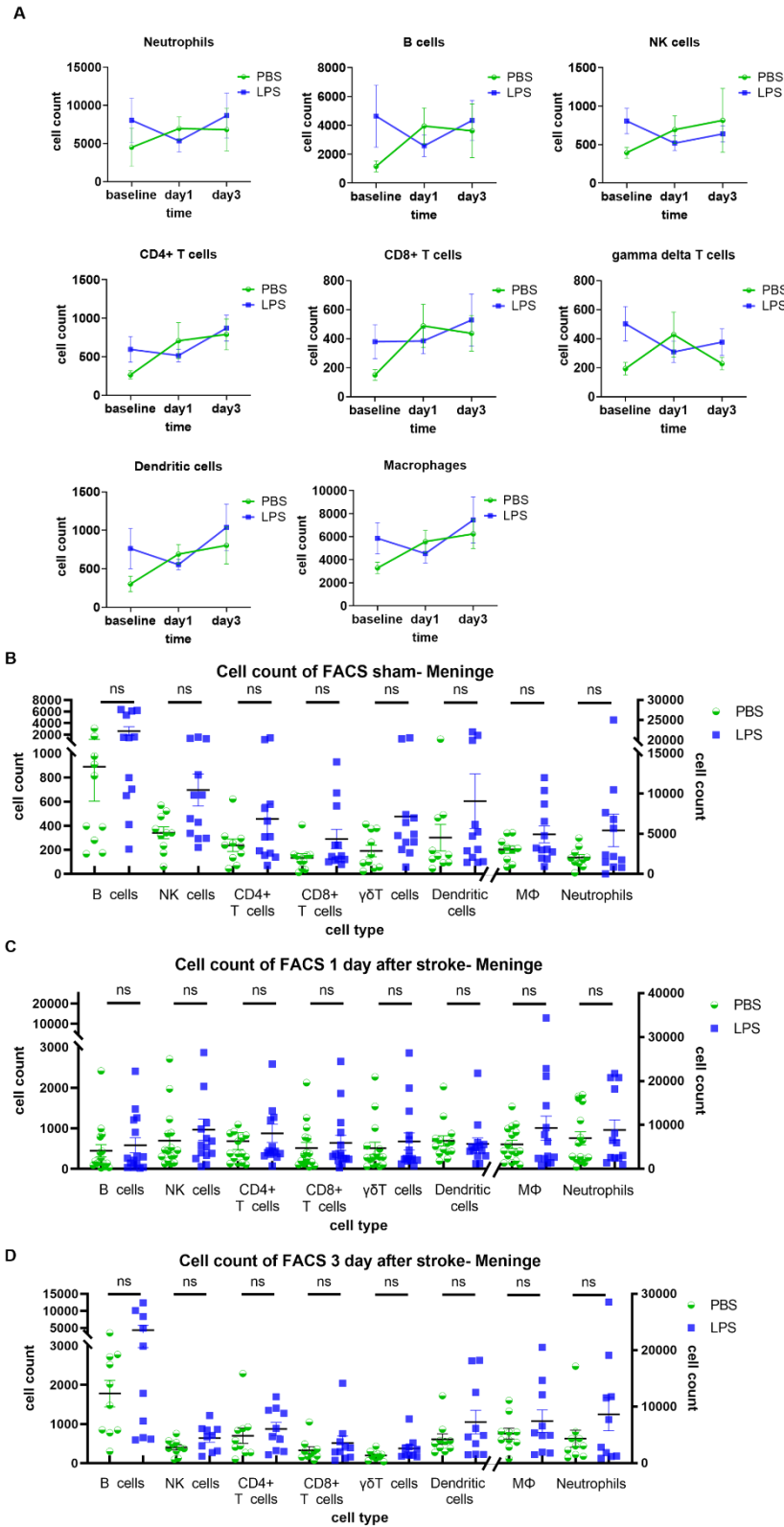


Figure 15. FACS analysis of meningeal dura in PBS- and LPS- injected mice in naïve, 1-day post-stroke and 3-day post-stroke conditions. (A) Timeline of cell count changes after stroke. (B, C, D) Detailed distribution of cell counts naïve (B), 1-day (C) and 3-day (D) after stroke in brain. All data are shown as mean \pm s.e.m. (ns: $p>0.05$. Statistics: unpaired t-test.) Abbreviation: PBS: phosphate-buffered saline; LPS: lipopolysaccharide; s.e.m: standard error mean; ns: not significant.

Interestingly, the prior LPS treatment to induce microglial immune tolerance tended to increase the immune cell count in all analyzed cell populations in the dural layer (**Figure 15A**). At day 1 and 3 post-ischemia the immune cell counts in the meninges increased as seen in the brain parenchyma, but no obvious differences between the LPS immune tolerance group and the PBS control group could be detected. Almost all the detected cells kept at similar level to baseline condition (**Figure 15 B, C and D**). However, even though cell counts were indistinguishable after stroke, the dynamics were different between the LPS and PBS group. Whereas the cell counts in the LPS group remained stable or slightly decreased after stroke, the cell counts in the PBS group increased.

Furthermore, the cell distributions are depicted as UMAP. Here, the strong consistency of all cell populations among the two groups (LPS and PBS) is reflected by the highly overlapping UMAP figures (**Figure 16**).

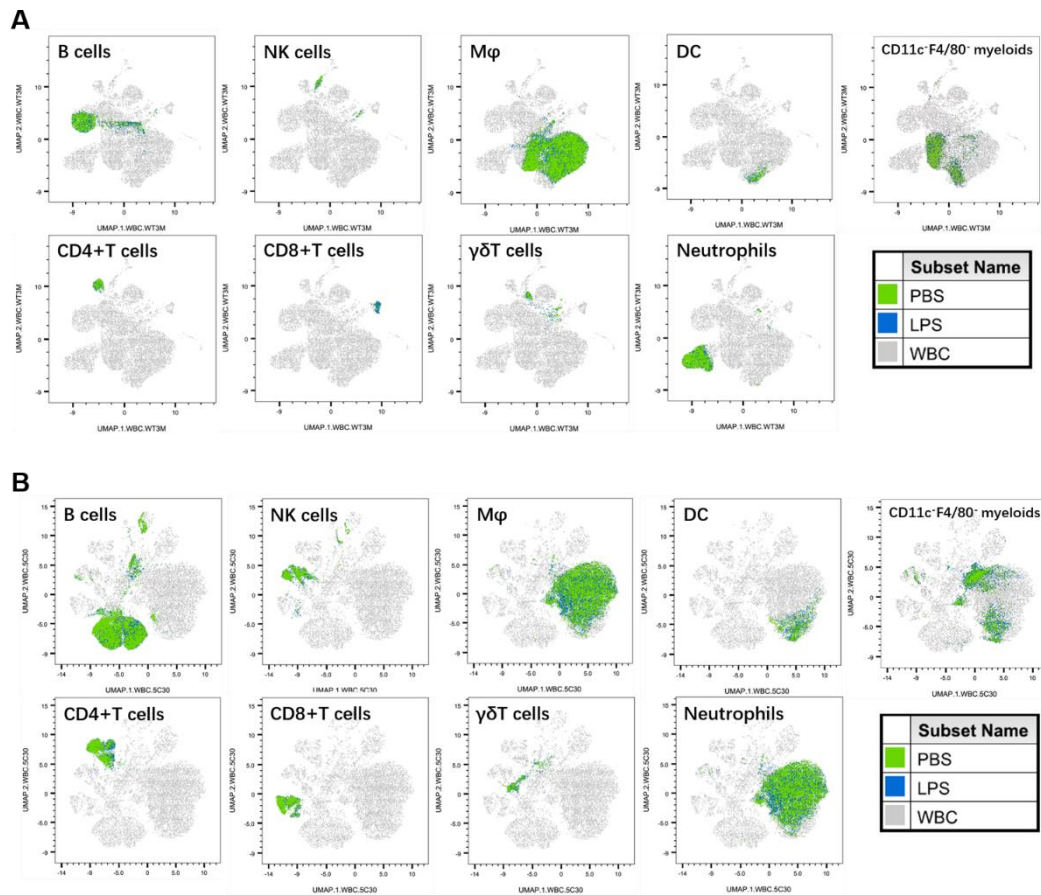


Figure 16. UMAP of cell distribution in different injection groups 1-day (A) and 3-day (B) after stroke in meninges. Abbreviation: WBC: white blood cells; PBS: phosphate-buffered saline; LPS: lipopolysaccharide; UMAP: Uniform Manifold Approximation and Projection.

4.2.3 T cells secrete similar proinflammatory cytokines after induction of immune tolerance

T cell activation in ischemic stroke is characterized by the production of inflammatory mediators which can contribute to tissue damage by enhancing the immune response in the brain (Zhang et al., 2021a). In order to investigate if immune tolerance in microglia impairs microglia-T cell interaction and thus the pro-inflammatory properties of T cells during stroke onset, T cell activation was investigated by measuring IFN- γ and TNF- α , two classical pro-inflammatory cytokines, in different T cell subtypes. A timeline reflecting cytokine level changes from baseline, day 1 and day 3 post-stroke are shown in **Figure 17**.

Overall, in the brain, LPS-induced immune tolerance in microglia does not effectively impact cytokine production in CD4⁺, CD8⁺ and $\gamma\delta$ T cells. Even though no significant

effects could be detected, TNF- α production by $\gamma\delta$ T cells was slightly impaired by LPS stimulation at all analyzed timepoints.

In the meningeal dura tissue, cytokine production in T cell subpopulations shows minor changes but does not reach significance. A tendency for slightly less cytokine producing cells in response to immune tolerance induction leads to an unspecific trend of decreased cytokine production levels in all analyzed T cell populations.

Lymph nodes are immune organs in the periphery, which locate far away from microglia and thus serve as control to exclude systemic effects of immune tolerance induction. In line, cytokine production, in particular IFN- γ , in the cervical lymph nodes, strongly overlaps between the LPS treatment and the PBS control group. For TNF- α , a slight but not significant decrease in the LPS group is visible, especially in $\gamma\delta$ T cells.

In summary, microglia immune tolerance does not affect peripheral immune cell infiltration and its T cell-specific activation in the brain and meningeal tissue in the acute inflammatory phase post-stroke.

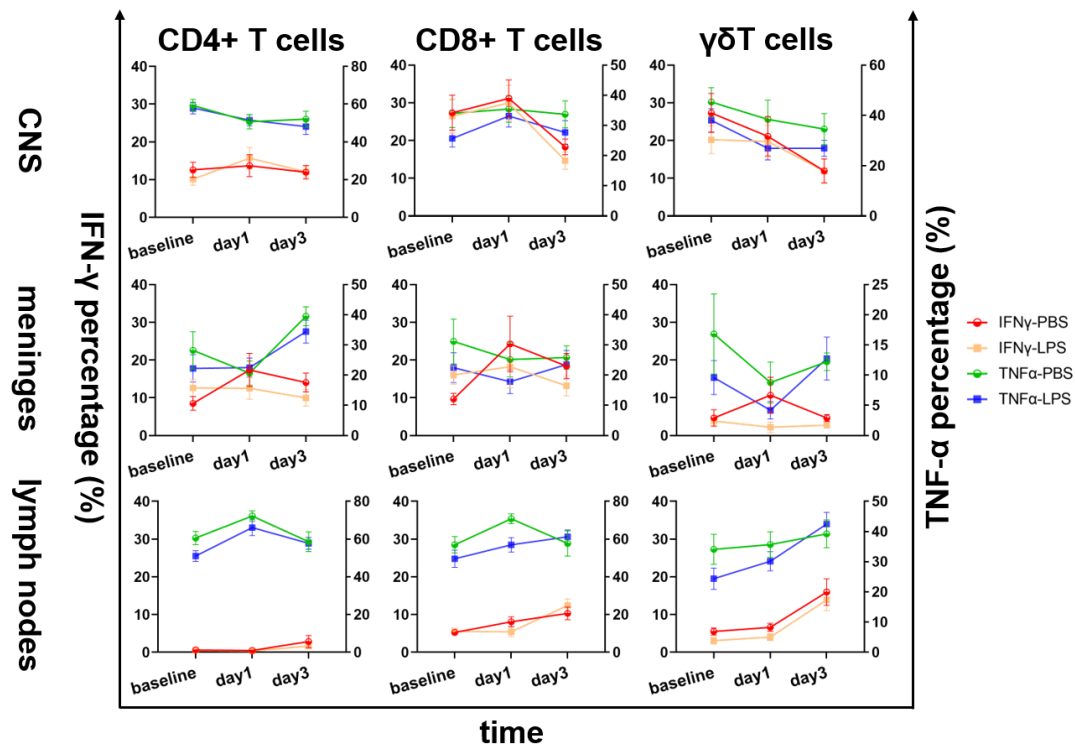


Figure 17. Cytokine levels of IFN- γ and TNF- α in CD4+T cells, CD8+ T cells and $\gamma\delta$ T cells from brains, meninges, and lymph nodes at different time point. Abbreviation: PBS, phosphate-buffered saline; LPS, lipopolysaccharide; IFN- γ , interferon- γ ; TNF- α , tumor necrotic factor- α .

4.3 Exploration of immune tolerance induction on long-term outcome post-stroke

During ischemia microglia do not only contribute to acute inflammation but also to chronic neurodegenerative and recovery mechanisms (Wang et al., 2022). Therefore, in a second cohort, we wanted to investigate the impact of microglial immune tolerance on regenerative mechanisms until 14 days post-ischemia. In total 28 mice (PBS, n=15; LPS, n=13) were included for the long-term stroke analysis with tMCAO stroke modelling performed with 50 minutes occlusion before reperfusion. Among all mice, totally 25 mice were involved in behavior studies (PBS, n=14; LPS, n=11).

4.3.1 Stroke lesion size slightly decreases after inductions of immune tolerance in microglia

In order to analyze potential changes in lesion size and atrophy volume up to 14 days post-ischemia, MRI measurements at day 1, 3 and 14 were included in the analysis.

When comparing acute tissue damage, the LPS group showed less stroke volume than the PBS group with a strong trend on day 1 and a significant result on day 3 post-stroke (day 1: PBS, 54.33 ± 10.76 , LPS, 46.01 ± 13.74 , $p=0.09$; day 3, PBS: 51.72 ± 10.01 , LPS, 39.20 ± 16.69 , $p=0.022$) (**Figure 18A and B**). Moreover, the lesion size dynamics from day 1 to day 3 (**Figure 18C**) indicated a significantly faster recovery of the LPS group with a decreasing volume of tissue damage (PBS, $-5.45 \pm 10.71\%$, LPS, $-19.35 \pm 4.95\%$, $p=0.022$).

Due to the large variance of tissue recovery, MRI at day 14 post-ischemia is used to calculate brain atrophy instead of tissue damage. As a consequence, the healthy tissue preserved rate instead of lesion size was recorded for identifying tissue repairing and preservation differences between the LPS and PBS group. The LPS group showed a gently higher preserved rate (PBS, $85.29 \pm 6.33\%$, LPS, $86.96 \pm 7.71\%$, $p=0.53$) (**Figure 18D**).

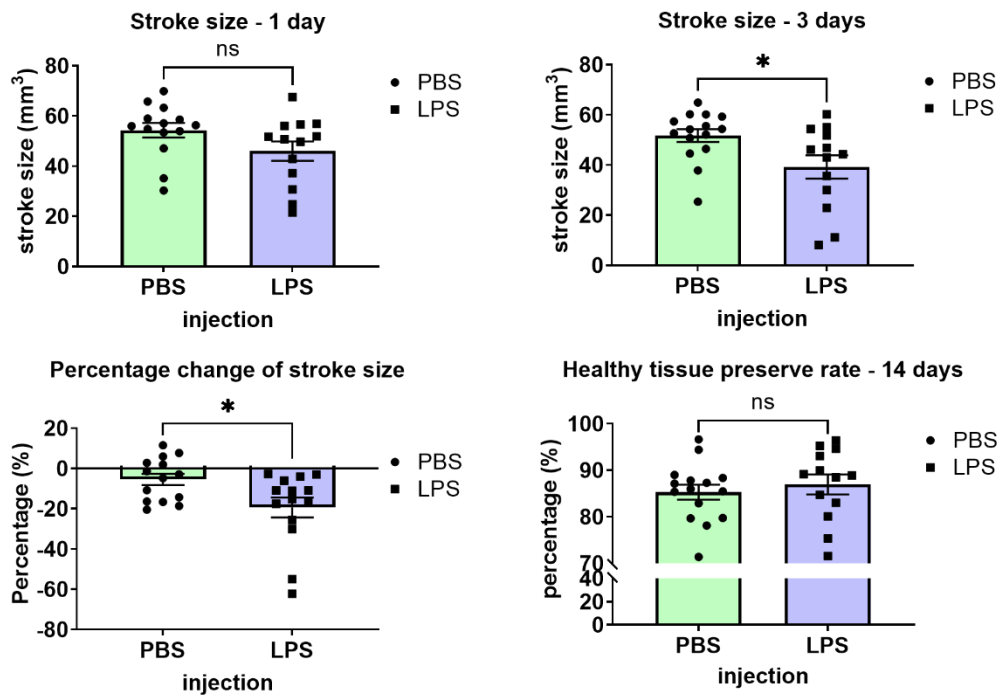


Figure 18. Stroke lesion size at different time points post-stroke. (A) Stroke lesion size comparison on 1 day after stroke. (B) Stroke lesion size comparison on 3 days after stroke. (C) Stroke recovery percentage from day 1 to day 3 after stroke. (D) Healthy tissue preserved rate on the ipsilateral hemisphere on day 14 after stroke calculated by measuring brain atrophy. Mouse count: PBS, n=15; LPS, n=13. (ns: $p>0.05$; *: $p<0.05$. Statistics: unpaired t-test.) Abbreviation: PBS, phosphate-buffered saline; LPS, lipopolysaccharide; ns: not significant.

4.3.2 Immune tolerance modified behavior outcome post-stroke

To observe the alteration of behavioral performance as an indicator of stroke recovery, an Open field test and a Y-maze test were applied to explore the locomotion, anxiety-behavior, and short spatial memory function respectively. For a better visualization, all data were transformed to the form of ratio to respective preinjection (baseline) values. To make the data comparable, preinjection data were first normalized by z-transformation by the injection groups, and add 1 to keep mean value as 1. Specially, due to the prenormalization, preinjection data were excluded from the further comparisons. The formula was as followed:

$$\text{standardized value} = 1 + \frac{(\text{original value} - \text{group mean value})}{\text{group standard deviation}}$$

4.3.2.1 Immune tolerance improved the locomotor functions in open field test 14 days post-ischemia

To investigate the anxiety-like behavior and locomotor function to observe a potential impact of microglial immune tolerance on stroke recovery, mice were used in the open field test in preinjection (baseline not shown), preoperative (4 weeks post LPS/PBS injections), postoperative (4-5 days post-stroke) and terminal stage (12-13 days post-stroke) as described in the methods sections (see in section 3.1.4).

Open field test includes parameters that reflect anxiety behavior (**Figure 19A**) and locomotor ability parameters (**Figure 19B**). When comparing the anxiety-like behavior with the control group, the LPS-treated mice exhibited stronger anxiety behavior at preoperative stage on the aspect of center zone count ($p=0.02$) and count percentage of center zone ($p=0.03$) (**Figure 19A**). However, both effects were not observable at the post-stroke time points. In contrast, locomotor activity performed better in the LPS group in the long-term post-stroke stage than the PBS group. This was particularly reflected as an overall significant better performance of distance travelled in all zones ($p=0.02$), and speed travelled in all zones ($p=0.02$), and a trend of overwhelming in speed travelled in peripheral zone ($p=0.09$), at terminal stage (**Figure 19B**). Mice did not exhibit a special preference of zone staying or moving according to the heatmap (**Figure 19C**).

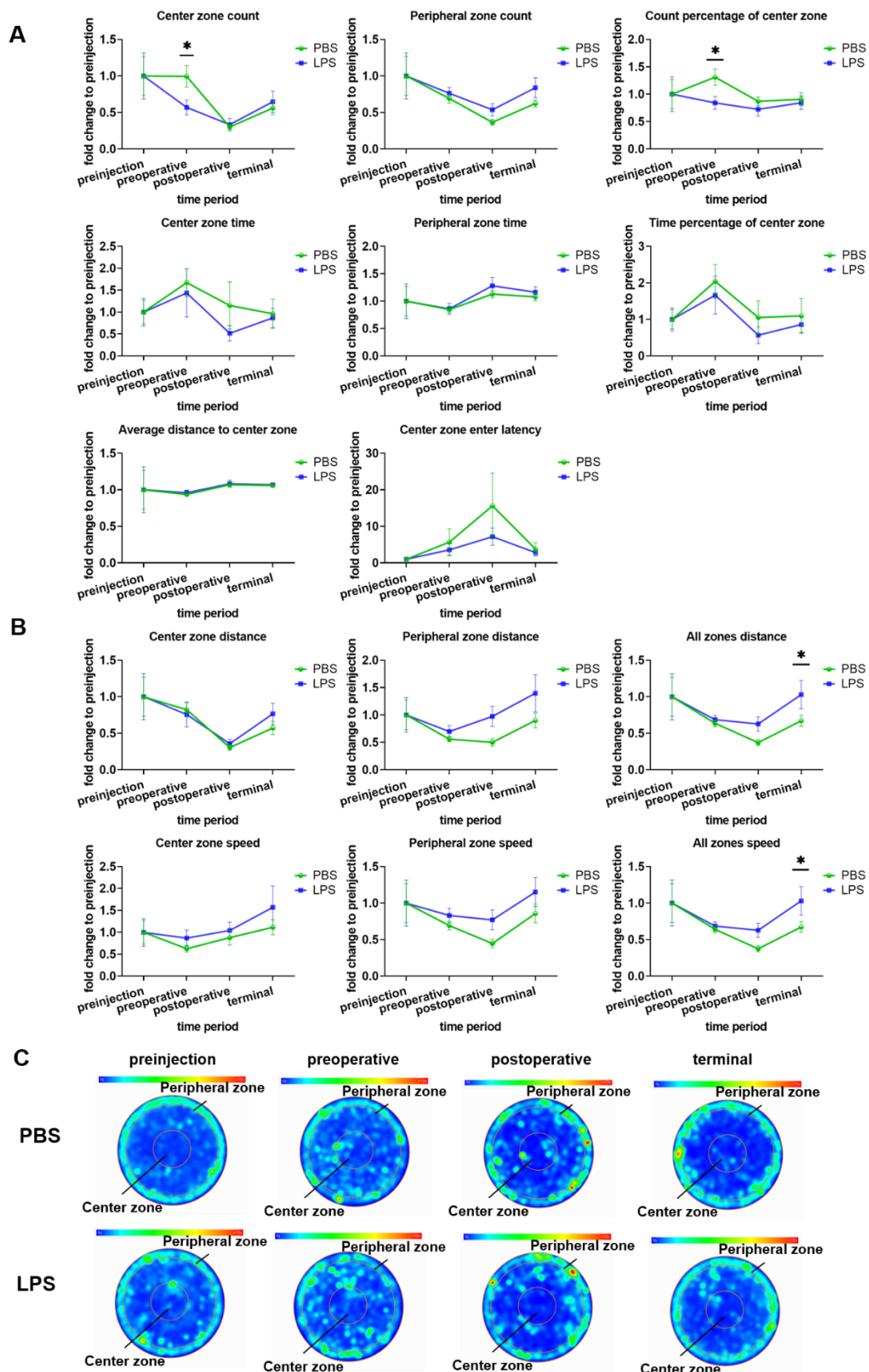


Figure 19. Results of open field testing to investigate anxieties and locomotor function post-stroke
 (A) Timeline of all tested open-field parameter for measuring anxiety level and mobility. Results are standardized to the ratio to preinjection data. (B) Heatmap of mice staying time in different location in

the open field arena. Mouse count: PBS, n=10; LPS, n=9. (ns: $p>0.05$; *: $p<0.05$; **: $p<0.01$. Statistics: two-way ANOVA.) Abbreviation: PBS: phosphate-buffered saline; LPS: lipopolysaccharide; ANOVA: analysis of variance.

4.3.2.2 Microglial immune tolerance does not improve short-term memory

Y-maze test was performed at the same time points as open field test in order to measure the short-term spatial memory function of mice. The details were the same as previously described (section 4.1.2). To begin with, we separately determined the absolute number of entry counts into the previous closed and always open arm (**Figure 20A**). Thereby, the closed arm entry counts reflect the willingness of exploration and short-term memory (Roth et al., 2021). Here we do not observe differences between treatment groups at none of the analyzed timepoints. Also, when calculated the relative entry ratio between the closed and the open arm (**Figure 20B**) mice from both treatment groups exhibited the similar bias to preferring the exploration of the closed arm (shown in detail in **Figure 20C**). The moving trace comparisons are shown in **Figure 20D** and no obvious differences are observed.

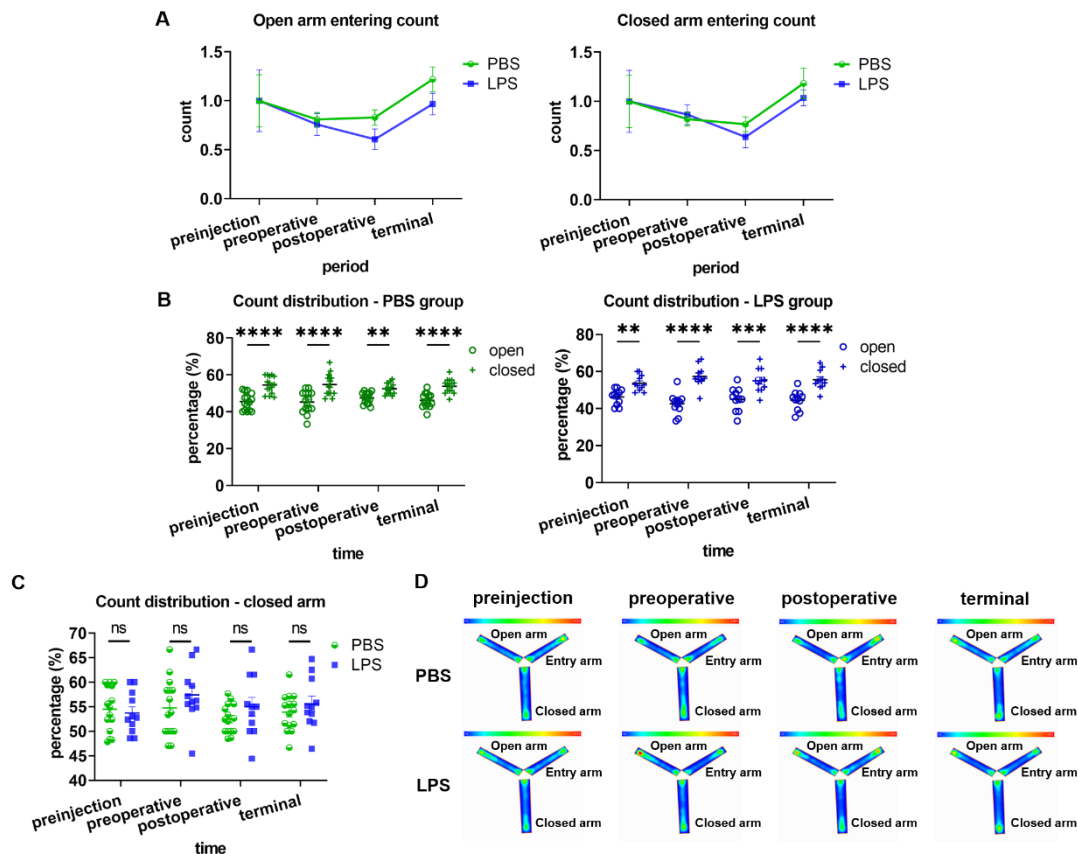


Figure 20. Results of Y-maze test in preinjection, preoperative, postoperative and terminal stage (A) Timeline of open arm entering count, closed arm entering count, in Y-maze arena from preinjection to terminal stage. Results were standardized to the ratio to preinjection data. (B) Comparison of distribution of different arms entering count. (C) Preference comparison of mice entering to closed arm. (D) Heatmaps of mice staying time in different location in Y-maze arena. Mouse count: PBS, n=10; LPS, n=9. (ns: $p > 0.05$; *: $p < 0.05$; **: $p < 0.01$; ***: $p < 0.005$; ****: $p < 0.001$. Statistics: two-way ANOVA.) All data are shown as mean \pm s.e.m. Abbreviation: PBS: phosphate-buffered saline; LPS: lipopolysaccharide; s.e.m: standard error mean; ns: not significant; ANOVA: analysis of variance.

4.3.3 Immune landscape 14 days post-stroke showed no changes in immune tolerance-induced mice

According to the immune cell analysis carried out during the acute phase post-stroke we were interested if microglia influence the subacute immune response of infiltrating immune cells and thus contribute to a dampened immune reaction in the brain that could explain the improved behavioral outcome after the induction of immune tolerance.

4.3.3.1 Cell counts and UMAP distribution showed similarities between PBS and LPS group in the CNS

Cell counts of the analyzed immune cells and subpopulations of infiltrated leukocytes were calculated similar to the analyses at day 1 and day 3 in section 4.2.2. However, in comparison to the number of infiltrated immune cells on day 1 (section 4.2.2), a dramatic increase of cell counts was observed in almost all kinds of cells except neutrophils and macrophages in both groups (B cells, NK cells, all measured T cells, DCs: around 100-1000; macrophages and microglia: around 6000-10000; see details in section 4.2.1, **Figure 13**). Though, no difference can be observed in the overall cell count between LPS and PBS groups at day 14 post-stroke (**Figure 21A**). The high overlap on UMAP visualizations also indicated a similarity on cell subpopulations (**Figure 21B**).

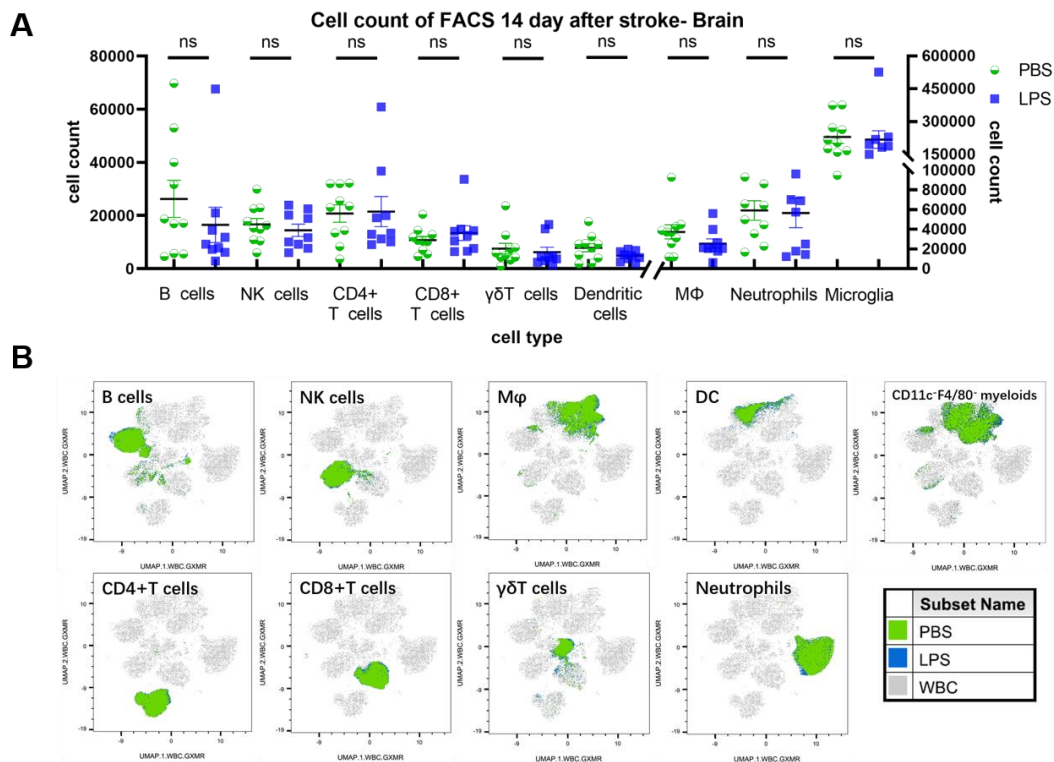


Figure 21. Quantification of infiltrating immune cells in the brain 14 days post-stroke (A) Major peripheral leukocytes and microglia count comparison between PBS and LPS groups 14 days after stroke. All data are shown as mean \pm s.e.m (B) UMAP of major peripheral leukocytes 14 days after stroke. Mouse count: PBS, n=10; LPS, n=9. (ns: $p > 0.05$. Statistics: unpaired t-test) Abbreviation: WBC: white blood cells; PBS: phosphate-buffered saline; LPS: lipopolysaccharide; UMAP: Uniform Manifold Approximation and Projection; s.e.m: standard error mean; ns: not significant.

4.3.3.2 Cell counts and subtypes are comparable between PBS and LPS groups in meninges

Similar to the brain parenchyma, meningeal cell counts were calculated as described in section 4.2.2 to investigate the condition of leukocytes. Unlike in the brain, macrophages are the dominating cell population in the meninges. However, the cell counts in the LPS and the PBS group were similar and showed no trends towards changes in cell number (**Figure 22A**). The UMAP also referred a similarity of leukocyte subpopulations (**Figure 22B**).

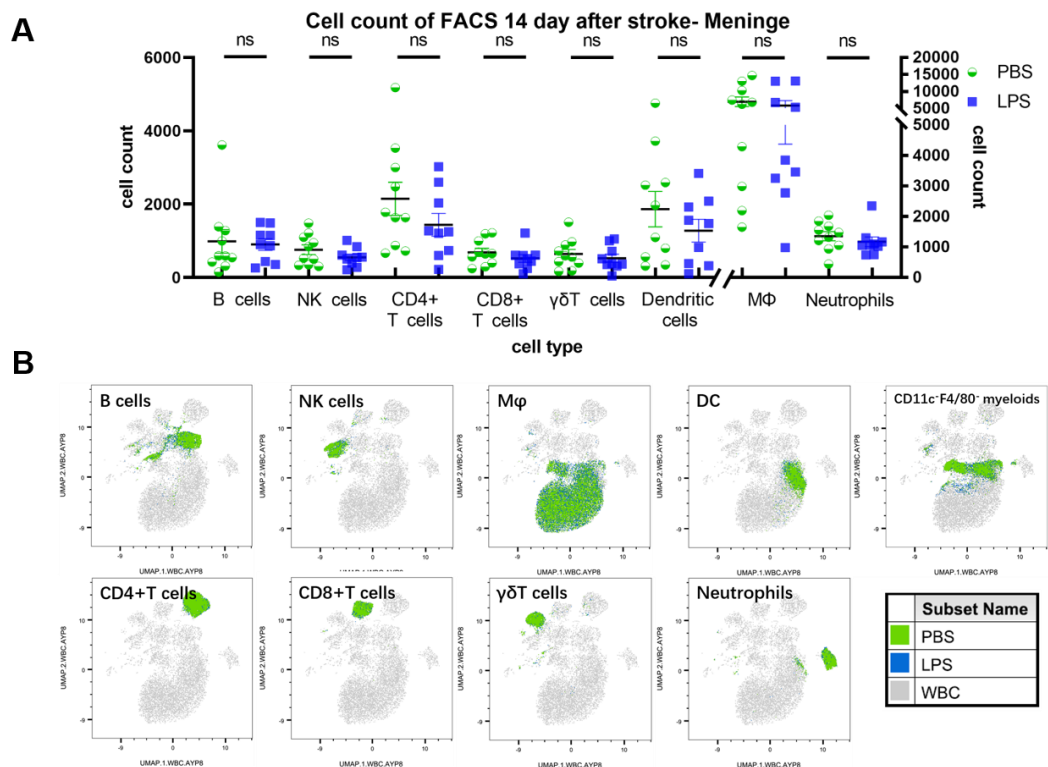


Figure 22. Quantification of leukocytes in the meninges 14 days post-stroke (A) Major peripheral leukocyte counts in comparison between PBS and LPS groups 14 days after stroke. All data are shown as mean \pm s.e.m (B) UMAP of major peripheral leukocytes 14 days after stroke. (ns: $p > 0.05$. Statistics: unpaired t-test) Abbreviation: WBC: white blood cells; PBS: phosphate-buffered saline; LPS: lipopolysaccharide; UMAP: Uniform Manifold Approximation and Projection; s.e.m: standard error mean; ns: not significant.

4.3.3.3 T cell functions are similar regarding pro-inflammatory cytokine releasing

In an additional experiment, T cells were stimulated for cytokine production in order to investigate the pro-inflammatory cytokine releasing function in PBS and LPS groups. Overall, the FACS analysis of the T cell-specific cytokine response shows that T cells

display a higher IFN- γ secretion and lower TNF- α secretion ability than in peripheral tissue (here measured in cervical LNs) at 14 days post-stroke. However, when comparing the LPS group with the PBS group, the cytokines secreted by CD4⁺ and CD8⁺ T cells stay at a similar level (**Figure 23**). The results indicate only a minor or no influence of immune tolerance on T cell-originated pro-inflammatory functions. Nevertheless, though not significant, it is still possible to observe a trend that LPS-treated $\gamma\delta$ T cells from CNS and meninges secrete less TNF- α and IFN- γ than PBS group.

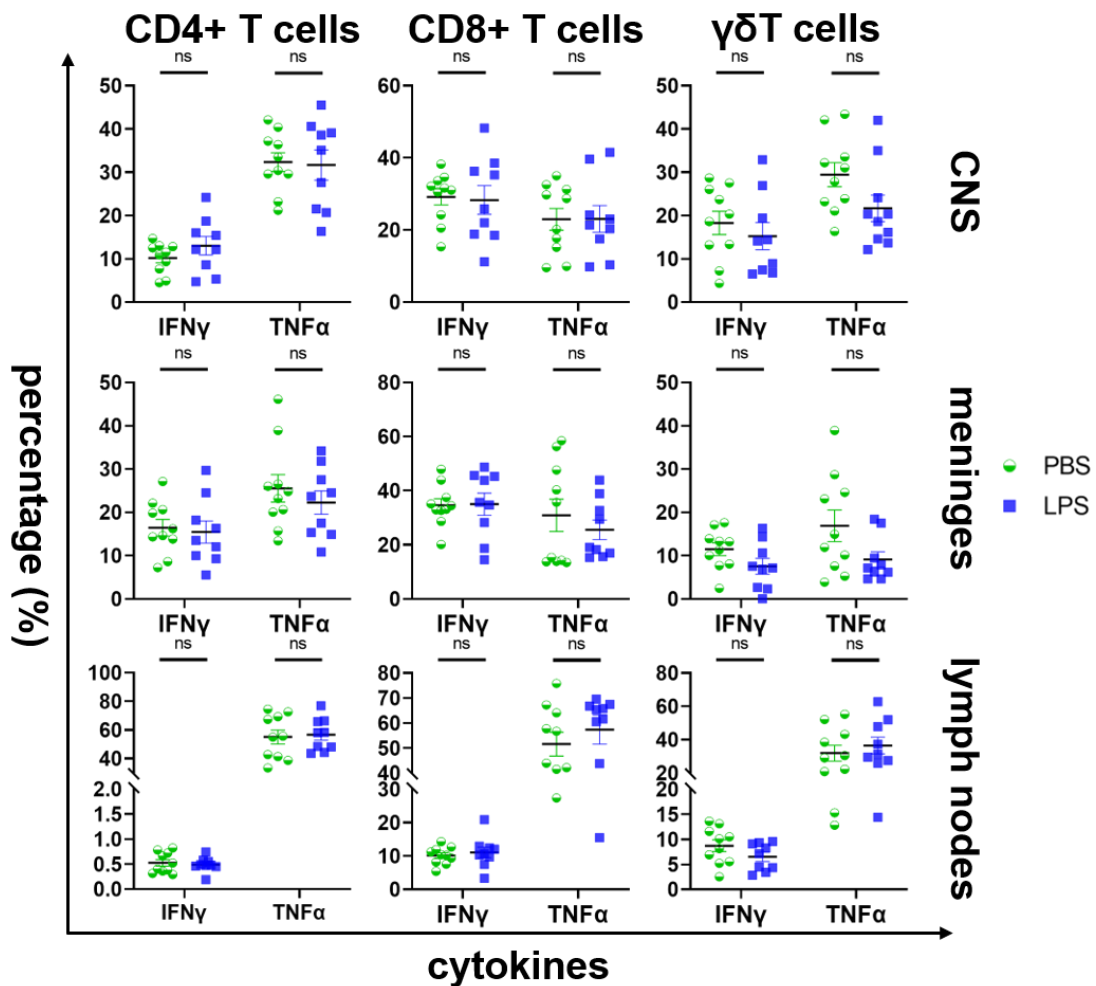


Figure 23. Cytokine levels of IFN- γ and TNF- α in CD4⁺T cells, CD8⁺ T cells and $\gamma\delta$ T cells from brains, meninges, and lymph nodes long-term post-stroke. All data are shown as mean \pm s.e.m. (ns: $p>0.05$) Abbreviation: PBS: phosphate-buffered saline; LPS: lipopolysaccharide; IFN- γ : interferon- γ ; TNF- α : tumor necrotic factor- α ; s.e.m: standard error mean; ns: not significant.

4.4 Exploration of microglia gene expression difference between cortex and subcortical regions

According to the results of stroke lesion size (section 4.3.1), we assumed that the microglia with immune tolerance induction play a protective role as early as 24-hours post-stroke. To investigate the gene expression deviation of microglia from cortical and subcortical regions from the ipsilateral hemisphere with or without prior immune tolerance induction, microglia cells were sorted 1-day post-ischemia and RNA was extracted. Sample pairs (cortical and subcortical microglia populations) with both RIN value over 6 and concentration over 300pg/ μ l were selected for bulk-RNA sequencing analysis. Finally, totally 10 sample pairs underwent bulk-RNA sequencing (PBS, n=5; LPS, n=5).

4.4.1 Quality control and sample distribution

All samples exhibited good sample quality, displayed as balanced GC pair percentage (around 50%) and less than 0.1% error bases (data not shown). The sample homogeneity is exhibited in **Figure 24** which shows the principal component analysis (PCA) result of the 4 tested conditions. On the aspect of PC1, LPS_cortical and LPS_subcortical samples exhibited a high homogeneity respectively. Both PBS-treated sample groups, however, had higher variations among groups.

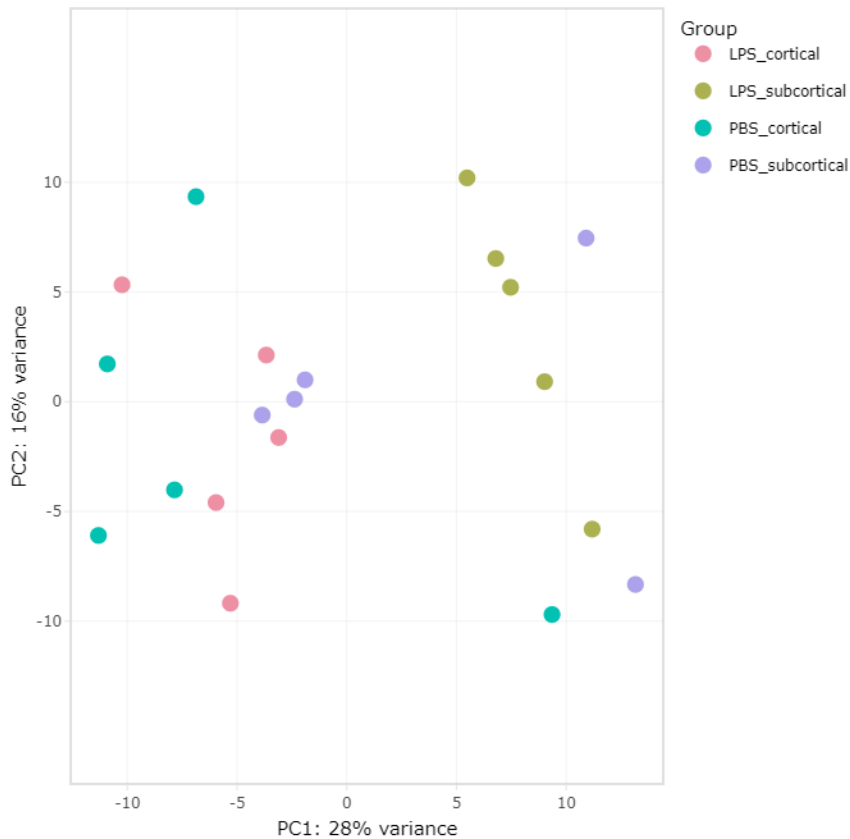


Figure 24. PCA plot of sample homogeneity check. PCA plot of samples from LPS_cortical (n=5), LPS_subcortical (n=5), PBS_cortical (n=5), and PBS_subcortical (n=5) samples. Abbreviations: PCA: principal component analysis; LPS: lipopolysaccharide; PBS: phosphate-buffered saline

4.4.2 Differentially expressed genes between the PBS and LPS group are only found in subcortical microglia

Differentially expressed genes (DEGs) were determined in a direct comparison between the respective brain region (PBS vs LPS in cortical and subcortical group) and significant DEGs were plotted on the heatmap on **Figure 25A**.

Interestingly, in the cortical microglia a highly consistent gene expression between the PBS and LPS conditions were found. None of the genes met the requirement of significant DEGs (**Figure 25B**). However, in the subcortical microglia population 10 genes were proven to be categorized as DEGs. Compared to control group samples (PBS), LPS-treated microglia exhibited higher expression levels of *Slc15a2*, *Hacd4*, *Adgre4*, *Abca9*, *Rnase6*, *Ablim1* and *Thrsp*, and lower levels of *Nqo1*, *Nfib* and *Ncmaph* (**Figure 25C, D**).

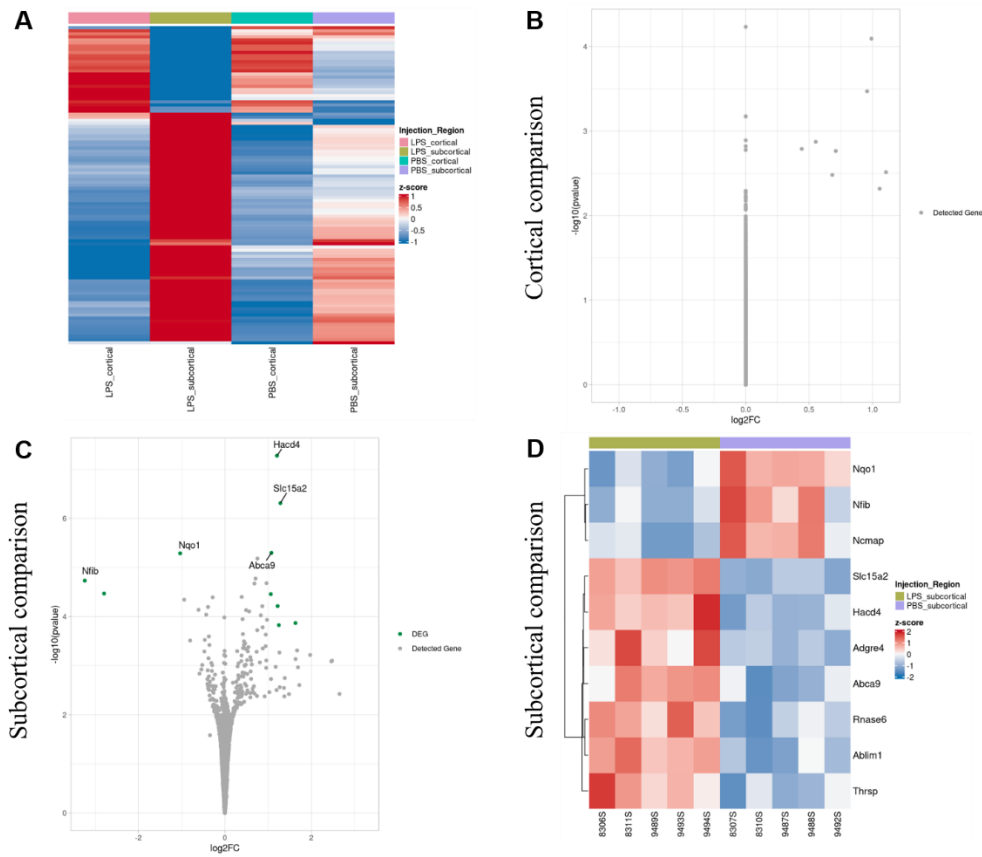


Figure 25. DEGs identified in the comparison of the PBS_cortical versus LPS_cortical group and PBS_subcortical versus LPS_subcortical samples. A: Heatmap of general DEG distributions among all groups; B: volcano plot of the gene expression level comparisons between PBS_cortical versus LPS_cortical group samples; C: volcano plot of the gene expression comparison between PBS_subcortical versus LPS_subcortical group samples; D: heatmap of DEGs between PBS_subcortical versus LPS_subcortical group samples. Abbreviations: DEG: differentially expressed gene; PBS: phosphate-buffered saline; LPS: lipopolysaccharide.

4.4.3 Downstream analyses of Bulk-RNA sequencing data indicated pathways involved in immune tolerance during stroke recovery

After detecting the single DEGs, gene enrichment analysis and transcription regulation analyses were performed to identify the involved pathways and the interactions between transcriptional factors (TFs) and their targets (regulons) during the process of stroke after induction of microglial immune tolerance induction.

As seen in **Figure 26**, compared to control microglia, LPS-treated microglia from the cortex showed significantly downregulated *Myc* targets pathways, oxidative phosphorylation pathways, *E2f* targets pathways as well as DNA repair-related pathways (**Figure 26A**), while microglia from the subcortical region exhibited

downregulated *Myc* targets pathways and oxidative phosphorylation pathways only (**Figure 26B**). There were no pathways upregulated with LPS-immune tolerance induction prior stroke.

Regarding TFs, cortical LPS-treated microglia show similar upregulated genes as microglia in the subcortical tissue (**Figure 26C and D**) compared to the PBS group. Upregulated genes such as *Lyl1*, *Tcf12*, and *Irf4*, and downregulated genes including *Zeb2*, *Zfp263*, and *Myc* were the same in the two different regions.

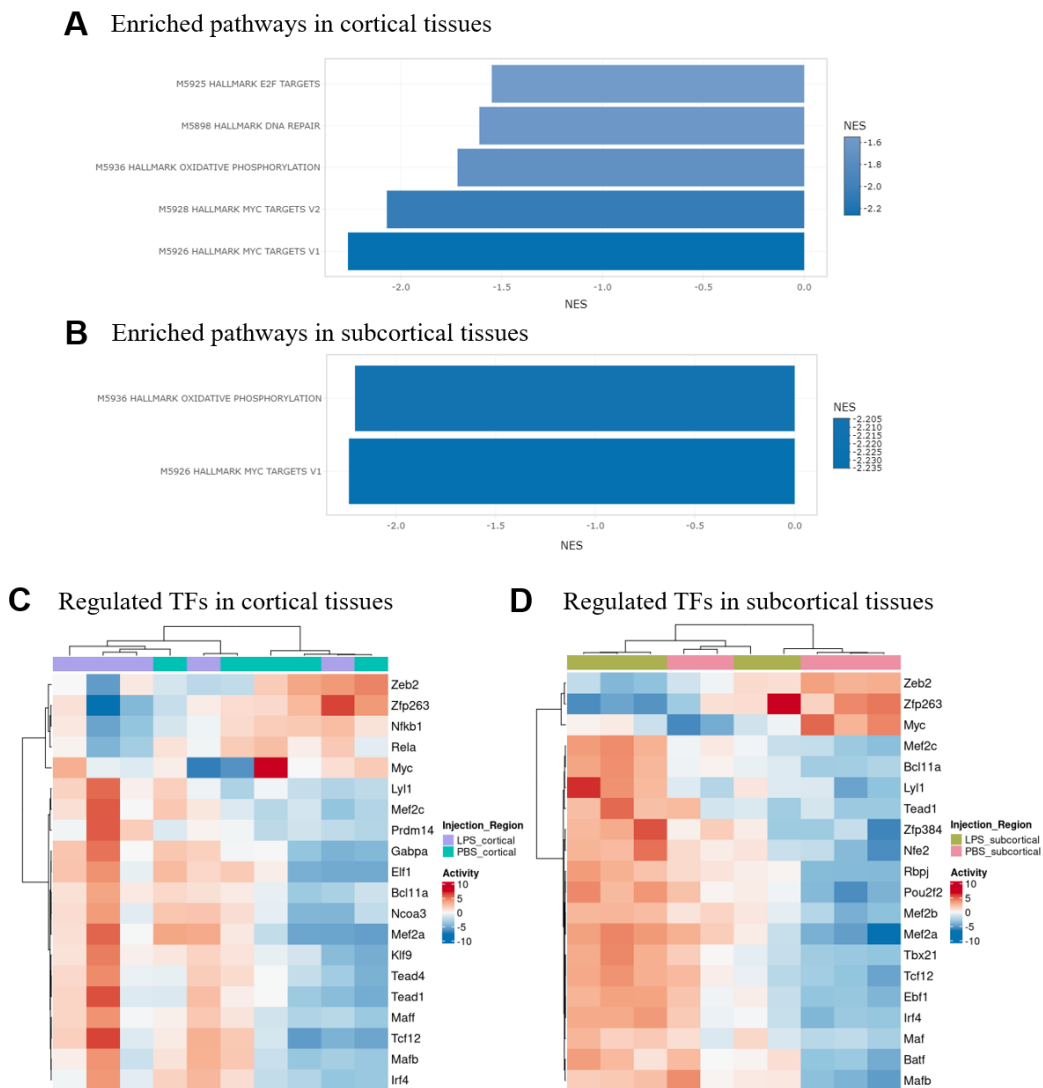


Figure 26. Downstream gene enrichment analysis and transcription regulation analysis. A: GSEA analysis of cortical microglia comparison between the PBS group (n=5) and the LPS group (n=5). B: GSEA analysis of subcortical microglia comparison between the PBS group (n=5) and the LPS group (n=5). C: Transcription regulatory activity analysis of cortical microglia comparison between the PBS group and the LPS group. D: Transcription regulatory activity analysis of subcortical microglia comparison between the PBS group and the LPS group. Abbreviations: GSEA: gene set enrichment analysis; PBS: phosphate-buffered saline; LPS: lipopolysaccharide.

5. Discussion

In this study, we explored the impact of microglial immune tolerance on inflammatory as well as regenerative stroke conditions to investigate potential protective mechanisms of immune tolerance to the induced brain damage. Overall, we observed a decreased stroke lesion size in the early post-stroke stage (day 1/3) and behavior alterations in the late post-stroke stage (day 14). Additionally, we identified microglial gene modifications which indicated an effect of microglial immune tolerance during the acute phase post-stroke.

5.1 Continuous peripheral LPS injections are able to induce immune tolerance in mice

In our study, continuous peripheral LPS administration was applied for immune tolerance induction. We successfully observed the described dramatic bodyweight loss on the first 3 injection days in the LPS group mice compared to the PBS group mice. The bodyweight loss of the LPS treated mice, however, stopped on the 3rd and 4th day, and turned into bodyweight gaining afterwards, indicating a successful immune tolerance induction.

Several studies have used peripheral injections of LPS to induce an inflammatory state in the CNS. Within that context, a single LPS injection followed by the initiation of a neuropathological stimulus pointed to a deterioration of several CNS diseases (Wendeln et al., 2018). However, repeated LPS injections, which cause a prolonged activation of the innate immune system, were able to diminish the pro-inflammatory condition and hence alleviate the subsequent injury (Lajqi et al., 2020, Wendeln et al., 2018). To induce immune tolerance in microglia, preconditioning via four consecutive intraperitoneal LPS injections have been described to efficiently induce a tolerance state of these cells in the brain (Wendeln et al., 2018). The acute exposure to LPS always leads to a pro-inflammatory stage that can be measured by acute bodyweight loss within the first 24h post-injection and observed by a sickness behavior with reduced activity of the mice.

Bodyweight change reflects the establishment of a systemic inflammation in the body. In this study, bodyweight of mice dropped drastically after the first exposure to LPS and gradually recovered afterwards. Such bodyweight drop kept in accordance with previous studies (Norden et al., 2016, Laugero and Moberg, 2000). The first exposure to LPS (first injection) in our setup shares the similar mechanism with immune training induced by a single LPS injection. It is known that the activation of innate immunity directly causes a rise of energy consumption in activated immune cells (Alhadidi and Shah, 2018). LPS in particular causes a metabolic alteration from oxidative phosphorylation to aerobic glycolysis to compensate the inadequate ATP production required to initiate and maintain the immune response. As a consequence, bodyweight as well as body temperature decreases, hence peripheral leukocyte counts increase. Both latter parameters are certainly alternatives to proof activation of innate immunity but were not measured within this study. However, bodyweight owns the advantages of its non-invasiveness as well as fast applicability, which causes the least influences on mice as well as the following experiments.

On the 3rd and 4th day of injection, the LPS-injected mice stopped losing weight, indicating a well-established immune tolerance. Such alteration also suggests a change of metabolic alteration. An *in vitro* study applied peripheral blood mononuclear cells from healthy human donors and induced endotoxin tolerance by LPS incubation. It turned out that tolerated cells exhibit an inhibition of lactate production, indicating a less favor of glycolysis and lower energy demand (Ferreira et al., 2022). Such changes showed the lower activity of immune cells, indicating the induction of immune tolerance by LPS.

After finishing the four LPS injections, bodyweight was monitored weekly to assure proper recovery by an increase in bodyweight. Indeed, the bodyweight in the LPS group increased steadily. As a result, we can observe a diminish of weight difference between PBS and LPS injected groups after the establishment of immune tolerance. As recovery from the systemically induced inflammation by LPS requires energy, we alleviated the bodyweight drop induced by LPS by adding extra nutrition to the LPS injected mice.

However, also 4 weeks after the LPS injections, there was still a slight difference, though without significance in bodyweight between the LPS group and the PBS control group. This result indicated that successful LPS preconditioning has a long-lasting effect, and still plays an unignorable role during the recovery process. To completely rule out a possible effect of an incomplete recovery, one could elongate the refractive time after the injections until mice are used to induce the secondary stimulus or provide stricter nutrition supplement.

5.2 Immune tolerance is able to alleviate stroke lesion size during the early but not the late-stage post-stroke

The function of microglial immune tolerance in stroke recovery is still not clear. In our study, we investigated the impact of microglial immune tolerance on lesion size as well as subsequent immune cell infiltration within the first 72h post-stroke and 14 days post-stroke. As expected, lesion sizes in the LPS treated mice, determined by MRI measurements, tended to be decreased upon immune tolerance induction and were significantly smaller on day 3 post-stroke compared to the control group ($p=0.022$). Moreover, the lesion recovery rate from day 1 to day 3 was higher in the LPS group than in the PBS group ($p=0.022$). Nevertheless, such significance did not appear in the long-term stage ($p=0.53$). This result proved our hypothesis that immune tolerance induction 4-weeks before stroke can alleviate stroke injury and protect the CNS.

Our results find that stroke injuries in the LPS-treated mice are milder and also recover faster in the acute phase than in control group mice. Stroke itself initiates a strong sterile inflammation reaction with microglia, as the residential macrophage in CNS, being the first cells to react to the onset of injury. The induction of microglia immune tolerance is theoretically possible to alleviate stroke injury. However, several published studies applied only a single LPS injection within 3 days before stroke modeling and found smaller stroke lesion size via brain section staining (Rosenzweig et al., 2007, Liang et al., 2011). Both studies emphasized the involvement of LPS-induced microglia activation, indicating that pre-activation of microglia is beneficial for stroke controlling

and recovery. In line with our data, another study used repeated LPS injections that verifiably activated microglia and subsequently observed an anti-inflammatory and protective effect on secondary occurring neurological pathologies (Wendeln et al., 2018).

The impact of microglia immune tolerance on long-term changes and subsequent tissue recovery was non-significant in this study. However, it is still observable that the LPS-treated mice preserved slightly more healthy tissue than control mice. Limited publications studied immune tolerance in a long-term stage of stroke recovery. Zhou et al. reported a long-lasting effect of immune tolerance in a sepsis model. More than 270 days after repeated low-dose LPS administration, mice still exhibited a better performance on behavior studies after the re-introduction of sepsis (Zhou et al., 2020). Since the epigenetic signature of innate immune cells can last for several months, the long-term protection by microglia immune tolerance is theoretically possible to preserve till 14 days post-stroke. We assume that our stroke evaluation method only based on a quantification of the preserved tissue rate on the 14th day post-stroke cannot emphasize the recovery effect appropriately. An in-depth study with further parameter determining tissue recovery is required for validating the long-term protection effect of immune tolerance on stroke recovery.

5.3 Immune tolerance did not alter the immune landscapes after stroke onset

To further investigate the effect of microglial immune tolerance and the subsequent immune cell infiltration and distribution, flow cytometric studies were performed in control, day 1, day 3, and day 14 mice. Stroke alters the immune landscape on CNS not only by activating CNS residential cells, but also recruiting peripheral cells. The adjacent barrier tissues, the meninges, have a close relationship with the brain parenchyma, and were shown to be changed in their immune cell composition upon stroke pathophysiology (Su et al., 2023), however, whether immune tolerance in microglia affects their immunogenicity is not known and was analyzed together with the brain parenchyma. In our study, the changing trend of cell count and distribution in

the LPS-treated mice largely remained similar to PBS-treated mice. Nevertheless, although no significance was observed, a trend of some cell counts being impacted by immune tolerance also indicated some alterations caused by immune tolerance after stroke onset. In particular, a tendency of less macrophages is detected both in day 1 and day 3 in the LPS group compared to the PBS group in the CNS. Moreover, the UMAP shows less overlapping of the macrophage subpopulation, indicating the variation of macrophages among two groups of mice on day 3. Brain macrophages derive from infiltrated monocytes from the periphery. Similar to microglia, they are responsible for pro-inflammatory cytokine release to induce an inflammatory state in the tissue and they can adopt a variety of phenotypes (Krishnan and Lawrence, 2019, Patir et al., 2024). The adaptation of macrophages to the microglial phenotype may indicate a possible compensation effect of microglial immune tolerance by pro-inflammatory macrophages during stroke, which has the potential to neutralize the neuroprotective effect of immune tolerance microglia.

In addition, we also observed slightly higher CNS B cell counts in the PBS group than in the LPS group on day 1 and day 14. Similar to other lymphocytes, B cells are recruited by innate immune cells and reach stroke lesion site by passing the damaged BBB. Until now, the general function of B cells during stroke is not entirely solved. Several studies hold the view that CNS B cells might play a role in post-stroke psychological impairment (Selvaraj et al., 2016, Doyle et al., 2015). Interestingly, this would be in accordance with our result that the LPS mice had better performance on neuropsychiatric function than the control mice. This result might also indicate a possible predictive function of B cells in post-stroke psychological disorders.

We observed a generally unchanged meningeal count with the influence of immune tolerance in stroke. Recently, an increasing number of studies validated that meninges are involved in stroke processes and publications indicated that meningeal innate immunity is involved in several diseases. In meningitis caused by *Neisseria meningitidis* infection, innate immune cells including local macrophages and DCs are activated by bacteria and recruit circulating inflammatory cells (Johswich, 2017).

Another study showed that the skull supplies the meninges and brain border with neutrophils and monocytes, especially under inflammatory circumstances (Cugurra et al., 2021), which support the idea that meninges are the intermediate station of cell migration during diseases. From the abovementioned findings, we initially postulated that modified innate immunity through the induction of immune tolerance can affect the recruitment of cells from circulation and adjacent tissues while stroke onset, and cause the immune reactions thereafter. However, based on our results, we cannot draw the conclusion about the influence of immune tolerance on meninges during stroke processes. Further studies are needed for validation.

In our results, T cell produced pro-inflammatory cytokines remained to a large extent similar in all tissues as well as all time stages (control, day 1, day 3 and day 14). However, some insignificant but still visible deviations are still obtained. Compared to the T cells from the PBS group mice, the LPS-treated T cells from the CNS and meninges produced a comparative lower level of TNF- α and IFN- γ before and after stroke onset, especially in day 1 and 3 (**Figure 17**). Such trend is especially obvious in the comparison of CNS $\gamma\delta$ T cells in all time points.

TNF- α and IFN- γ are pro-inflammatory cytokines. They are majorly produced by microglia, infiltrating T cells (especially CD4⁺ Th1 cells) or NK cells (Yilmaz et al., 2006, Teymuri Kheravi et al., 2021). Released pro-inflammatory cytokines including TNF- α and IFN- γ upregulate the major histocompatibility (MHC) molecule expression level on CNS cells, and further cause the recognition and damage reaction of T cells (Arumugam et al., 2005). In experimental stroke, lymphocyte-deficiency transgenic mice and antibody-mediated T cell depletion mice are both observed with smaller stroke volume (Gill and Veltkamp, 2016). The results explain that microglial immune tolerance is probably protecting the CNS by influencing acquired immunity during stroke through a decrease of pro-inflammatory cytokine production in T cells. On the other hand, the indifference of pro-inflammatory T cells in peripheral lymph nodes indicates the lower connection with microglia during immune tolerance induction. Such consistency also indicates the specific function of microglia and innate immune

tolerance in CNS.

5.4 Immune tolerance alters anxiety-like behavior and locomotor function at different stages but does not influence short-term spatial memory function

In order to measure the impact of microglial immune tolerance on the functional outcome post-stroke, we designed behavior experiments focusing on anxiety-like behavior, locomotor tendency, and short-term spatial memory functions. On the aspect of Open field results to measure anxiety and locomotor functions, the LPS-injected mice performed with better locomotor functions, which exhibited longer travelled distance ($p=0.02$) and faster speed ($p=0.02$) in the whole arena than the PBS mice. This effect was only observable at 14 days but not at the acute post-stroke stage. To exclude effects of LPS injection alone on behavior functions, we analyzed mice with LPS/PBS injections only. 4 weeks after the first injection, we observed an initiation of anxiety-like behavior in mice treated with LPS, which exhibited as longer staying time ($p=0.02$) as well as larger staying time proportion ($p=0.03$) in the center zone than PBS-treated mice, but no effects were observed in locomotor functions. This indicates that the improvement in locomotion seen at 14 days post-stroke is a specific effect of immune memory induced in microglia whereas changes in anxiety may be due to the LPS injections itself. The Open field test is a multi-functional behavior test to distinguish the locomotor tendency and anxiety-like behaviors among mice (Manwani et al., 2011, Ye et al., 2022). It is reported that microglia depletion in rats altered their performance in the Open field test, indicating a relationship between microglia and the locomotor development (Nelson and Lenz, 2017).

The observed an initiation of anxiety-like behavior only 4 weeks after LPS administration, may be a similar effect as in a study that applied GM-CSF to induce innate immune tolerance and successfully affected the anxiety-like behavior after chronic stress modelling (Chen et al., 2022). However, in that study immune tolerance alleviated anxiety. The opposite trend in our results might indicate an influence of the impaired physical constitution caused by LPS (reduced bodyweight) and the related

energy for recovery. However, Kraeuter et al. also mentioned that the anxiety results should be interpreted together with other tests results such as elevated plus maze (Kraeuter et al., 2019a). Such anxiety performance needs further validation. Moreover, the anxiety-like changes disappeared after stroke onset. It may indicate that stroke-related anxiety is so strong that can even diminish the deviation caused by immune tolerance.

We didn't observe any difference in Y-maze tests. Instead, we observed mice in all stages and groups showing a preference of entering the closed arm (all closed arm entry percentage >50%). The Y-maze test reflects short-term spatial memory function. A tendency of exploring unvisited region is the normal reaction. The unbiased arm visiting refers to the hippocampus functional impairment (Kraeuter et al., 2019b). This finding means that the short-term spatial memory function impairment is not that significantly affected by microglial-mediated and initiated immune responses during stroke processes, and thus innate immune tolerance has no impact on this part.

However, although there was no significantly better recovery of stroke lesion in LPS-treated mice than PBS-treated mice (section 4.3.1, **Figure 18D**, healthy tissue preserved rate comparison: $p>0.05$), the difference of behavior performance still exists. It provides evidence of a functional repair caused by immune tolerance which is independent to structural recovery in the CNS.

5.5 Differentially expressed genes and pathways involved in microglia-mediated immune tolerance

For a detailed overview about microglial adaptations on a genetic level due to the induction of immune tolerance prior ischemic stroke, we analyzed gene expression by RNA-sequencing of microglia at day 1 post-stroke. By separating cortical and subcortical regions we were able to analyze the DEGs between microglia from LPS-injected mice and control mice in both cortex and subcortical tissue. In addition, we explored related pathways that are possibly differentially regulated between our treatment groups. To our surprise, no DEGs were detected from the comparison

between cortical microglia in the two groups. DEGs directly reflect the regulation condition of a certain gene and indicate the possible pathways. That none of the detected genes met our threshold of DEG in the comparison between cortical microglia, is in line with unpublished results in our lab showing morphological differences in microglia only in the subcortical region but not in the cortical part (these results are part of the doctoral thesis of Ege Bursali). We assume that there exists a larger heterogeneity of non-active, active and highly active microglia in the cortex due to the varying orientation of the microglia to the lesion size. This may cover the effect of potential changes in microglial in close vicinity of the lesion. Another reason could be the overwhelming inflammatory reaction that might mask the effect of immune tolerance. 10 DEGs were found in microglia isolated from the subcortical region, including upregulated *Slc15a2*, *Hacd4*, *Adgre4*, *Abca9*, *Rnase6*, *Ablim1* and *Thrsp*, and downregulated *Nqo1*, *Nfib* and *Ncmap* genes with LPS injection. Among the abovementioned genes, only a few of them are studied in the context of ischemic stroke. *Ablim1*, for example, is a gene related with axon guidance and outgrowth. Though rarely reported in the field of cerebrovascular diseases, it is a possible gene for the post-stroke repair (Orozco and Edbauer, 2013). Another regulated gene is *Nfib*, which is closely related to neuronal cell development and is expressed on microglia. *Nfib* is reported to be correlated with some mental disorders, brain tumor and Parkinson's disease (El-Hodiri et al., 2022). So far, it is hard to identify its role. But our result shows that *Nfib* downregulation occurs in a less inflammation-involved condition, indicating its possible pro-inflammatory role in stroke that is dampened during immune tolerance. Nevertheless, also some well-studied genes are found which interestingly show an unexpected adverse trend toward our results. *Nqo1*, a gene highly related with microglia and participating in anti-ROS during stroke, is observed downregulated in LPS-treated subcortical microglia. It is not in accordance to our finding because *Nqo1* is related with post-stroke repairment and anti-inflammation (Simpson and Oliver, 2020). Our result indicates less repairment effect in immune tolerance mice during stroke restoration. In a gene set enrichment analysis, we observed 5 downregulated pathways in LPS-

inducted microglia. In particular, we find the downregulation of the *Myc* pathway of the LPS group microglia in both cortical and subcortical tissues. Microglia alter the energy metabolism pattern after immune tolerance induction. The *Myc* pathway is correlated with microglia proliferation which is less mentioned in stroke studies. In a sciatic nerve injury model, the *Myc* gene was upregulated in spinal cord microglia shortly after the injury onset. Knockout of the *Myc* gene led to an inhibition of the *Myc/Cdk1* pathway and stopped early phase microglia proliferation (Tan et al., 2022). Similarly, excessive microglia proliferation causes strong inflammation after stroke injury. The enrichment analysis result about *Myc* pathway provides another mechanism of immune tolerance alleviating stroke, which controls the quantity of microglia and therefore moderates inflammatory insult. In our study, there is a decreasing trend of microglia number with immune tolerance induction compared to the control group on day1, day 3 and day 14 (**Figure 13 and 21**), which supports the anti-inflammatory function of *Myc* post-stroke.

Furthermore, the *E2f* pathway is downregulated in LPS-treated microglia specifically in cortex. *E2f* is an activator sub-family transcription factor consisting of *E2f1* and *E2f2* and is related to cell proliferation and cell cycle-related neuronal death. However, *E2f* and its pathway are less studied on the aspect of ischemic stroke. In other neurological diseases such as traumatic spinal cord injury, *E2f1* and *E2f2* expression was increased in activated microglia, and led to the inflammatory injury. Either intrathecal injection of *E2f* receptor antagonist or *E2f1* or *E2f2* knockout significantly alleviated spinal cord injury (Wu et al., 2015). Our result proves that LPS-induced immune tolerance inhibits the *E2f* pathway and hence controls the inflammatory injury of stroke in the cortex.

However, the oxidative phosphorylation level (OXPHO) and DNA repairment are both downregulated in LPS group microglia. Such results are in fact not beneficial to anti-inflammation or restoration after stroke onset. DNA repairment is obviously a process of tissue repairment after insult. OXPHO process requires oxygen and provides more energy than glycolysis, and possibly promotes the anti-inflammatory microglia proliferation (Devanney et al., 2020). We assume that the abovementioned pathways

are involved but overwhelmed by other anti-inflammatory processes. Further validations are needed to identify the exact function of these pathways in immune tolerance and stroke.

Besides the analysis of DEGs and related pathways, a transcription regulatory activity estimation was performed to infer the involved pathways at the level of proteins and TFs. TFs were found similar regulated in both cortex and subcortical microglia, and several genes with validated protective functions were detected in our results. In detail, in the result of transcriptional regulatory analysis, we can easily find a group of TFs that share the same regulation condition among cortical and subcortical microglia. Downregulation of *Zeb2*, *Zfp263*, and *Myc*, as well as upregulation of *Lyl1*, *Tcf12*, and *Irf4* are shared in the LPS groups in both cortical and subcortical microglia. It indicates that though with different DEGs mentioned above, the general regulation pathways keep similar between cortex and subcortical region with the induction of immune tolerance during stroke. The TFs are generally anti-inflammatory. For example, downregulation of *Myc*, as mentioned above, controls the microglia proliferation and limits inflammatory reactions (Tan et al., 2022). Upregulated *Irf4* gene involves the *Irf5/Irf4* regulatory axis. In a study, it was shown that the inhibition of *Irf5* caused *Irf4* upregulation, which promoted the anti-inflammatory polarization of microglia, quenched the pro-inflammatory response and then improved stroke outcome (Al Mamun et al., 2020). However, genes such as *Zeb2*, which exhibited protective role, also were downregulated in our research. It is related with the TGF- β pathway and promotes post-stroke repair (Wei et al., 2022). The adverse trend is not in line with our observation in the MRI analysis (section 4.3.1), potentially indicating its minor impact on immune tolerance-related stroke protection.

To sum up to the bulk sequencing results, we find pathways and TFs but only minor DEGs that are related immune tolerance mechanisms during stroke. Though with several controversial results, the major findings are correlated with the experimental results and help to explain the protective roles of immune tolerance during stroke repairment.

5.6 Limitations of the study

Besides our findings, that microglial immune tolerance can shape their inflammatory response in the acute phase post-ischemia and thus contribute to less tissue damage, this study inevitably had some drawbacks. First of all, the stroke occlusion strategy varied among different experiments (but never within study groups). The adjustment was applied to reduce the burden and stress of the mice during the experiments and was required to adopt to the surgeons' personal surgical technique. Furthermore, the incubation period for immune tolerance induction remained concerned by the unignorable p value of final bodyweight ($p=0.052$). Although not significant, the result might also indicate a potential effect on mouse growing and development. A longer incubation time is a possible solution. Eventually, this study tended to investigate the immune tolerance of microglia, which is characterized by their epigenetic modification. So far, this part was only assumed from previous publications (Wendeln et al., 2018) but will be confirmed in future studies. The RNA sequencing analysis of bulk microglia gave first insights into the consequences of LPS-induced microglial immune tolerance on a genetic level. However, not all microglia from the cortical and subcortical tissue were in direct contact to the ischemic tissue. Thus, they were not activated and missed to respond with an LPS-induced immune reaction. To specify the analysis to microglia activated by stroke a scRNAseq or the inclusion of a microglial activation marker such as Galectin-3 for microglial sorting could have helped for an in-depth analysis (Garcia-Revilla et al., 2022). To sum up, this study validated the protection function of immune tolerance in stroke with different experimental methods, and made a step forward to the underlying mechanisms. Upcoming studies are still needed for further explorations.

6. Summary

Stroke is a disease with high morbidity and mortality. It causes heavy burdens on patients, care-givers and the society. Besides the primary tissue damage through the hypoxic event, secondary inflammation contributes to delayed cell death in the brain parenchyma. The innate immune system in the CNS, especially microglia, can be primed by peripheral LPS administration, to induce an immune tolerance stage. We hypothesized that LPS-induced CNS innate immune tolerance in microglia is able to alleviate stroke-associated inflammation and improve outcomes. In order to test this hypothesis, acute (short-term) and subacute (long-term) studies post-ischemia were conducted. In the short-term study, FACS analysis was performed to validate the alteration of the immune landscape in the CNS, including brain and meninges upon microglia immune tolerance. Of note, no statistical difference in the immune cell composition could be observed. Also, the FACS results at day 14 post-ischemia showed a generally unchanged immune landscape within the LPS immune tolerance group after compared to the control group. However, when investigating the impact of immune-tolerance in microglia on lesion size and functional outcome, LPS-injected mice showed a significant smaller lesion size on day 3 and better recovery rate from day 1 to day 3. Furthermore, a tendency of smaller stroke sizes in the LPS-group on day 1 and day 14 were also observed. Moreover, the LPS group performed better in anxiety-like behavior 4 weeks after immune tolerance induction and in locomotor function in the open field test 14 days post-stroke, but don't show improvement on short-term spatial memory. In bulk-RNA sequencing, the downstream analysis revealed an anti-inflammatory transformation of microglia function in both cortical and subcortical microglia in LPS-treated mice on the aspect of downregulation of oxidative phosphorylation, *E2f* pathway and *Myc* pathway. In this study, we demonstrate the anti-inflammatory functions of innate immune tolerance induction on stroke recovery, indicating a therapeutic potential on targeting CNS innate immunity.

Zusammenfassung

Der Schlaganfall ist eine Krankheit mit hoher Morbidität und Mortalität, die für Patienten, Pflegepersonal und die Gesellschaft eine große Belastung darstellt. Neben der primären Gewebeschädigung durch das hypoxische Ereignis trägt eine sekundäre Entzündung zum verzögerten Zelltod im Hirnparenchym bei. Das angeborene Immunsystem im ZNS, insbesondere repräsentiert durch Mikroglia, kann durch periphere Injektionen von LPS aktiviert und in eine entzündungshemmende Immuntoleranzphase gebracht werden. Um zu überprüfen, dass die LPS-induzierte Immuntoleranz in Mikroglia in der Lage ist, die Entzündungsreaktion des Schlaganfalls zu lindern, wurden Kurz- und Langzeitexperimente durchgeführt. Zu Beginn wurde in der Kurzzeitstudie (1/3 Tage nach Schlaganfall) eine FACS-Analyse durchgeführt, um Veränderungen der Immunzellzusammensetzung im Gehirn sowie den Hirnhäuten zu überprüfen. Hierbei wurde kein statistischer Unterschied zwischen der LPS-Gruppe und der Kontrollgruppe festgestellt. Auch die langfristigen FACS-Ergebnisse (14 Tage nach Schlaganfall) zeigen eine im Allgemeinen unveränderte Immunlandschaft nach Induktion von Immuntoleranz in Mikroglia im Vergleich zur Kontrollgruppe. Bei der Untersuchung der Auswirkungen der Immuntoleranz in den Mikroglia auf die Größe der Schlaganfallläsion und das funktionelle Outcome konnte jedoch eine signifikant kleinere Läsionsgröße an Tag 3 und ein stärkerer Rückgang der Läsion von Tag 1 bis Tag 3 beobachtet werden. Eine Tendenz zu einer geringeren Schlaganfallgröße nach LPS-induzierter Immuntoleranz in Mikroglia an Tag 1 und Tag 14 wurde ebenfalls beobachtet. Darüber hinaus zeigte die LPS-Gruppe 4 Wochen nach der Immuntoleranzinduktion (ohne Schlaganfall) ein verändertes Angstverhalten, sowie eine verstärkte Fortbewegung im Openfield-Test 14 Tage nach dem Schlaganfall, jedoch keine Verbesserung des Kurzzeitgedächtnisses. In einer sich anschließenden Sequenzierung des Transkriptoms der Mikroglia zeigte die durchgeführte Analyse eine entzündungshemmende Veränderung der Mikrogliafunktion sowohl in den kortikalen als auch in den subkortikalen Mikroglia in LPS-behandelten Mäusen unter dem Aspekt der Herunterregulierung der oxidativen Phosphorylierung, des E2f-Signalweges und

des Myc Signalweges. In dieser Studie konnten wir die entzündungshemmende Wirkung der Induktion einer angeborenen Immuntoleranz auf die Erholung nach einem Schlaganfall nachweisen, was auf ein therapeutisches Potenzial der angeborenen Immunität im ZNS hinweist.

7. Bibliography

- Ahmed, S. H., He, Y. Y., Nassief, A., Xu, J., Xu, X. M., Hsu, C. Y. & Faraci, F. M. 2000. Effects of lipopolysaccharide priming on acute ischemic brain injury. *Stroke*, 31, 193-9.
- Al Mamun, A., Chauhan, A., Qi, S., Ngwa, C., Xu, Y., Sharmeen, R., Hazen, A. L., Li, J., Aronowski, J. A., Mccullough, L. D. & Liu, F. 2020. Microglial IRF5-IRF4 regulatory axis regulates neuroinflammation after cerebral ischemia and impacts stroke outcomes. *Proc Natl Acad Sci U S A*, 117, 1742-1752.
- Alhadidi, Q. & Shah, Z. A. 2018. Cofilin Mediates LPS-Induced Microglial Cell Activation and Associated Neurotoxicity Through Activation of NF-kappaB and JAK-STAT Pathway. *Mol Neurobiol*, 55, 1676-1691.
- Arumugam, T. V., Granger, D. N. & Mattson, M. P. 2005. Stroke and T-cells. *Neuromolecular Med*, 7, 229-42.
- Azad, T. D., Veeravagu, A. & Steinberg, G. K. 2016. Neurorestoration after stroke. *Neurosurg Focus*, 40, E2.
- Beuker, C., Schafflick, D., Strecker, J. K., Heming, M., Li, X., Wolbert, J., Schmidt-Pogoda, A., Thomas, C., Kuhlmann, T., Aranda-Pardos, I., N, A. G., Kumar, P. A., Werner, Y., Kilic, E., Hermann, D. M., Wiendl, H., Stumm, R., Meyer Zu Horste, G. & Minnerup, J. 2022. Stroke induces disease-specific myeloid cells in the brain parenchyma and pia. *Nat Commun*, 13, 945.
- Borst, K., Dumas, A. A. & Prinz, M. 2021. Microglia: Immune and non-immune functions. *Immunity*, 54, 2194-2208.
- Campbell, B. C. V., De Silva, D. A., Macleod, M. R., Coutts, S. B., Schwamm, L. H., Davis, S. M. & Donnan, G. A. 2019. Ischaemic stroke. *Nat Rev Dis Primers*, 5, 70.
- Chen, D., Yu, S. P. & Wei, L. 2014. Ion channels in regulation of neuronal regenerative activities. *Transl Stroke Res*, 5, 156-62.
- Chen, X. & Holtzman, D. M. 2022. Emerging roles of innate and adaptive immunity in Alzheimer's disease. *Immunity*, 55, 2236-2254.
- Chen, Z., Liu, H., Ye, Y., Chen, D., Lu, Q., Lu, X. & Huang, C. 2022. Granulocyte-macrophage colony-stimulating factor-triggered innate immune tolerance against chronic stress-induced behavioral abnormalities in mice. *Int Immunopharmacol*, 109, 108924.
- Cheong, J. G., Ravishankar, A., Sharma, S., Parkhurst, C. N., Grassmann, S. A., Wingert, C. K., Laurent, P., Ma, S., Paddock, L., Miranda, I. C., Karakaslar, E. O., Nehar-Belaid, D., Thibodeau, A., Bale, M. J., Kartha, V. K., Yee, J. K., Mays, M. Y., Jiang, C., Daman, A. W., Martinez De Paz, A., Ahimovic, D., Ramos, V., Lercher, A., Nielsen, E., Alvarez-Mulett, S., Zheng, L., Earl, A., Yallowitz, A., Robbins, L., Lafond, E., Weidman, K. L., Racine-Brzostek, S., Yang, H. S., Price, D. R., Leyre, L., Rendeiro, A. F., Ravichandran, H., Kim, J., Borczuk, A. C., Rice, C. M., Jones, R. B., Schenck, E. J., Kaner, R. J., Chadburn, A., Zhao, Z., Pascual, V., Elemento, O., Schwartz, R. E., Buenrostro, J. D., Niec, R. E., Barrat, F. J., Lief, L., Sun, J. C., Ucar, D. &

- Josefowicz, S. Z. 2023. Epigenetic memory of coronavirus infection in innate immune cells and their progenitors. *Cell*, 186, 3882-3902 e24.
- Chu, H. X., Broughton, B. R., Kim, H. A., Lee, S., Drummond, G. R. & Sobey, C. G. 2015. Evidence That Ly6C(hi) Monocytes are Protective in Acute Ischemic Stroke by Promoting M2 Macrophage Polarization. *Stroke*, 46, 1929-37.
- Crupi, R., Di Paola, R., Esposito, E. & Cuzzocrea, S. 2018. Middle Cerebral Artery Occlusion by an Intraluminal Suture Method. *Methods Mol Biol*, 1727, 393-401.
- Cruz-Carrillo, G. & Camacho-Morales, A. 2021. Metabolic Flexibility Assists Reprogramming of Central and Peripheral Innate Immunity During Neurodevelopment. *Mol Neurobiol*, 58, 703-718.
- Cugurra, A., Mamuladze, T., Rustenhoven, J., Dykstra, T., Beroshvili, G., Greenberg, Z., Baker, W., Papadopoulos, Z., Drieu, A., Blackburn, S., Kanamori, M., Brioschi, S., Herz, J., Schuettpelz, L., Colonna, M., Smirnov, I. & Kipnis, J. 2021. Skull and vertebral bone marrow are myeloid cell reservoirs for the meninges and CNS parenchyma. *Science*, Jul 23, eabf7844.
- Denorme, F., Rustad, J. L. & Campbell, R. A. 2021. Brothers in arms: platelets and neutrophils in ischemic stroke. *Curr Opin Hematol*, 28, 301-307.
- Devanney, N. A., Stewart, A. N. & Gensel, J. C. 2020. Microglia and macrophage metabolism in CNS injury and disease: The role of immunometabolism in neurodegeneration and neurotrauma. *Exp Neurol*, 329, 113310.
- Divangahi, M., Aaby, P., Khader, S. A., Barreiro, L. B., Bekkering, S., Chavakis, T., Van Crevel, R., Curtis, N., Dinardo, A. R., Dominguez-Andres, J., Duivenvoorden, R., Fanucchi, S., Fayad, Z., Fuchs, E., Hamon, M., Jeffrey, K. L., Khan, N., Joosten, L. a. B., Kaufmann, E., Latz, E., Matarese, G., Van Der Meer, J. W. M., Mhlanga, M., Moorlag, S., Mulder, W. J. M., Naik, S., Novakovic, B., O'Neill, L., Ochando, J., Ozato, K., Riksen, N. P., Sauerwein, R., Sherwood, E. R., Schlitzer, A., Schultze, J. L., Sieweke, M. H., Benn, C. S., Stunnenberg, H., Sun, J., Van De Veerdonk, F. L., Weis, S., Williams, D. L., Xavier, R. & Netea, M. G. 2021. Trained immunity, tolerance, priming and differentiation: distinct immunological processes. *Nat Immunol*, 22, 2-6.
- Doyle, K. P., Quach, L. N., Sole, M., Axtell, R. C., Nguyen, T. V., Soler-Llavina, G. J., Jurado, S., Han, J., Steinman, L., Longo, F. M., Schneider, J. A., Malenka, R. C. & Buckwalter, M. S. 2015. B-lymphocyte-mediated delayed cognitive impairment following stroke. *J Neurosci*, 35, 2133-45.
- Easton, A. S. 2013. Neutrophils and stroke - can neutrophils mitigate disease in the central nervous system? *Int Immunopharmacol*, 17, 1218-25.
- El-Hodiri, H. M., Campbell, W. A., Kelly, L. E., Hawthorn, E. C., Schwartz, M., Jalligampala, A., Mccall, M. A., Meyer, K. & Fischer, A. J. 2022. Nuclear Factor I in neurons, glia and during the formation of Muller glia-derived progenitor cells in avian, porcine and primate retinas. *J Comp Neurol*, 530, 1213-1230.
- Feigin, V. L., Owolabi, M. O. & World Stroke Organization-Lancet Neurology Commission Stroke Collaboration, G. 2023. Pragmatic solutions to reduce the

- global burden of stroke: a World Stroke Organization-Lancet Neurology Commission. *Lancet Neurol*, 22, 1160-1206.
- Feil, K., Reidler, P., Kunz, W. G., Kupper, C., Heinrich, J., Laub, C., Muller, K., Voglein, J., Liebig, T., Dieterich, M. & Kellert, L. 2020. Addressing a real-life problem: treatment with intravenous thrombolysis and mechanical thrombectomy in acute stroke patients with an extended time window beyond 4.5 h based on computed tomography perfusion imaging. *Eur J Neurol*, 27, 168-174.
- Felger, J. C., Abe, T., Kaunzner, U. W., Gottfried-Blackmore, A., Gal-Toth, J., Mcewen, B. S., Iadecola, C. & Bulloch, K. 2010. Brain dendritic cells in ischemic stroke: time course, activation state, and origin. *Brain Behav Immun*, 24, 724-37.
- Feng, L., Tian, R., Mu, X., Chen, C., Zhang, Y., Cui, J., Song, Y., Liu, Y., Zhang, M., Shi, L., Sun, Y., Li, L. & Yi, W. 2022. Identification of Genes Linking Natural Killer Cells to Apoptosis in Acute Myocardial Infarction and Ischemic Stroke. *Frontiers in Immunology*, 13.
- Ferreira, B. L., Sousa, M. B., Leite, G. G. F., Brunialti, M. K. C., Nishiduka, E. S., Tashima, A. K., Van Der Poll, T. & Salomao, R. 2022. Glucose metabolism is upregulated in the mononuclear cell proteome during sepsis and supports endotoxin-tolerant cell function. *Front Immunol*, 13, 1051514.
- Garcia-Alonso, L., Holland, C. H., Ibrahim, M. M., Turei, D. & Saez-Rodriguez, J. 2019. Benchmark and integration of resources for the estimation of human transcription factor activities. *Genome Res*, 29, 1363-1375.
- Garcia-Culebras, A., Duran-Laforet, V., Pena-Martinez, C., Ballesteros, I., Pradillo, J. M., Diaz-Guzman, J., Lizasoain, I. & Moro, M. A. 2018. Myeloid cells as therapeutic targets in neuroinflammation after stroke: Specific roles of neutrophils and neutrophil-platelet interactions. *J Cereb Blood Flow Metab*, 38, 2150-2164.
- Garcia-Revilla, J., Boza-Serrano, A., Espinosa-Oliva, A. M., Soto, M. S., Deierborg, T., Ruiz, R., De Pablos, R. M., Burguillos, M. A. & Venero, J. L. 2022. Galectin-3, a rising star in modulating microglia activation under conditions of neurodegeneration. *Cell Death Dis*, 13, 628.
- Geckin, B., Konstantin Fohse, F., Dominguez-Andres, J. & Netea, M. G. 2022. Trained immunity: implications for vaccination. *Curr Opin Immunol*, 77, 102190.
- Gelderblom, M., Koch, S., Strecker, J. K., Jorgensen, C., Garcia-Bonilla, L., Ludewig, P., Schadlich, I. S., Piepke, M., Degenhardt, K., Bernreuther, C., Pinnschmidt, H., Arumugam, T. V., Thomalla, G., Faber, C., Sedlacik, J., Gerloff, C., Minnerup, J., Clausen, B. H., Anrather, J. & Magnus, T. 2023. A preclinical randomized controlled multi-centre trial of anti-interleukin-17A treatment for acute ischaemic stroke. *Brain Commun*, 5, fcad090.
- Gelderblom, M., Leypoldt, F., Steinbach, K., Behrens, D., Choe, C. U., Siler, D. A., Arumugam, T. V., Orthey, E., Gerloff, C., Tolosa, E. & Magnus, T. 2009. Temporal and spatial dynamics of cerebral immune cell accumulation in

- stroke. *Stroke*, 40, 1849-57.
- Gelderblom, M., Weymar, A., Bernreuther, C., Velden, J., Arunachalam, P., Steinbach, K., Orthey, E., Arumugam, T. V., Leypoldt, F., Simova, O., Thom, V., Friese, M. A., Prinz, I., Holscher, C., Glatzel, M., Korn, T., Gerloff, C., Tolosa, E. & Magnus, T. 2012. Neutralization of the IL-17 axis diminishes neutrophil invasion and protects from ischemic stroke. *Blood*, 120, 3793-802.
- Gill, D. & Veltkamp, R. 2016. Dynamics of T cell responses after stroke. *Curr Opin Pharmacol*, 26, 26-32.
- Gong, P., Liu, Y., Gong, Y., Chen, G., Zhang, X., Wang, S., Zhou, F., Duan, R., Chen, W., Huang, T., Wang, M., Deng, Q., Shi, H., Zhou, J., Jiang, T. & Zhang, Y. 2021. The association of neutrophil to lymphocyte ratio, platelet to lymphocyte ratio, and lymphocyte to monocyte ratio with post-thrombolysis early neurological outcomes in patients with acute ischemic stroke. *J Neuroinflammation*, 18, 51.
- Guzik, A. & Bushnell, C. 2017. Stroke Epidemiology and Risk Factor Management. *Continuum (Minneap Minn)*, 23, 15-39.
- Hackett, C. J. 2003. Innate immune activation as a broad-spectrum biodefense strategy: prospects and research challenges. *J Allergy Clin Immunol*, 112, 686-94.
- Hamner, M. A., Ye, Z., Lee, R. V., Colman, J. R., Le, T., Gong, D. C., Ransom, B. R. & Weinstein, J. R. 2015. Ischemic Preconditioning in White Matter: Magnitude and Mechanism. *J Neurosci*, 35, 15599-611.
- Han, J., Gu, X., Li, Y. & Wu, Q. 2020. Mechanisms of BCG in the treatment of bladder cancer-current understanding and the prospect. *Biomed Pharmacother*, 129, 110393.
- Handley, A., Medcalf, P., Hellier, K. & Dutta, D. 2009. Movement disorders after stroke. *Age Ageing*, 38, 260-6.
- Helboe, K. S., Eddelien, H. S. & Kruuse, C. 2023. Visual symptoms in acute stroke - A systematic review of observational studies. *Clin Neurol Neurosurg*, 229, 107749.
- Hossmann, K. A. 2012. The two pathophysiologies of focal brain ischemia: implications for translational stroke research. *J Cereb Blood Flow Metab*, 32, 1310-6.
- Howells, D. W., Porritt, M. J., Rewell, S. S., O'collins, V., Sena, E. S., Van Der Worp, H. B., Traystman, R. J. & Macleod, M. R. 2010. Different strokes for different folks: the rich diversity of animal models of focal cerebral ischemia. *J Cereb Blood Flow Metab*, 30, 1412-31.
- Hu, P., Yang, Q., Kong, L., Hu, L. & Zeng, L. 2018. Relationship between the anxiety/depression and care burden of the major caregiver of stroke patients. *Medicine (Baltimore)*, 97, e12638.
- Hughes, H. K., Moreno, R. J. & Ashwood, P. 2023. Innate immune dysfunction and neuroinflammation in autism spectrum disorder (ASD). *Brain Behav Immun*, 108, 245-254.
- Janeway, C. A., Jr. & Medzhitov, R. 2002. Innate immune recognition. *Annu Rev*

- Immunol*, 20, 197-216.
- Jemmerson, R., Dubinsky, J. & Brustovetsky, N. 2005. Cytochrome C release from CNS mitochondria and potential for clinical intervention in apoptosis-mediated CNS diseases. *Antioxid Redox Signal*, Sep-Oct, 1158-72.
- Jian, Z., Liu, R., Zhu, X., Smerin, D., Zhong, Y., Gu, L., Fang, W. & Xiong, X. 2019. The Involvement and Therapy Target of Immune Cells After Ischemic Stroke. *Front Immunol*, 10, 2167.
- Johswich, K. 2017. Innate immune recognition and inflammation in Neisseria meningitidis infection. *Pathog Dis*, 75.
- Jr., H. P. A., Bendixen, B. H., Kappelle, L. J., Biller, J., Love, B. B., Gordon, D. L. & Iii, E. E. M. 1993. Classification of subtype of acute ischemic stroke. Definitions for use in a multicenter clinical trial. TOAST. Trial of Org 10172 in Acute Stroke Treatment. *Stroke*, 24, 35-41.
- Kanazawa, M., Ninomiya, I., Hatakeyama, M., Takahashi, T. & Shimohata, T. 2017. Microglia and Monocytes/Macrophages Polarization Reveal Novel Therapeutic Mechanism against Stroke. *Int J Mol Sci*, 18.
- Kang, L., Yu, H., Yang, X., Zhu, Y., Bai, X., Wang, R., Cao, Y., Xu, H., Luo, H., Lu, L., Shi, M. J., Tian, Y., Fan, W. & Zhao, B. Q. 2020. Neutrophil extracellular traps released by neutrophils impair revascularization and vascular remodeling after stroke. *Nat Commun*, 11, 2488.
- Karsy, M., Brock, A., Guan, J., Tausky, P., Kalani, M. Y. & Park, M. S. 2017. Neuroprotective strategies and the underlying molecular basis of cerebrovascular stroke. *Neurosurg Focus*, 42, E3.
- Kazemi, A., Azimian, J., Mafi, M., Allen, K. A. & Motalebi, S. A. 2021. Caregiver burden and coping strategies in caregivers of older patients with stroke. *BMC Psychol*, 9, 51.
- Krauter, A. K., Guest, P. C. & Sarnyai, Z. 2019a. The Open Field Test for Measuring Locomotor Activity and Anxiety-Like Behavior. *Methods Mol Biol*, 1916, 99-103.
- Krauter, A. K., Guest, P. C. & Sarnyai, Z. 2019b. The Y-Maze for Assessment of Spatial Working and Reference Memory in Mice. *Methods Mol Biol*, 1916, 105-111.
- Krishnan, S. & Lawrence, C. B. 2019. Old Dog New Tricks; Revisiting How Stroke Modulates the Systemic Immune Landscape. *Front Neurol*, 10, 718.
- Kumar Saini, S. & Singh, D. 2024. Mitochondrial mechanisms in Cerebral Ischemia-Reperfusion Injury: Unravelling the intricacies. *Mitochondrion*, 77, 101883.
- Lajqi, T., Stojiljkovic, M., Williams, D. L., Hudalla, H., Bauer, M., Witte, O. W., Wetzker, R., Bauer, R. & Schmeer, C. 2020. Memory-Like Responses of Brain Microglia Are Controlled by Developmental State and Pathogen Dose. *Front Immunol*, 11, 546415.
- Laugero, K. & Moberg, G. 2000. Effects of acute behavioral stress and LPS-induced cytokine release on growth and energetics in mice. *Physiol Behav*, Jan, 415-22.
- Lenz, K. M. & Nelson, L. H. 2018. Microglia and Beyond: Innate Immune Cells As Regulators of Brain Development and Behavioral Function. *Front Immunol*, 9,

698.

- Liang, J., Wang, J., Saad, Y., Warble, L., Becerra, E. & Kolattukudy, P. E. 2011. Participation of MCP-induced protein 1 in lipopolysaccharide preconditioning-induced ischemic stroke tolerance by regulating the expression of proinflammatory cytokines. *J Neuroinflammation*, 8, 182.
- Lier, J., Streit, W. J. & Bechmann, I. 2021. Beyond Activation: Characterizing Microglial Functional Phenotypes. *Cells*, 10.
- Liesz, A., Hu, X., Kleinschnitz, C. & Offner, H. 2015. Functional role of regulatory lymphocytes in stroke: facts and controversies. *Stroke*, 46, 1422-30.
- Lin, L., Wang, X. & Yu, Z. 2016. Ischemia-reperfusion Injury in the Brain: Mechanisms and Potential Therapeutic Strategies. *Biochem Pharmacol (Los Angel)*, 5.
- Lin, T. Y., Jiang, D., Chen, W. R., Lin, J. S., Zhang, X. Y., Chen, C. H., Hsu, C. L., Lai, L. C., Chen, P. H., Yang, K. C., Sansing, L. H. & Chang, C. F. 2023. Trained immunity induced by high-salt diet impedes stroke recovery. *EMBO Rep*, 24, e57164.
- Liu, H., Liu, K., Pei, L., Gao, Y., Zhao, L., Sun, S., Wu, J., Li, Y., Fang, H., Song, B. & Xu, Y. 2020. Monocyte-to-High-Density Lipoprotein Ratio Predicts the Outcome of Acute Ischemic Stroke. *J Atheroscler Thromb*, 27, 959-968.
- Longa, E., Weinstein, P., Carlson, S. & Cummins, R. 1989. Reversible middle cerebral artery occlusion without craniectomy in rats. *Stroke*, Jan, 84-91.
- Malone, M. K., Ujas, T. A., Britsch, D. R. S., Cotter, K. M., Poinsette, K. & Stowe, A. M. 2023. The immunopathology of B lymphocytes during stroke-induced injury and repair. *Semin Immunopathol*, 45, 315-327.
- Manwani, B., Liu, F., Xu, Y., Persky, R., Li, J. & McCullough, L. D. 2011. Functional recovery in aging mice after experimental stroke. *Brain Behav Immun*, 25, 1689-700.
- Marsh, J. D. & Keyrouz, S. G. 2010. Stroke prevention and treatment. *J Am Coll Cardiol*, 56, 683-91.
- Mayer-Barber, K. D. & Barber, D. L. 2015. Innate and Adaptive Cellular Immune Responses to Mycobacterium tuberculosis Infection. *Cold Spring Harb Perspect Med*, 5.
- Mcbride, D. W. & Zhang, J. H. 2017. Precision Stroke Animal Models: the Permanent MCAO Model Should Be the Primary Model, Not Transient MCAO. *Transl Stroke Res*.
- McDonough, A. & Weinstein, J. R. 2020. The role of microglia in ischemic preconditioning. *Glia*, 68, 455-471.
- Neher, J. J. & Cunningham, C. 2019. Priming Microglia for Innate Immune Memory in the Brain. *Trends Immunol*, 40, 358-374.
- Nelson, L. H. & Lenz, K. M. 2017. Microglia depletion in early life programs persistent changes in social, mood-related, and locomotor behavior in male and female rats. *Behav Brain Res*, 316, 279-293.
- Netea, M. G., Dominguez-Andres, J., Barreiro, L. B., Chavakis, T., Divangahi, M., Fuchs, E., Joosten, L. a. B., Van Der Meer, J. W. M., Mhlanga, M. M., Mulder,

- W. J. M., Riksen, N. P., Schlitzer, A., Schultze, J. L., Stabell Benn, C., Sun, J. C., Xavier, R. J. & Latz, E. 2020. Defining trained immunity and its role in health and disease. *Nat Rev Immunol*, 20, 375-388.
- Norden, D. M., Trojanowski, P. J., Villanueva, E., Navarro, E. & Godbout, J. P. 2016. Sequential activation of microglia and astrocyte cytokine expression precedes increased Iba-1 or GFAP immunoreactivity following systemic immune challenge. *Glia*, 64, 300-16.
- Nour, M., Scalzo, F. & Liebeskind, D. S. 2013. Ischemia-reperfusion injury in stroke. *Interv Neurol*, 1, 185-99.
- Ochando, J., Mulder, W. J. M., Madsen, J. C., Netea, M. G. & Duivenvoorden, R. 2023. Trained immunity - basic concepts and contributions to immunopathology. *Nat Rev Nephrol*, 19, 23-37.
- Orozco, D. & Edbauer, D. 2013. FUS-mediated alternative splicing in the nervous system: consequences for ALS and FTL. *J Mol Med (Berl)*, 91, 1343-54.
- Ortega, F., Berninger, B. & Costa, M. R. 2013. Primary culture and live imaging of adult neural stem cells and their progeny. *Methods Mol Biol*, 1052, 1-11.
- Pan, J., Konstas, A. A., Bateman, B., Ortolano, G. A. & Pile-Spellman, J. 2007. Reperfusion injury following cerebral ischemia: pathophysiology, MR imaging, and potential therapies. *Neuroradiology*, 49, 93-102.
- Pannell, M., Meier, M. A., Szulzewsky, F., Matyash, V., Endres, M., Kronenberg, G., Prinz, V., Waiczies, S., Wolf, S. A. & Kettenmann, H. 2016. The subpopulation of microglia expressing functional muscarinic acetylcholine receptors expands in stroke and Alzheimer's disease. *Brain Struct Funct*, 221, 1157-72.
- Paolicelli, R. C., Sierra, A., Stevens, B., Tremblay, M. E., Aguzzi, A., Ajami, B., Amit, I., Audinat, E., Bechmann, I., Bennett, M., Bennett, F., Bessis, A., Biber, K., Bilbo, S., Blurton-Jones, M., Boddeke, E., Brites, D., Brone, B., Brown, G. C., Butovsky, O., Carson, M. J., Castellano, B., Colonna, M., Cowley, S. A., Cunningham, C., Davalos, D., De Jager, P. L., De Strooper, B., Denes, A., Eggen, B. J. L., Eyo, U., Galea, E., Garel, S., Ginhoux, F., Glass, C. K., Gokce, O., Gomez-Nicola, D., Gonzalez, B., Gordon, S., Graeber, M. B., Greenhalgh, A. D., Gressens, P., Greter, M., Gutmann, D. H., Haass, C., Heneka, M. T., Heppner, F. L., Hong, S., Hume, D. A., Jung, S., Kettenmann, H., Kipnis, J., Koyama, R., Lemke, G., Lynch, M., Majewska, A., Malcangio, M., Malm, T., Mancuso, R., Masuda, T., Matteoli, M., Mccoll, B. W., Miron, V. E., Molofsky, A. V., Monje, M., Mracsko, E., Nadjar, A., Neher, J. J., Neniskyte, U., Neumann, H., Noda, M., Peng, B., Peri, F., Perry, V. H., Popovich, P. G., Pridans, C., Priller, J., Prinz, M., Ragozzino, D., Ransohoff, R. M., Salter, M. W., Schaefer, A., Schafer, D. P., Schwartz, M., Simons, M., Smith, C. J., Streit, W. J., Tay, T. L., Tsai, L. H., Verkhratsky, A., Von Bernhardi, R., Wake, H., Wittamer, V., Wolf, S. A., Wu, L. J. & Wyss-Coray, T. 2022. Microglia states and nomenclature: A field at its crossroads. *Neuron*, 110, 3458-3483.
- Patir, A., Barrington, J., Szymkowiak, S., Brezzo, G., Straus, D., Alfieri, A., Lefevre, L., Liu, Z., Ginhoux, F., Henderson, N. C., Horsburgh, K., Ramachandran, P.

- & Mccoll, B. W. 2024. Phenotypic and spatial heterogeneity of brain myeloid cells after stroke is associated with cell ontogeny, tissue damage, and brain connectivity. *Cell Rep*, 43, 114250.
- Prinz, M., Jung, S. & Priller, J. 2019. Microglia Biology: One Century of Evolving Concepts. *Cell*, 179, 292-311.
- Prinz, M., Masuda, T., Wheeler, M. A. & Quintana, F. J. 2021. Microglia and Central Nervous System-Associated Macrophages-From Origin to Disease Modulation. *Annu Rev Immunol*, 39, 251-277.
- Püntener, U., Booth, S., Perry, V. & Teeling, J. 2012. Long-term impact of systemic bacterial infection on the cerebral vasculature and microglia. *J Neuroinflammation*, Jun 27, 146.
- Qian, J., Liang, T., Xu, Y., Liu, Z. P., Jing, L. L. & Luo, H. B. 2024. Effect of the Novel Free Radical Scavenger 4'-Hydroxyl-2-Substituted Phenylnitronyl Nitroxide on Oxidative Stress, Mitochondrial Dysfunction and Apoptosis Induced by Cerebral Ischemia-Reperfusion in Rats. *Neuroscience*, 540, 1-11.
- Radak, D., Katsiki, N., Resanovic, I., Jovanovic, A., Sudar-Milovanovic, E., Zafirovic, S., Mousad, S. & Isenovic, E. 2017. Apoptosis and Acute Brain Ischemia in Ischemic Stroke. *Curr Vasc Pharmacol*, 15.
- Rolfes, L., Ruck, T., David, C., Mencl, S., Bock, S., Schmidt, M., Strecker, J. K., Pfeuffer, S., Mecklenbeck, A. S., Gross, C., Gliem, M., Minnerup, J., Schuhmann, M. K., Kleinschnitz, C. & Meuth, S. G. 2022. Natural Killer Cells Are Present in Rag1(-/-) Mice and Promote Tissue Damage During the Acute Phase of Ischemic Stroke. *Transl Stroke Res*, 13, 197-211.
- Rosenzweig, H. L., Minami, M., Lessov, N. S., Coste, S. C., Stevens, S. L., Henshall, D. C., Meller, R., Simon, R. P. & Stenzel-Poore, M. P. 2007. Endotoxin preconditioning protects against the cytotoxic effects of TNFalpha after stroke: a novel role for TNFalpha in LPS-ischemic tolerance. *J Cereb Blood Flow Metab*, 27, 1663-74.
- Roth, S., Yang, J., Cramer, J. V., Malik, R. & Liesz, A. 2021. Detection of cytokine-induced sickness behavior after ischemic stroke by an optimized behavioral assessment battery. *Brain Behav Immun*, 91, 668-672.
- Saini, V., Guada, L. & Yavagal, D. R. 2021. Global Epidemiology of Stroke and Access to Acute Ischemic Stroke Interventions. *Neurology*, 97, S6-S16.
- Schaafsma, W., Zhang, X., Van Zomeren, K. C., Jacobs, S., Georgieva, P. B., Wolf, S. A., Kettenmann, H., Janova, H., Saiepour, N., Hanisch, U. K., Meerlo, P., Van Den Elsen, P. J., Brouwer, N., Boddeke, H. W. & Eggen, B. J. 2015. Long-lasting pro-inflammatory suppression of microglia by LPS-preconditioning is mediated by RelB-dependent epigenetic silencing. *Brain Behav Immun*, 48, 205-21.
- Schadlich, I. S., Vienhues, J. H., Jander, A., Piepke, M., Magnus, T., Lambertsen, K. L., Clausen, B. H. & Gelderblom, M. 2022. Interleukin-1 Mediates Ischemic Brain Injury via Induction of IL-17A in gammadelta T Cells and CXCL1 in Astrocytes. *Neuromolecular Med*, 24, 437-451.
- Scheyltjens, I., Van Hove, H., De Vlaminck, K., Kancheva, D., Bastos, J., Vara-Perez,

- M., Pombo Antunes, A. R., Martens, L., Scott, C. L., Van Ginderachter, J. A., Saeys, Y., Guilliams, M., Vandamme, N. & Movahedi, K. 2022. Single-cell RNA and protein profiling of immune cells from the mouse brain and its border tissues. *Nat Protoc*, 17, 2354-2388.
- Selvaraj, U. M., Poinatte, K., Torres, V., Ortega, S. B. & Stowe, A. M. 2016. Heterogeneity of B Cell Functions in Stroke-Related Risk, Prevention, Injury, and Repair. *Neurotherapeutics*, 13, 729-747.
- Simpson, D. S. A. & Oliver, P. L. 2020. ROS Generation in Microglia: Understanding Oxidative Stress and Inflammation in Neurodegenerative Disease. *Antioxidants (Basel)*, 9.
- Somebang, K., Rudolph, J., Imhof, I., Li, L., Niemi, E. C., Shigenaga, J., Tran, H., Gill, T. M., Lo, I., Zabel, B. A., Schmajuk, G., Wipke, B. T., Gyoneva, S., Jandreski, L., Craft, M., Benedetto, G., Plowey, E. D., Charo, I., Campbell, J., Ye, C. J., Panter, S. S., Nakamura, M. C., Eckalbar, W. & Hsieh, C. L. 2021. CCR2 deficiency alters activation of microglia subsets in traumatic brain injury. *Cell Rep*, 36, 109727.
- Sousa, C., Golebiewska, A., Poovathingal, S. K., Kaoma, T., Pires-Afonso, Y., Martina, S., Coowar, D., Azuaje, F., Skupin, A., Balling, R., Biber, K., Niclou, S. P. & Michelucci, A. 2018. Single-cell transcriptomics reveals distinct inflammation-induced microglia signatures. *EMBO Rep*, 19.
- Spiteri, A. G., Wishart, C. L., Pamphlett, R., Locatelli, G. & King, N. J. C. 2022. Microglia and monocytes in inflammatory CNS disease: integrating phenotype and function. *Acta Neuropathol*, 143, 179-224.
- Stroke Therapy Academic Industry Roundtable (STAIR). 1999. Recommendations for standards regarding preclinical neuroprotective and restorative drug development. *Stroke*, 30, 2752-2758.
- Stambas, J., Lu, C. & Tripp, R. A. 2020. Innate and adaptive immune responses in respiratory virus infection: implications for the clinic. *Expert Rev Respir Med*, 14, 1141-1147.
- Stolp, J., Zaitso, M. & Wood, K. J. 2019. Immune Tolerance and Rejection in Organ Transplantation. *Methods Mol Biol*, 1899, 159-180.
- Su, Y., Zheng, H., Shi, C., Li, X., Zhang, S., Guo, G., Yu, W., Zhang, S., Hu, Z., Yang, J., Xia, Z., Mao, C. & Xu, Y. 2023. Meningeal immunity and neurological diseases: new approaches, new insights. *J Neuroinflammation*, 20, 125.
- Subramanian, A., Tamayo, P., Mootha, V., Mukherjee, S., Ebert, B., Gillette, M., Paulovich, A., Pomeroy, S., Golub, T., Lander, E. & Mesirov, J. 2005. Gene set enrichment analysis: a knowledge-based approach for interpreting genome-wide expression profiles. *Proc Natl Acad Sci U S A*, 102, 15545-50.
- Szabo, K. 2014. Hippocampal stroke. *Front Neurol Neurosci*, 34, 150-6.
- Tan, W., Su, P. P., Leff, J., Gao, X., Chen, J., Guan, A. K., Kalyanasundaram, G., Ma, A. & Guan, Z. 2022. Distinct phases of adult microglia proliferation: a Myc-mediated early phase and a Tnfrsf3-mediated late phase. *Cell Discov*, 8, 34.
- Teymuri Kheravi, M., Nayebifar, S., Aletaha, S. M. & Sarhadi, S. 2021. The Effect of Two Types of Exercise Preconditioning on the Expression of TrkB, TNF-

- alpha, and MMP2 Genes in Rats with Stroke. *Biomed Res Int*, 2021, 5595368.
- Tsao, C. W., Aday, A. W., Almarzooq, Z. I., Anderson, C. a. M., Arora, P., Avery, C. L., Baker-Smith, C. M., Beaton, A. Z., Boehme, A. K., Buxton, A. E., Commodore-Mensah, Y., Elkind, M. S. V., Evenson, K. R., Eze-Nliam, C., Fugar, S., Generoso, G., Heard, D. G., Hiremath, S., Ho, J. E., Kalani, R., Kazi, D. S., Ko, D., Levine, D. A., Liu, J., Ma, J., Magnani, J. W., Michos, E. D., Mussolino, M. E., Navaneethan, S. D., Parikh, N. I., Poudel, R., Rezk-Hanna, M., Roth, G. A., Shah, N. S., St-Onge, M. P., Thacker, E. L., Virani, S. S., Voeks, J. H., Wang, N. Y., Wong, N. D., Wong, S. S., Yaffe, K., Martin, S. S., American Heart Association Council On, E., Prevention Statistics, C. & Stroke Statistics, S. 2023. Heart Disease and Stroke Statistics-2023 Update: A Report From the American Heart Association. *Circulation*, 147, e93-e621.
- Var, S. R., Shetty, A. V., Grande, A. W., Low, W. C. & Cheeran, M. C. 2021. Microglia and Macrophages in Neuroprotection, Neurogenesis, and Emerging Therapies for Stroke. *Cells*, 10.
- Wang, X. & Quinn, P. J. 2010. Lipopolysaccharide: Biosynthetic pathway and structure modification. *Prog Lipid Res*, 49, 97-107.
- Wang, Y., Leak, R. K. & Cao, G. 2022. Microglia-mediated neuroinflammation and neuroplasticity after stroke. *Front Cell Neurosci*, 16, 980722.
- Wei, R., Zhang, L., Hu, W., Shang, X., He, Y. & Zhang, W. 2022. Zeb2/Axin2-Enriched BMSC-Derived Exosomes Promote Post-Stroke Functional Recovery by Enhancing Neurogenesis and Neural Plasticity. *J Mol Neurosci*, 72, 69-81.
- Wendeln, A.-C., Degenhardt, K., Kaurani, L., Gertig, M., Ulas, T., Jain, G., Wagner, J., Häsler, L. M., Wild, K., Skodras, A., Blank, T., Staszewski, O., Datta, M., Centeno, T. P., Capece, V., Islam, M. R., Kerimoglu, C., Staufenbiel, M., Schultze, J. L., Beyer, M., Prinz, M., Jucker, M., Fischer, A. & Neher, J. J. 2018. Innate immune memory in the brain shapes neurological disease hallmarks. *Nature*, 556, 332-338.
- West, M. A. & Heagy, W. 2002. Endotoxin tolerance: A review. *Crit Care Med*, 30.
- Wicks, E. E., Ran, K. R., Kim, J. E., Xu, R., Lee, R. P. & Jackson, C. M. 2022. The Translational Potential of Microglia and Monocyte-Derived Macrophages in Ischemic Stroke. *Front Immunol*, 13, 897022.
- Wu, J., Sabirzhanov, B., Stoica, B. A., Lipinski, M. M., Zhao, Z., Zhao, S., Ward, N., Yang, D. & Faden, A. I. 2015. Ablation of the transcription factors E2F1-2 limits neuroinflammation and associated neurological deficits after contusive spinal cord injury. *Cell Cycle*, 14, 3698-712.
- Wu, K. L., Chan, S. H. & Chan, J. Y. 2012. Neuroinflammation and oxidative stress in rostral ventrolateral medulla contribute to neurogenic hypertension induced by systemic inflammation. *J Neuroinflammation*, Sep 7, 9:212.
- Xiong, B., Li, A., Lou, Y., Chen, S., Long, B., Peng, J., Yang, Z., Xu, T., Yang, X., Li, X., Jiang, T., Luo, Q. & Gong, H. 2017. Precise Cerebral Vascular Atlas in Stereotaxic Coordinates of Whole Mouse Brain. *Front Neuroanat*, 11, 128.
- Xu, Q., Zou, Y., Miao, Z., Jiang, L. & Zhao, X. 2023. Transient receptor potential ion

- channels and cerebral stroke. *Brain Behav*, 13, e2843.
- Yan, H., Kawano, T., Kanki, H., Nishiyama, K., Shimamura, M., Mochizuki, H. & Sasaki, T. 2023. Role of Polymorphonuclear Myeloid-Derived Suppressor Cells and Neutrophils in Ischemic Stroke. *J Am Heart Assoc*, 12, e028125.
- Ye, M., Xiang, H., Liu, H., Hu, Z., Wang, Y., Gu, Y., Lu, X. & Huang, C. 2022. Innate immune tolerance against adolescent intermittent alcohol exposure-induced behavioral abnormalities in adult mice. *Int Immunopharmacol*, 113, 109250.
- Yilmaz, G., Arumugam, T. V., Stokes, K. Y. & Granger, D. N. 2006. Role of T lymphocytes and interferon-gamma in ischemic stroke. *Circulation*, 113, 2105-12.
- Zbesko, J. C., Frye, J. B., Bechtel, D. A., Gerardo, D. K., Stokes, J., Calderon, K., Nguyen, T. V., Bhattacharya, D. & Doyle, K. P. 2021. IgA natural antibodies are produced following T-cell independent B-cell activation following stroke. *Brain Behav Immun*, 91, 578-586.
- Zhang, D., Ren, J., Luo, Y., He, Q., Zhao, R., Chang, J., Yang, Y. & Guo, Z. N. 2021a. T Cell Response in Ischemic Stroke: From Mechanisms to Translational Insights. *Front Immunol*, 12, 707972.
- Zhang, H., Chen, T., Ren, J., Xia, Y., Onuma, A., Wang, Y., He, J., Wu, J., Wang, H., Hamad, A., Shen, C., Zhang, J., Asara, J. M., Behbehani, G. K., Wen, H., Deng, M., Tsung, A. & Huang, H. 2021b. Pre-operative exercise therapy triggers anti-inflammatory trained immunity of Kupffer cells through metabolic reprogramming. *Nat Metab*, 3, 843-858.
- Zheng, Y., He, R., Wang, P., Shi, Y., Zhao, L. & Liang, J. 2019. Exosomes from LPS-stimulated macrophages induce neuroprotection and functional improvement after ischemic stroke by modulating microglial polarization. *Biomater Sci*, 7, 2037-2049.
- Zhou, X. Y., Gao, R., Hu, J., Gao, D. P., Liao, Y. L. & Yang, J. J. 2020. Trained Innate Immunity by Repeated Low-Dose Lipopolysaccharide Injections Displays Long-Term Neuroprotective Effects. *Mediators Inflamm*, 2020, 8191079.
- Zotter, M., Piechowiak, E. I., Balasubramaniam, R., Von Martial, R., Genceviciute, K., Blanquet, M., Slavova, N., Sarikaya, H., Arnold, M., Gralla, J., Jung, S., Fischer, U., El-Koussy, M. & Heldner, M. R. 2021. Endovascular therapy in patients with large vessel occlusion due to cardioembolism versus large-artery atherosclerosis. *Ther Adv Neurol Disord*, 14, 1756286421999017.

8. Acknowledgements

Thanks to my supervisor Dr. Karoline Degenhardt. Your patient teaching helps me develop from an animal experiment starter to a lab person with important skills. The help from you is not limited to my research and skills. It is really helpful to listen to your suggestion about my life and studies. Our discussions on projects finally lead me to current graduation. Sometimes we talk about topics about lives and travelling, and I can always get a lot of interesting experience. It is my proud to learn from you and also be a friend of you!

Thanks to PD Dr. Mathias Gelderblom and Prof. Tim Magnus. Your efforts in advance provide me with an excellent study and research environment. It is also your help with my application of studying here. Thank you for your help with my contact to our ERSI lab.

Thanks to my colleagues Dr. Mingming Zha, Dr. Yuqi Gui, Hind Haj Ahmad, Jiani Jiang, Tina Fischer, Mamta Panda, Sara Isla Cainzos, Katrin Lessmann, Javier Randez Garbayo, Dr. Santra Brenna. It is glad to work with my excellent colleagues in the lab. We learn from each other, discuss about our topics, and I can always get either advice or inspiration. And especially many thanks to Dr. Mingming Zha. We have experienced a lot of special things, and always help each other. Now I'm almost graduate as well, and sincerely hope we can have a bright future and a nice working environment.

Thanks to our technician team, Lennart Pöls, Karolin Gustmann, Jasmin Pabla, and Tobias Großhauser. All your assistance in my project and experiments are all reflected on my results. We are also good friends. It is always happy to chat with you about variety of topics. You are also kind to listen to me, and share many cool things with me. Lennart becomes my best friend here, and I can always share my thought with him (also our shared hobbies). And by the way, sincerely hope Lennart can master Japanese one day.

Thanks to the help of people in other departments. Thanks to Tobias Mummert, Prof. Michael Kaul, Dr. Thomas Lindner with animal MRI. Thanks to Christiana Pahrman and Maike Westphal for kindly helping me with the scale every week. Thanks to Regine

Thiele, Melanie Lachmann-Schwemm, and Dr. Anne Rissiek with FACS sorting (from helping to teaching!). Thanks to Prof. Immo Prinz and Dr. Likai Tan with data analysis (also thanks for the help from Prof. Prinz with scholarship application!). Thanks for Dr. Christian Müller and Philipp Dirksen for the assistance on RNA-sequencing analysis. Your help provide me large convenience, and your kindness is always my extra gift.

Thanks to my wife, Peipei Wei. We study together and live together. Only you face every difficulty together with me. In the past several years, we have experienced different but colorful life. Though with sorrow and pain, we have still harvested a wonderful and unique life experience together. Hope our futures go brighter and higher. Lastly, thanks to Chinese Scholarship Council (CSC). The precious scholarship let me have the possibility to study in UKE. As a student from a normal family, it is a too expensive hope to study aboard. I finally have a special life in Germany, and learned a lot.

It's the ending chapter of this story. I will memorize every smile and tear, gratitude to every friend and foe, and calmly step forward to the next part of my life. At last, wish every attendance in my life enjoy the part with me.

9. Resume

Lebenslauf entfällt aus datenschutzrechtlichen Gründen.

10. Eidesstattliche Versicherung

Ich versichere ausdrücklich, dass ich die Arbeit selbständig und ohne fremde Hilfe, insbesondere ohne entgeltliche Hilfe von Vermittlungs- und Beratungsdiensten, verfasst, andere als die von mir angegebenen Quellen und Hilfsmittel nicht benutzt und die aus den benutzten Werken wörtlich oder inhaltlich entnommenen Stellen einzeln nach Ausgabe (Auflage und Jahr des Erscheinens), Band und Seite des benutzten Werkes kenntlich gemacht habe. Das gilt insbesondere auch für alle Informationen aus Internetquellen.

Soweit beim Verfassen der Dissertation KI-basierte Tools („Chatbots“) verwendet wurden, versichere ich ausdrücklich, den daraus generierten Anteil deutlich kenntlich gemacht zu haben. Die „Stellungnahme des Präsidiums der Deutschen Forschungsgemeinschaft (DFG) zum Einfluss generativer Modelle für die Text- und Bilderstellung auf die Wissenschaften und das Förderhandeln der DFG“ aus September 2023 wurde dabei beachtet.

Ferner versichere ich, dass ich die Dissertation bisher nicht einem Fachvertreter an einer anderen Hochschule zur Überprüfung vorgelegt oder mich anderweitig um Zulassung zur Promotion beworben habe.

Ich erkläre mich damit einverstanden, dass meine Dissertation vom Dekanat der Medizini-schen Fakultät mit einer gängigen Software zur Erkennung von Plagiaten überprüft werden kann.

Datum

Unterschrift